A. D. Myshkis
V. G. Babskii, N. D. Kopachevskii
L. A. Slobozhanin, A. D. Tyuptsov

Low-Gravity Fluid Mechanics

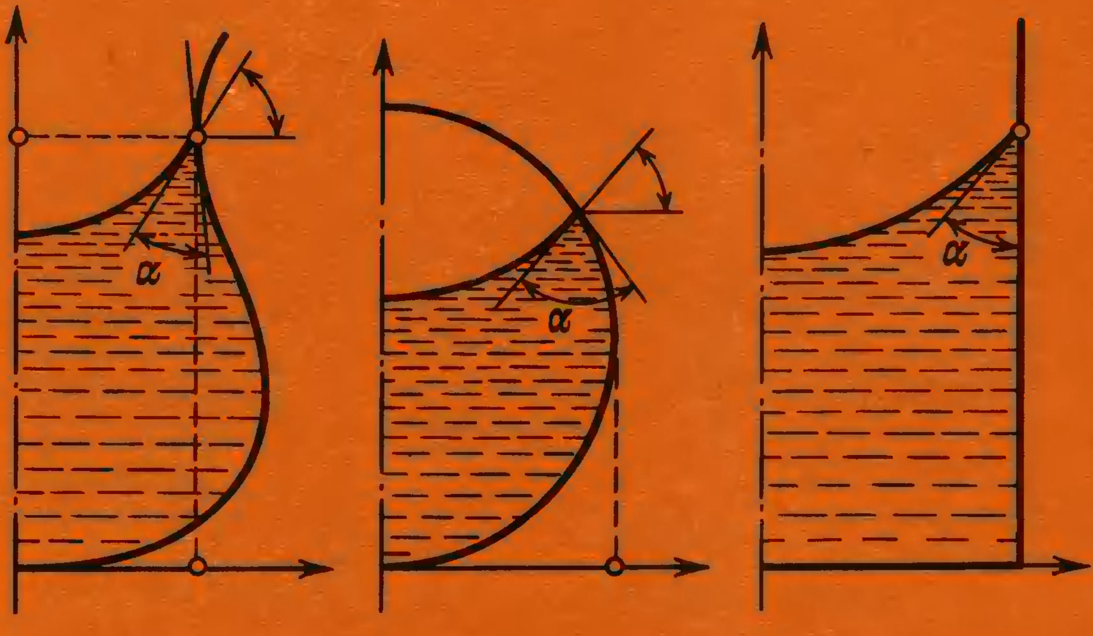

Springer-Verlag

Low-Gravity Fluid Mechanics

Mathematical Theory of Capillary Phenomena

By A. D. Myshkis
V. G. Babskii N. D. Kopachevskii
L. A. Slobozhanin A. D. Tyuptsov

Translated by R. S. Wadhwa

With 218 Figures

Springer-Verlag Berlin Heidelberg New York
London Paris Tokyo

Anatolii D. Myshkis

Moscow Institute of Railway Engineers, Ul. Obraztsova 15,
SU-103055 Moscow, USSR

Vitalii G. Babskii

Institute of Molecular Biology and Genetics, Ukrainian Academy of Sciences,
SU-252627 Kiev, USSR

Nikolai D. Kopachevskii

Simferopol State University, SU-333000 Simferopol, USSR

Lev A. Slobozhanin

Physico-Technical Institute of Low Temperatures, Ukrainian Academy of Sciences, Lenin Prospect 47,
SU-310164 Khar'kov, USSR

Anatolii D. Tyuptsov

Physico-Technical Institute of Low Temperatures, Ukrainian Academy of Sciences, Lenin Prospect 47,
SU-310164 Khar'kov, USSR

Translator: *R. S. Wadhwa*

28-3-224 Menzhinsky St., SU-129281 Moscow, USSR

This edition is based on the original Russian edition: *Gidromekhanika Nevesomosti*

ISBN 3-540-16189-9 Springer-Verlag Berlin Heidelberg New York
ISBN 0-387-16189-9 Springer-Verlag New York Berlin Heidelberg

Library of Congress Cataloging-in-Publication Data. Gidromekhanika nevesomosti. English Low-gravity fluid mechanics. Translation of: Gidromekhanika nevesomosti. 1. Fluid mechanics. 2. Capillarity – Mathematical models. 3. Liquids – Effect of reduced gravity on. I. Myshkis, A. D. (Anatoliĭ Dmitrievich) QA901.G5313 1987 532'.6 86-33926

Printed in Germany

Typesetting: Asco Trade Typesetting Limited, Hongkong
Offset printing: Druckhaus Beltz, 6944 Hemsbach; Bookbinding: J. Schäffer GmbH & Co. KG., 6718 Grünstadt
2153/3150-543210

Preface

We are extremely grateful to Springer-Verlag and to Prof. Dr. W. Beiglböck for bringing out the English edition of our book. We are also thankful to Dr. R. S. Wadhwa for a qualified translation. While preparing the manuscript for translation, we took the opportunity to go through the whole text, make necessary amendments, supplement the original material with new results, and considerably enlarge the lists of references.

We hope that this book will serve to strengthen the bonds of international cooperation in this field.

July 1986 *The authors*

Translator's Note

The final form of the bibliography contains a (free) English translation of all the Russian books and papers published in the USSR. This has been done at the request of the authors and with the concurrence of Prof. Beiglböck. The titles are not always exact, and some of the works have already been translated into English or other European languages. Unfortunately, the authors were not in a position to provide detailed information on this subject.

R.S. Wadhwa

Preface to the Russian Edition

What shall I do ...
With their weightlessness
In this ponderous world?

M. Tsvetaeva, *The Poet*

This book deals with the behavior of a liquid in zero-gravity or conditions close to it. The surge of interest in zero-gravity problems stems from the progress attained in the field of spaceflight, where such conditions can be attained for long periods of time. Hence the very term "zero-gravity" has a romantic halo about it: although spaceflights have become an accepted fact of life, they are not by any means everyday occurrences. Each new spaceflight involves the best that the present-day level of scientific and technical advancement can offer, and may be considered as a quest for the unknown.

It was this fascination of the unexplored that prompted the authors of this book to acquaint themselves with the problems of low-gravity fluid mechanics in 1963. The feeling, obviously, was shared by others as well. The American physicist *Benedikt* [16], who compiled the collection of articles "Weightlessness", even proposed a new term, "epihydrodynamics", for low-gravity fluid mechanics to emphasize the novelty of this branch of science.

As a matter of fact, this novelty is confined only to the application of the results of investigations. The problems themselves hardly contain anything new, and their specific properties (which often play a determining role) are due to surface tension. However, problems of fluid mechanics taking surface tension into consideration have been investigated for well over a century. These problems arise during investigation of phenomena in capillaries, thin films, drops, etc. in which the capillary forces become significant. (In this connection, the terms *capillary fluid* and *capillary hydrodynamics* are quite frequently employed [94].)

Since the important factor is the ratio of capillary and gravitational forces rather than their absolute values, we can expect a similarity between capillary effects and the behavior of a fluid under zero- or near-zero-gravity conditions. This analogy was qualitatively confirmed in the earliest experiments on the simulation of zero-gravity conditions in airplanes (moving in a Keplerian trajectory) or in containers in free fall. Later, experiments were carried out on artificial Earth satellites. At a press conference held on 21 August 1962, the Soviet cosmonaut P. R. Popovich reported the first results of the observation of water in a bulb in spaceflight. In a telecast from the American space station "Skylab" on 14 January 1974, drops of water suspended in air were shown to viewers all over the world. In special experiments conducted on board "Apollo 14" on 7 February 1971, the American astronaut S. A. Roosa observed thermocapillary convection in a liquid, a typical phenomenon in zero-gravity conditions [72].

With the development and complication of space technology, an increase in the duration of spaceflights and a diversification of the type of investigations conducted on board spaceships, the role of fluids is constantly growing. They are used in rocket engines and power units, in life-support (and survival) systems, in temperature control equipment, for conducting various technological experiments, etc. [8, 53, 100, 152].

Naturally, the construction and operation of such systems and equipment would be inconceivable without preliminary experimental and theoretical investigations of the behavior of a liquid under zero-gravity conditions.

However, experiments in space are rare and expensive, and the simulation of zero-gravity on Earth is fraught with considerable technological complications, thus limiting purely empirical investigation. For this reason, mathematical modelling or the theoretical investigation of the behavior of a liquid in zero-gravity has become significant.

Such analysis, supported by well-developed computational algorithms and detailed investigation of various model problems, must provide the bulk of qualitative and quantitative results and predict the influence of various factors in extremal situations. As a rule, even the simplest examples of the problems considered here do not admit a solution in terms of elementary functions. Only the use of computers has led to significant advancement in the mathematical investigation of the behavior of a liquid under zero-gravity conditions.

This book is devoted entirely to the mathematical theory of fluid mechanics under zero-gravity or, to be more precise, to an analysis of the problems of fluid mechanics under zero-gravity from the point of view of applied mathematics. This theory has been developed quite significantly over the last few years and has proved to be much richer in content than had originally been expected. It is appropriate to recall in this connection that according to *Batchelor* [13], a significant and characteristic property of fluid mechanics is that it embraces various mechanical and physical processes; although each of these processes can be assumed to be quite clear from the point of view of fundamental physics, together they may lead to many unexpected effects.

It should be noted that this book deals with the statics and small movements of a liquid (roughly speaking, with nonlinear statics and linear dynamics on a nonlinear static background), since the theory of considerably nonlinear movements of a capillary liquid has been worked out quite inadequately so far. The problems discussed are of interest to a wide range of readers. Engineers in the field of space technology and specialists in mechanics interested in the applications of problems will be excited by the qualitatively new aspects in the behavior of a liquid in zero- and near-zero-gravity, the corresponding methods of computation, and the results of calculations presented in the form of numerous graphs and tables. Researchers in mathematics and theoretical branches of mechanics will be interested in the possibility of formulating new mathematical problems admitting a direct physical interpretation and requiring methods of functional analysis and mathematical physics, which, up to now, have not been worked out in detail.

To meet the requirements of both these categories of readers, the authors have employed the following technique while writing this book: the material presented in the main part contains the formulation of problems, description of the qualitative and quantitative results that do not require an advanced level of mathematics, and the methods and results of computations. The auxiliary parts containing the detailed mathematical analysis and various digressions are indicated by a vertical grey line in the margin and may be skipped if desired.

The book consists of a Foreword, Introduction (Chap. 1), and eight chapters divided into three parts: Part I (Chaps. 2 – 4) deals with problems of hydrostatics, Part II (Chaps. 5 – 7) is devoted to the theory of small oscillations, and Part III (Chaps. 8, 9) describes convection in zero-gravity. Separate lists of references have been compiled: one for the Introduction and Preface, and one following each part of the book. These lists are quite exhaustive and contain all pertinent references known to the authors.[1] However, the results of these investigations are not given equal coverage; while some works (for example, as the reader may guess, the results of the authors' investigations) are described in detail, others are mentioned only in passing, either under the heading "Reference Commentaries" or in the Introductions. While making this distinction, the authors have been guided by their endeavor to present an integral pattern for each part of the theory, although it is hard to say if they have succeeded entirely in their attempt.

The authors are extremely grateful to Prof. B.I. Verkin, Director of the Physico-Technical Institute of Low Temperatures at Kharkov, and Member of the Academy of Sciences of the Ukrainian SSR, for suggesting the investigation of the behavior of a liquid in zero-gravity, for a discussion of the first results, for continued benevolence, and for persistent support in the investigations which form the basis of the material of this book. We are also thankful to the staff of the Applied Mathematics Department of this Institute, including Drs. I.D. Borisov, I.I. Ievlev, N.N. Morozovskaya, N.S. Shcherbakova, G.B. Shcherbina, I.L. Sklovskaya, Yu.B. Sklovskii, M.A. Svechkareva (Belyayeva), L.A. Temkin, and V.S. Temkina, who participated in the investigations on which the material of this book is based.

Sincere thanks are also due to Drs. F.L. Chernous'ko, S.G. Krein, I.A. Lukovskii, N.N. Moiseev, V.I. Polezhaev, V.V. Rumyantsev, L.S. Srubshchik, and V.I. Yudovich for close and fruitful cooperation and for helpful discussions. We also acknowledge with thanks the participation of the editor, Dr. V.A. Samsonov, who made several critical remarks and offered numerous suggestions that ultimately led to the elimination of many shortcomings in the original manuscript.

---

[1] Unfortunately, many American works on this subject, published in the form of technical reports by NASA as well as various companies and universities, were not accessible to the authors.

Contents

Part I **Statics**

Part II **Small Oscillations**

Part III Convection

"The outstanding contributions made by Poisson and Laplace to the mathematical theory of capillary phenomena have completely exhausted this subject and brought it to such a level of perfection that there is hardly anything more to be gained by their further investigation."

A. Yu. Davidov, *Theory of Capillary Phenomena* (Moscow 1851)

1. Introduction

1.1 On Zero-Gravity

Gravitational forces play an important, and often dominating, role in many physical phenomena and processes under ordinary terrestrial conditions. From the point of view of mechanics, the gravitational force field is manifested in that each free mass point experiences an acceleration $\boldsymbol{g}$ whose magnitude and direction depend only on the position of the point and, perhaps, on time. However, the acceleration depends on the system of coordinates in which its motion is considered. Hence the gravitational force field also depends on the choice of the coordinate system.

Let K and K' be two systems of coordinates and $\boldsymbol{g}$ and $\boldsymbol{g}'$ be the corresponding acceleration fields. If the system K' performs translation with respect to K with an acceleration $\boldsymbol{a}$, the vectors $\boldsymbol{g}$ and $\boldsymbol{g}'$ are connected at each point A through the relation

$$\boldsymbol{g}'_A = \boldsymbol{g}_A - \boldsymbol{a}.$$

In particular, it follows that if $\boldsymbol{g}_A = \boldsymbol{0}$; i.e., if there is no gravitational field in K, the inertial force field generated in K' due to its accelerated motion is equivalent to a uniform gravitational field and $\boldsymbol{g}'_A = -\boldsymbol{a}$.

If the system K' is fixed to a mass point O' and together with it performs free translatory motion; i.e., motion caused only by a gravitational field, then $\boldsymbol{a} = \boldsymbol{g}_{O'}$,

$$\boldsymbol{g}'_A = \boldsymbol{g}_A - \boldsymbol{g}_{O'},$$

and $\boldsymbol{g}'_{O'} = \boldsymbol{0}$. Besides, the uniformity of the gravitational field in the system K indicates that there is no gravitational field in K'.

Real gravitational fields are not uniform. However, their nonuniformity is usually perceptible only in regions of space whose size is comparable with the distance from the center of the source of gravity (Earth, Moon, Sun and other celestial bodies). Hence, even though gravitational forces and accelerations do not completely vanish on board in the case of the free flight of a space ship, their value is smaller than under terrestrial conditions by several orders of magnitude and they do not play significant role in many physical phenomena. It is in this sense that the term *zero-gravity* should be understood in the description of conditions of space flight.

A brief simulation of zero-gravity under terrestrial conditions is possible with the help of freely falling containers, as well as airplane flights in Keplerian trajectories. *Zero-gravity towers* (wells), in which a container with measuring and recording instruments is allowed to fall freely under the action of gravity, are widely used.[1] However, it is clear that this mainly permits only short-duration active processes involving the transition of a liquid from the condition corresponding to the normal acceleration due to gravity ($g_0 = 9.81\ m/s^2$) up to the zero-gravity condition, since the liquid does not really attain the state of rest for a few seconds. Hence, such experiments are unsuitable for investigating hydrostatics or steady-state processes. The same conclusion can be drawn about the conditions realized in airplanes flying in Keplerian trajectories [137, 155].

In experiments on airplanes with a fixed object, a load factor $g/g_0 \lesssim 0.02$ can be maintained for 30 s, while in a container floating on bracing wires, a value $g/g_0 \lesssim 0.01$ can be attained for 5 to 10 s [137]. Lower g-loading can be attained in a freely floating container, but the duration of the experiment is curtailed in this case to just 2–3 s and the harmful influence of initial disturbances created while releasing the container becomes quite significant.

For some problems of hydrostatics, it is possible to imitate low-gravity conditions in thin containers or in slits between transparent parallel plates inclined to the horizontal at a certain angle φ [80]. In many processes of hydromechanics, only the component of gravitational force in the direction of the slit is effective, and imitation of various load factors g/g_0 from 0 to 1 is possible by a horizontal to vertical rotation of the plates (in this case, $g/g_0 = \sin \varphi$). Experimental verification has shown that the equilibrium shapes of the liquid surface are in good agreement with the theoretical solution of the plane problem, although the effect of wetting of plates has not been taken into account. This method was applied to investigate the phenomenon of boiling in weak gravitational fields [79]. However, it is obvious that such a method of simulation of processes has very limited applications in fluid mechanics.

One of the first problems when investigating zero-gravity fluid mechanics is comparing and estimating the influence of various forces, and indicating the dominant ones. The gravitational forces acting on a mass point can be divided into the following categories:

(1) forces outside the spaceship, caused by the nonuniformity of the external gravitational field;
(2) forces of gravitational interaction with the structural elements of an apparatus and its contents (internal gravitation or self-gravitation).

Intermolecular forces have to be considered in many cases.

Additional acceleration and force fields on board a spaceship are also created by factors like aerodynamic deceleration in orbital flights, interaction of the electric charge of the apparatus with the Earth's magnetic field, solar pressure, and rotation of the apparatus (in order to maintain its orientation). Table 1.1, borrowed from [114], presents the order of accelerations due to all these factors (except intermolecular forces). Methods and results of more accurate calculations of real accelerations on board a spaceship are described in [93]. Measurements of acceleration made on board the orbital station "Salyut 6" with the help of precise accelerometers were published in [71]. In the next paragraph, we estimate the magnitude of accelerations in a liquid caused by intermolecular forces.

---

[1] In order to eliminate aerodynamic resistance and hence better reproduce zero-gravity conditions, the object under investigation is thrown into a large falling container, or air is pumped out of the gravity tower (well). For example, at a vacuum of 10^{-1} torr, accelerations that are just 10^{-5} of the terrestrial value of g_0 are realized in a freely falling container.

Table 1.1. Relative accelerations (loading factors) in space

Source	Altitude of circular orbit [km]	
	240	1610
Aerodynamic origin (maximum solar activity)	7.0×10^{-6}	4.6×10^{-12}
Geomagnetism	9.5×10^{-12}	5.1×10^{-13}
Light pressure	3.1×10^{-9}	3.1×10^{-9}
Internal gravitation	3.3×10^{-8}	3.3×10^{-8}
In-flight orientation control	4.3×10^{-7}	2.4×10^{-7}
External gravitation (nonuniformity of Earth's gravitational field)	4.3×10^{-7}	2.4×10^{-7}

Remark. The values of acceleration are given with respect to the acceleration due to gravity, $g_0 = 9.80665$ m/s^2. The following initial data were given: mass of the spaceship, 45.36 t; diameter (of the spherical spaceship), 19.2 m; area of the mid-section, 290 m^2; drag coefficient, 2.0; distance of an elementary volume of the liquid from the center of gravity (or rotation), 3.05 m.

1.2 Surface or Capillary Forces

The possibility that intermolecular interactions could considerably influence the behavior of a liquid was first revealed by investigations of capillary phenomena. Intermolecular forces, unlike gravitational and Coulomb forces, are short-range forces, and their intensity decreases rapidly with increasing distance between molecules. Hence the *free* potential energy of a certain mechanical system—"liquid-rigid body (vessel)"—due to intermolecular interaction, i.e., that part of the energy which varies with the shape or position of a liquid in a vessel, is concentrated only in narrow layers (of the thickness of several intermolecular separations) near the interfaces between different media and is called *surface energy*. The energy $\mathcal{U}$ of each such layer is proportional to the area S of the corresponding interface:

$$\mathcal{U} = \sigma S,$$

while the proportionality factor $\sigma > 0$ is equal to the surface energy density of the layer. The variation $\Delta\mathcal{U} = \sigma\Delta S$ of the energy calculated in this way is equal to the change in the potential energy of a uniformly stretched homogeneous elastic film whose tension (i.e., the force per unit length of the film cross section) is equal to σ. This led to an analogy between the interface of two media and a stretched elastic film, which was first introduced by Young in 1805 and has since become a classical part of the theory of capillary phenomena. Hence, σ is called *surface tension* or the *coefficient of surface tension*, and the corresponding forces which tend to decrease the area S of the surface are called *surface forces* or, in keeping with historical tradition, capillary forces.

The magnitude of the surface tension depends on the physical properties of the media in contact. On the free surface of a liquid, σ depends on temperature T and on the pressure of the gas (vapor). As these parameters increase, σ decreases and becomes equal to zero at the critical temperature T_{cr}. The dependence of σ on T is described quite accurately by

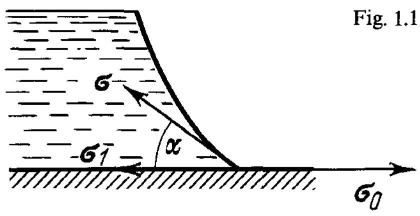

Fig. 1.1

the empirical relation

$$\sigma = k(T - T_{cr}),$$

where k is a constant depending on the nature of the liquid. (Other empirical dependences $\sigma(T)$ and the theoretical concepts associated with them can be found in [2, 110, 131].)

The following two cases can arise if a liquid having a free surface comes in contact with a rigid body:

(1) complete wetting, when the entire surface of the rigid body is covered either by the liquid or by its thin film (this situation is typical for cryogenic fluids);
(2) partial wetting, when the liquid covers only a part of the surface of the rigid body.

The case of partial wetting is frequently encountered. Here, the liquid forms a certain dihedral angle α (Fig. 1.1) at the *wetting line* bounding the wetted part of the rigid surface. This angle is called the boundary-, contact- or *wetting angle.*

It follows from the analogy between the interface of two media and an elastic film that the Dupré-Young condition

$$\sigma_0 = \sigma_1 + \sigma \cos \alpha,$$

must be satisfied at the wetting line in the state of equilibrium. Here σ, σ_0, σ_1, are the values of the surface tension at the liquid-gas, gas-solid and liquid-solid boundaries, respectively.

In all problems on the statics and dynamics of a liquid considered in this book, the classical concepts are employed and σ and angle α are assumed to be the initial parameters whose values (or their dependence on temperature and pressure) may be specified uniquely.

At present, there is no physical theory that allows us to calculate the values of surface tension and the wetting angle or at least to predict the existence of a completely definite boundary angle for given media in contact. (We shall return to the question of the boundary angle in Sect. 2.1.6d.)

The values of surface tension obtained by empirical methods for a number of "liquid-gas" pairs (at atmospheric pressure) and the values of contact angles for some "liquid-solid" pairs (in air) are compiled in Tables 1.2 [16, 26, 77, 114] and 1.3 [11, 16, 114].

The values of surface tension and the wetting angle are quite sensitive to impurities and, especially, surfactants on the interfaces, [95]. The observed value of the boundary angle also depends on the roughness of the solid surface. Since purity and roughness are rarely controlled with sufficient accuracy in measurements of σ and α and are not indicated in publications, the data contained in different references are quite varied, complicating their practical application. In many cases, however, useful qualitative, and at times

Table 1.2. Surface tension for some "liquid-gas" and "liquid-liquid" pairs

Substance	Medium in contact	Temperature [°C]	Surface tension σ [dyne/cm]
Hydrogen	Vapor of the substance	−252.0	2.0
Nitrogen		−195.9	8.3
Nitrogen		−183.0	6.2
Oxygen		−182.7	13.0
Ethyl alcohol		20.0	22.0
Mercury		0	513.0
Mercury		20.0	475.0
Mercury	Chloroform	20.0	357
Water	Olive oil	20.0	20.0
Water	Air	20.0	72.75
Water		100	58.8
Gold		1130	1102
Gold	Vapor of the substance	1070	612
Silver		1060	750

Table 1.3. Contact angle for some "liquid-solid" pairs in air

Solid	Liquid	Contact angle [deg]	Solid	Liquid	Contact angle [deg]
Glass	Water	0	Steel	Hydrogen	0
Glass	Mercury	128–148	Steel	Nitrogen	0
Glass	Hydrogen	0	Steel	Oxygen	0
Glass	Nitrogen	0	Paraffin	Hydrogen	106
Glass	Oxygen	0	Aluminium	Nitrogen	7
Steel	Water	70–90	Platinum	Oxygen	1.5

quantitative, conclusions can be drawn on the basis of only approximate information on capillarity parameters.

It should be also noted that most of the known methods for determining surface tension and boundary angle are based on low-order approximation formulas for:

(1) the height to which a liquid rises in a capillary or solid fiber [1, 36, 120];
(2) the shapes of drops or bubbles; and
(3) the velocity of propagation of capillary waves.

It is possible that the application of more accurate numerical results, including those given in this book, and precise measuring instruments may lead to more reliable values of these basic parameters of capillary forces. (Examples are already available; see [151].) A detailed list of works concerning the measurement of σ by static methods is contained in [96] (see also [19, 111, 128]).

Before concluding this section, let us estimate the values of accelerations created in a liquid by surface forces. The magnitude F of these forces can be roughly estimated by the relation

$$F \approx \sigma L,$$

where L is the characteristic length. If the mass of the liquid is estimated as $m \approx \rho L^3$ (ρ is the density), the characteristic acceleration $a \approx F/m$ for the liquid particles and the relative acceleration (load factor) $n = a/g_0$ will be equal to

$$a \approx \sigma/(\rho L^2), \quad n \approx \sigma/(\rho g_0 L^2).$$

By way of example, let us take liquid water at 20° C. In this case, $\rho = 1$ g/cm^2 and $\sigma = 72.75$ dyne/cm. Assuming that the volume of the water is 1 m^3 and $L = 100$ cm, we obtain $n \approx 7.4 \times 10^{-6}$. Comparing this value with the load factors presented in Table 1.1, we find that surface forces and aerodynamic deceleration are most pronounced in the orbit with altitude 240 km. With increasing distance from the Earth, the aerodynamic deceleration falls off rapidly, and so does the role of geomagnetism and the external gravitational field. The effect of surface forces becomes dominant at altitudes of 500–600 km and higher.

It should be noted, however, that as the volume of the liquid increases, so do the self-gravitational accelerations, while those, caused by surface tension decrease. Self-gravitation also increases with increasing mass of the spaceship. Hence, self-gravitational forces must be taken into account when considering comparatively large masses of the liquid (apparatus). For example, let us find the radius R of a free liquid sphere for which these forces become comparable with the surface forces. For this purpose, we equate the accelerations $a_G = a_\sigma$, created in a liquid by the corresponding forces:

$$Gm_1/R^2 = \sigma/(\rho 4R^2) \quad \text{or} \quad (4/3)\pi\rho GR = \sigma/(4\rho R^2).$$

Here, ρ and m_1 are the density and mass of the liquid; $G = 0.6668 \times 10^{-7}$ dyne cm^2/g is the gravitational constant. This leads to the following approximate relation

$$R = \sqrt[3]{\sigma/16G\rho^2}.$$

For $\rho = 1$ g/cm^3 and $\sigma = 72.75$ dyne/cm (water at 20° C), we obtain the value $R \approx 4.5$ m.

In all the problems of fluid mechanics considered in this book, it is assumed that the surface tension forces or self-gravitational forces play an important role (possibly in addition to other forces). We shall always use the term *zero-gravity* when the behavior of a liquid is considered on board a spaceship in free flight; i.e., when the translatory acceleration of the spaceship is due entirely to gravitational forces. We shall also consider the *near-zero-gravity (or low-gravity) conditions* in the case of small deviations from free-flight regime. Such deviations occur, for example, in flights with low propulsive thrusts. The inertial forces generated in this case are equivalent to a weak gravitational field.

1.3 On the History of the Problem

Apparently, the Belgian physicist J. Plateau was the first scientist to clearly formulate the problem of the influence of zero-gravity on the shape of a liquid mass. One of his earlier works, published in 1849, bears a quite modern title: "Sur les figures d'equilibre d'une masse liquide sans pesanteur" [118]. Plateau created "zero-gravity" by introducing a certain quantity of oil in a mixture of water and alcohol having the same density. It is remarkable that the scientists at "General Dynamics-Astronautics" in the USA repeated these experiments more than a century later while investigating the equilibrium configurations of a liquid and a gas in the model of a tank of liquid hydrogen in the rocket "Saturn" [117]. (Other examples of similar, present-day investigations are also available.) Hence the Plateau method, also called the *method of neutral buoyancy*, remains one of the most effective methods for terrestrial simulation of problems concerning the equilibrium and stability of a liquid under low-gravity.

In another celebrated experiment conducted by *Plateau* [119, 7], a spherical oil drop rotated in a mixture of water and alcohol having the same density. In this case, one could clearly see the formation of a ring separated from the bulk fluid by centrifugal forces, and a subsequent disintegration of this ring into separate parts. Since this could be associated with the formation of planets and their satellites, it served as the experimental verification of Laplace's cosmological hypothesis. This analogy, however, is only superficial. In Laplace's hypothesis, the shape of a rotating body depends only on the ratio of the forces of gravitational interaction between its parts and centrifugal forces, while in Plateau's experiment, surface tension plays a significant role. In this connection, Rayleigh, and (following a suggestion made by Appell) Globa-Mikhailenko, Boussinesq and Charrueau investigated theoretically the shapes of a rotating liquid under zero-gravity conditions in the presence of surface tension.[2] We shall return to this problem in Sects. 2.5 and 3.7.

It has been mentioned that as we go over to zero- or low-gravity, the surface tension of the liquid gains importance. Consequently, the problems that emerge in many cases (to within a change of scale) are the same as those for liquids in capillaries. In view of this, we shall briefly touch upon the development of the mathematical theory of capillary phenomena.

The rising of a liquid in capillaries was first observed by Leonardo da Vinci in 1490. Mariotte described the interaction of spheres floating on the free surface of a liquid, caused by capillary forces. The concept of surface tension, however, was introduced only in 1751 by Segner. A certain amount of empirical material was accumulated up to the 19th century, and in 1805, Young formulated the mathematical theory of capillarity by proceeding from the analogy between the free surface of a liquid having surface tension, and an elastic film. A deeper and more physical approach based on the consideration of the interaction between neighboring particles was adopted by Laplace in 1806. This method was perfected in certain respects by Gauss in 1830, using the principle of possible displacements and the related principle of minimum potential energy.

Over the last century, many authors have solved a number of problems in the mathematical theory of capillary phenomena. This theory was actively investigated by Poisson, Kirchhoff, Maxwell, Rayleigh, Poincaré, Neumann and numerous other famous (and not-so-famous) scientists. We shall not go into the details of their results, but refer the reader to the excellent review by *Minkovsky* [104] and the monograph by *Bakker* [10], where the results of these investigations are described as well as the history of the problem. (The review [17] also contains a historical account of the fundamental investigations of capillary phenomena.) These works describe the basic equations as well as their

---

[2] However, it is now clear that these works do not describe Plateau's experiment. As a matter of fact, the phenomena observed in this experiment are determined by the ratio of surface tension forces to viscous stresses at the interface, while centrifugal forces are not involved. The erroneous application of Plateau's method for investigating the rotation of a drop in zero-gravity is also mentioned in the review [161].

exact and approximate solutions, some of which will be considered in this book. In particular, many of these investigations deal with the calculation of the axisymmetric and cylindrical shapes of the liquid-gas interface in capillaries. Here, the equilibrium equation based on Laplace's law is reduced to an ordinary nonlinear differential equation whose solution posed a serious computational problem at the time. In 1857, the Royal Society earmarked a sum of 50 pounds sterling to meet the costs of computations. The results were published by *Bashforth* and *Adams* [12] in 1883 in tabular form.[3] These tables were later used by many authors (including *Shuleikin* [142] in one of his first reports on the behavior of a liquid upon the loss of gravity). *Kirchhoff* [78] has devoted two chapters to the analytical results of equilibrium shapes of a capillary liquid in his classical "Mechanics".

Dupré was the first to investigate equilibrium stability of a suspended liquid or a liquid lying over a lighter liquid. The theory of these experiments was developed by *Maxwell* [101]. Subsequent research into this kind of instability in the case of a plane interface was carried out, among others, by *Rayleigh* [129] and *Taylor* [150] (also see the monograph by *Chandrasekhar* [20] dealing with hydrodynamic stability). Experimental and theoretical studies of the stability of a liquid in zero-gravity were initiated by Plateau and Rayleigh (a detailed analysis of their results is given in [102]). Remarkable physical intuition allowed Rayleigh to demonstrate, using simple and clear examples, the basic regularities of phenomena (at times quite complicated ones, too) which not only are interesting in themselves, but also shed light on other, still unclear, effects [149].[4]

Oscillations of an ideal and viscous capillary liquid (including the so-called capillary waves) also represents a classical problem of fluid mechanics, and many important results in this direction are described in the monograph by *Lamb* [92]. Such dynamic properties are of special interest. As a matter of fact, the flow of a liquid in a fixed vessel under conditions close to zero-gravity as a rule constitutes part of the more general problem of the motion and stability of the system "body + liquid". The latter can be reduced to a system of equations in generalized coordinates of a rigid body, if we know the values of the natural frequencies of the oscillating liquid and the set of eigenfunctions describing the modes; i.e., the shapes of oscillations of the liquid in an immovable cavity.

Zhukovskii [166] was the first to analyze the motion of a body with cavities filled by an ideal liquid. Subsequently, the most significant results in this field were obtained (without taking the surface tension forces into consideration) by *Moiseev* and *Rumyantsev* [107], *Krein* [87], and *Chernous'ko* [24]. These investigations laid the foundations for all subsequent studies of the problems involving a capillary liquid. Over the last 20 years, *Rumyantsev* [107, 132–135] and his team have also considered the problem of stability of motion of a body with a capillary liquid, while *Moiseev* and *Chernous'ko* [23, 24, 106] have studied the problems of hydrostatics and small oscillations under zero-gravity conditions.

The oddity and diversity of the behavior of a liquid with surface tension arouses and stimulates the fantasy of scientists, spurring them on to discoveries in fields that are sometimes quite remote from fluid mechanics, e.g., nuclear physics (it is sufficient to recall

---

[3] Some of the modern investigations using computers still present results in the form of tables. *Padday* [112] noted that his most comprehensive tables were more than 400 pages long.

[4] We feel that many of the problems discussed in this book are so "Rayleigh-like" in their formulation that they could have been solved by Rayleigh himself, had he had a modern computer at his disposal.

the liquid-drop model of the atomic nucleus), solid-state physics, etc. A fascinating account of all this is given by *Geguzin* [59] in his book "The Drop". Even the innocent soap bubble was not ignored; the famous mathematician Courant loved to illustrate his lectures on Plateau's problem by demonstrating the evolution of the shapes of soap films on wire frames (see [33]; one of the authors witnessed such a demonstration).

Another direction in the theory of low-gravity phenomena taking self-gravitational forces into account, pertains to the classical mathematical investigations of the shapes of planets, started by Newton. Until very recently, the simultaneous action of capillary and self-gravitational forces was not considered since these factors were ascribed to phenomena of quite different scales.

1.4 Subject Matter of the Book

This book is devoted to the classical problems of fluid mechanics under zero- or low-gravity conditions, including, first of all, problems of hydrostatics. Investigations of the equilibrium shapes of the free surface of a liquid, initiated in the middle of the last century, are developed in Chap. 2. To begin with, the equations and boundary conditions of the equilibrium problem are introduced on the basis of the stationary principle of the potential energy $\mathcal{U}$. After this, the main emphasis is laid on numerical and approximation methods for solving the nonlinear problem thus obtained. The axisymmetric equilibrium surfaces in gravitational and centrifugal force fields are considered in detail. An algorithm is proposed for these problems, allowing a graphic determination of the shape of the equilibrium surface formed in a given vessel for known values of the volume and wetting angle of the liquid. The required universal nomograms are also constructed for this case. The plane equilibrium problem (related to the axisymmetric problem in respect of dimensions) is also considered in detail. Finally, various methods (boundary–layer method, method of perturbations and method of small variations) for solving the spatial problem are described.

It is natural to ask which of the obtained equilibrium surfaces are stable, i.e., can be realized in practice for systems that can be described adequately by the mathematical model under consideration. This problem is considered in Chap. 3. While extensive literature is available on the equilibrium problems discussed in Chap. 2, few works have been devoted to the stability of equilibrium surfaces.

In view of the expansion

$$\mathcal{U} - \mathcal{U}_0 = \delta\mathcal{U} + \tfrac{1}{2}\delta^2\mathcal{U} + \cdots$$

and the equality $\delta\mathcal{U} = 0$, a generalization of the Lagrange theorem on the correspondence of the stable equilibrium to the minimum of the potential energy $\mathcal{U}$ reduces the problem of stability to the investigation of the sign of $\delta^2\mathcal{U}$. The conditions under which $\delta^2\mathcal{U} > 0$ are determined in Chap. 3.

An algorithm for the numerical solution of the formulated problem is proposed for the axisymmetric and plane cases. Universal nomograms have been constructed to judge the stability or instability of the axisymmetric or cylindrical equilibrium surfaces obtained. For vessels of simple geometric shapes, the boundaries of the stability region are determined in the space of physical parameters. Smooth vessels as well as vessels with fractured surfaces are considered.

Most of the results have been obtained with the help of a computer, and some of them are of principle. It is shown, in particular, that all annular equilibrium shapes of a rotating liquid are unstable. This contradicts *Charrueau*'s [21] statement about the existence of stable annular shapes, which was derived by considering axisymmetric perturbations only.

The equilibrium equation contains several physical parameters. An analysis of the dependence of the solutions of this equation on these parameters leads to the problem of bifurcation of the solutions, which is directly connected with the stability problem. As a rule, critical equilibrium states serve as the bifurcation points. Chapter 4 deals with problems of bifurcation of the equilibrium shapes of a liquid. The concept of a stability margin for equilibrium states of a liquid, which is analogous to the well-known concept of the depth of a potential well but has not been investigated in detail so far, is also introduced in this chapter. An analysis of bifurcation of solutions allows us to find the stability margin (depth of the potential energy minimum) for subcritical equilibrium states that are close to critical, and to find the nature of variation of the equilibrium surface of a liquid upon transition to the supercritical region. The latter explains how a liquid loses its stability.

Chapters 5–7 are devoted to the problems of small (linear) oscillations of an ideal and viscous liquid. Consideration of the surface tension forces in the general formulation leads to theoretical and computational difficulties. In this case, the boundary condition on the free surface of a liquid contains differential operators whose order (for a viscous liquid) is equal to or (for an ideal liquid) higher than the order of the differential operator in the equation for the inner part of the region where the flow is investigated. Nevertheless, the problem of small oscillations can be reduced in many cases to the familiar eigenvalue problem for the operator equation in a Hilbert space. This permits us to analyze the spectral structure, observe similarities in various concrete problems, establish their connection with the theory of oscillations of mechanical systems, and propose effective computational methods.

The problem of the oscillations of an ideal capillary liquid in an arbitrary partially filled vessel under the action of the potential field of mass forces is formulated in Chap. 5. The equations and boundary conditions in this case are derived from the Hamilton-Ostrogradskii principle

$$\delta \mathscr{L} \equiv \delta \int_{t_1}^{t_2} (\mathscr{T} - \mathscr{U})\, dt = 0$$

of the stationary action $\mathscr{L}$ ($\mathscr{T}$ is the kinetic energy of the system). After this, the problem of natural oscillations is reduced to the operator equation

$$\mathscr{B} u = \omega^2 \mathscr{A} u$$

($\mathscr{A}$ and $\mathscr{B}$ are the kinetic and potential energy operators). Investigation of this equation proves the completeness of the characteristic shapes of oscillations of the liquid and the properties of the spectrum of frequencies ω. These properties form the basis of the variational methods for approximately computing frequencies and oscillation shapes. The problem of the oscillations of a system of immiscible liquids is also considered. Finally, Chap. 5 deals with the formulation of the problem of an ideal rotating liquid. Using the example of the rotating column, the structure of the spectrum of normal oscillations is determined. This has led to the discovery of a phenomenon which is characteristic of a rotating capillary liquid, viz., the presence of surface and internal waves whose behavior is qualitatively different in the bulk of the liquid and at its free surface. The mathematical theory of this phenomenon is developed in the last section of Chap. 5.

Various methods of calculating the frequencies of oscillations of an ideal capillary liquid in vessels of different shapes are developed in Chap. 6. These include variational and other methods connected with the approximate solution of a system of one-dimensional integral equations that are equivalent to the problem of oscillations of a liquid in an axisymmetric or "plane" vessel under the action of uniform gravitational fields of various intensities. The results of calculations are presented in the form of typical curves, tables and asymptotic formulas.

Chapter 7 is devoted to the oscillations of a viscous liquid; this problem has not been investigated in detail so far. Several classical problems that permit the separation of variables are presented. On the basis of these problems, we can draw general conclusions about the structure of the spectrum and the nature of normal oscillations of a viscous capillary liquid in a vessel. In particular, it is shown that, unlike noncapillary liquids, capillary liquids do not exhibit aperiodic motions with an arbitrarily slow damping. Some problems for low-viscosity liquids are solved by the boundary-layer method. The last section of this chapter deals with the operator formulation of the problem of normal oscillations of a viscous capillary rotating liquid that partially fills a vessel of an arbitrary shape. The equations and boundary conditions can be transformed in this case to the eigenvalue problem for a weakly perturbed self-conjugate operator acting in a Hilbert space. General conclusions about spectral structure can then be drawn on the basis of one of the Keldysh theorems.

The theoretical investigation of stationary thermal convection resulting from self-gravitation or thermocapillary effect is carried out in Chaps. 8 and 9, respectively. The importance of this problem arises from the practical absence of the natural convection which is usually caused by an external force field, under zero or low gravity. Nevertheless, it turns out that even under these conditions, self-gravitation or the thermocapillary effect[5] may also lead to convection. This facilitates the mixing of the fluid, levels out the temperature and is therefore favorable from the technical point of view. Self-gravitation, which generates Archimedean forces in a nonuniformly heated liquid, can lead to really significant convection even in vessels having linear dimensions of the order of a few meters. The surface tension gradient caused by nonuniform heating of the liquid may also be responsible for convection in relatively small masses.

Model problems of convection in a self-gravitating liquid due to nonuniform heating are discussed in detail in Chap. 8. The conditions for the emergence of convection and the nature of convective flows are investigated. Finally, Chap. 9 describes certain problems of thermocapillary convection.

---

[5] As far back as 1872, *Marangoni* [138] wrote that if, for some reason, a surface tension difference is created across the free surface of a liquid, the liquid will move to the region of higher surface tension. Such effects are called the *Marangoni effects* and include, in particular, *thermocapillary convection* caused by the temperature dependence of surface tension. The theory of convection due to the nonuniformity of surface tension is being rapidly developed at present.

It should be noted that the description of the mathematical apparatus has been given much attention in the last three chapters, while the number of completely solved problems is comparatively small. This is due to the complexity of the problems considered in these chapters.

Of course, many problems in the previous chapters are also complicated. In spite of the optimism of the 135-year-old epigraph, the mathematical theory of capillary phenomena on the whole still appears to be far from perfect. In particular, large-amplitude motions of a capillary liquid, which are most interesting from a practical point of view, are still a hard nut to crack even for modern computers, not to mention the theoretical difficulties involved.[6]

Among the problems directly linked to the material covered in this book but not considered here is the Plateau's problem of constructing the surface Γ with the minimum area, stretched over a given contour γ. This is the shape assumed by a film under zero-gravity when subjected to the surface tension forces. Plateau's problem inspired many publications (see, for example, [32, 108]) and provided an impetus for the creation of parametric problems in variational calculus. Investigations of Plateau's problem still continue, but are devoted more to theorems on solvability and solution properties than to the effective construction of a solution.

Over the last few years, the general problems of capillary hydrostatics have also been actively investigated on the level of "pure" mathematics. Many theorems have been proved on the existence, uniqueness, and regularity of the solution of respective boundary–value problems, and on the influence of the initial data on this solution. Rigorous estimates have been made and theorems connected with the substantiation of variational methods have been proved. These problems have been analyzed by *Concus*, *Finn*, *Gerhardt*, *Giusti*, *Ural'tseva*, and many other scientists. We shall not describe the results of these investigations since they are not directly related to the subject matter of this book. Instead, we draw the reader's attention to some of the papers dealing with these problems: [4, 5, 22, 27–30, 34, 39–52, 60–70, 74, 75, 83–86, 97–99, 113, 115, 136, 143–145, 147, 148, 154, 156–159, 162–164]. The theorems on solvability and representation of the solutions of some (as a rule, time-independent) problems of capillary hydrodynamics were proved at the same level; besides *Pukhnachev*'s works mentioned above (see footnote 6), we would like to indicate papers [6, 14, 15, 73, 81, 91, 109, 130, 140, 141, 146, and 153]. Some still unsolved mathematical problems arising during the investigation of low-gravity fluid mechanics are listed in our paper [9]. The specific area of fluid mechanics dealing with the nonlinear theory of capillary waves has also been left out of this book (see, for example, [105]).

The problems of the mechanics of a flexible non-expandable film containing a liquid are akin to those considered in this book. In the stretched state, the film acts like the surface tension forces, but the force of tension is not given and is determined in the course of solution of the problem from the condition of nonexpandability of the film (see the works of *Chernous'ko* et al. [25, 88–90, 116]).

Our book does not cover many problems which are definitely of practical interest to those dealing with low-gravity fluid mechanics. These problems include the motion of drops and bubbles, expulsion of liquids from vessels, flow of a capillary liquid in a channel,

---

[6] One of the first attempts to overcome these difficulties was made by *Pukhnachev* [122–127].

as well as capillary phenomena in the presence of electric and magnetic fields. Some of these problems are discussed in the monograph by *Povitskii* and *Lyubin* [121].[7]

Capillary phenomena are known to be extremely sensitive to all types of impurities. The authors hope that a certain "sterility" in the presentation of the material will do credit to the book.

---

[7] Some of the works which are undoubtedly of practical interest but have not been included in this book are mentioned here. Nonlinear problems of determination of the shape of an axisymmetric surface upon emptying or filling of a cylindrical or spherical vessel are solved numerically in [3, 38]. Questions related to the draining of a liquid from a cylindrical vessel performing transverse oscillations are considered in [139, 165]. The splashing of a liquid in a cylinder in weak force fields is discussed in [31, 37, 82]. Paper [103] describes the behavior of the free surface of a liquid in a cylindrical vessel upon a sudden transition to zero-gravity conditions and subsequent vertical shock. One of the methods of taking surface tension forces into account when calculating unsteady flows of a liquid is discussed in [35]. The results of the approximate solution of the problem on the deformation of a floating rising bubble in an ideal liquid are given in [18, 76]. A detailed review of the investigations concerning the motion of bubbles is given in [160].

A new area that deserves attention is associated with the analysis of the dynamic behavior of liquid media with solid and gaseous inclusions under the action of controlled periodic disturbances [54–58]. In this case, vibrational effects of a resonant nature have been observed experimentally. In many respects, these effects are similar to those observed under zero-gravity conditions.

Part I

Statics

2. Equilibrium Shapes of a Liquid

This chapter is devoted to the equilibrium shapes of the surface of a capillary liquid contained in a vessel which is either in a zero-gravity state or is subjected to a certain mass-force field.

We deal mainly with algorithms for finding such equilibrium shapes for different situations of practical importance, as well as with certain limiting cases. As a rule, the mass forces are assumed to be of gravitational or inertial origin, the latter resulting from a uniformly accelerated translation or from the uniform rotation of a vessel. From a mathematical point of view, the relative equilibrium of rotating mechanical systems is equivalent to the equilibrium in an altered force field. For the sake of clarity, however, we single out the case of rotating systems. Since in Chap. 3, we shall be investigating the stability of the equilibrium surfaces obtained here, we do not delve into the analysis of surfaces which are known beforehand to be unstable.

2.1 Equilibrium Conditions

2.1.1 Basic Assumptions and Notations

Throughout this book, we shall assume that a liquid is incompressible and homogeneous. For the sake of definiteness, we shall say that a liquid and its vapor, or a certain gas, completely fill a vessel, although in the problem we consider, they may fill the entire space or a part of the space bounded by a solid wall and extending to infinity. The surface of the vessel is assumed to be absolutely rigid, i.e., indeformable and (for the time being) smooth. The vessel is assumed to be capable of non-inertial motion. *All further analysis in Part I will be carried out in the coordinate system fixed to the vessel.*

Let us suppose that a liquid with density ρ and a gas whose density can be neglected occupy connected domains Ω and Ω_0 in space.[1] The interface between the liquid and the gas is denoted by Γ, while their contact surfaces with the vessel walls are denoted by Σ and Σ_0, respectively. The corresponding surface tensions are denoted by σ, $\tilde{\sigma}$ and σ_0, respectively. Let γ be the *line of contact* between the liquid, the gas and the vessel wall, and α_0 and α be the dihedral angles which the gas and the liquid, respectively, form along the line γ (Fig. 2.1). Note that the contact surfaces and the line γ may be unconnected.

The liquid, the gas and the material of the walls are assumed to be homogeneous and their physical properties stable in the sense that the quantities ρ, as well as σ, σ_0, and $\tilde{\sigma}$ have quite definite constant values.

We shall assume that all the mass forces acting on the liquid (including the inertial

[1] The case of unconnected domains, Ω and Ω_0, (i.e., domains consisting of two or more parts) will be considered in Sect. 2.1.6.

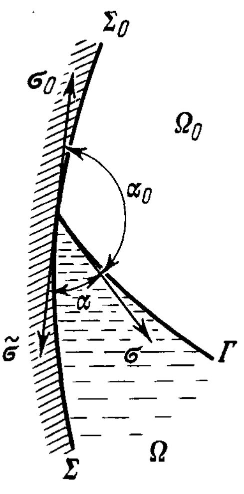

Fig. 2.1

forces of the translational motion of the coordinate system) are independent of time and of the domain Ω occupied by it. The volume density of these forces is denoted by $\rho \boldsymbol{F}(\boldsymbol{x})$. The mass-force field is assumed to have a potential

$$\boldsymbol{F} = -\nabla \Pi. \tag{2.1.1}$$

The necessary condition for the existence of equilibrium states of a liquid is that $\boldsymbol{F}(\boldsymbol{x})$ be a potential field. The time-independence of this field also becomes necessary (with rare exceptions) when the liquid has a free surface.

The total potential energy $\mathcal{U}$ of a liquid in a vessel, associated with surface and mass forces, has a stationary value in the equilibrium state [114]. This permits a formal mathematical derivation of the equilibrium conditions. These conditions will be derived in Sect. 2.1.4; however, let us first consider them in the form in which they are usually encountered in hydrostatics.

2.1.2 Hydrostatic Conditions

In order for a liquid in a vessel to be in equilibrium, the following well-known hydrostatic conditions must be satisfied:

(a) Euler's condition

$$\nabla p = \rho \boldsymbol{F} \qquad (\text{in } \Omega) \tag{2.1.2}$$

(p is the pressure in the liquid). This means that the force field $\boldsymbol{F}(\boldsymbol{x})$ must be a potential one.

(b) Laplace's condition for the pressure drop at the interface between the liquid and the gas:

$$p_0 - p = \sigma(k_1 + k_2), \tag{2.1.3}$$

where $p_0 = \text{const}$ is the pressure in the gas, while k_1 and k_2 are the curvatures of the principal normal sections[2] of the surface Γ (each of these curvatures is considered to be positive if the corresponding normal section is convex toward the domain Ω).

(c) The Dupré-Young condition on the contact line

$$\sigma \cos \alpha = \sigma_0 - \tilde{\sigma} \quad (\text{or } \sigma \cos \alpha_0 = \tilde{\sigma} - \sigma_0), \tag{2.1.4}$$

according to which the contact of a liquid and a gas with a solid can be stable only if

$$|\sigma_0 - \tilde{\sigma}| \leqslant \sigma. \tag{2.1.5}$$

Henceforth, we shall assume that this inequality is satisfied. (The case when this is not true will be considered in Sect. 2.1.6.)

The values α and α_0 of the dihedral angles given by condition (2.1.4) are called the *contact angles* of a liquid and a gas, respectively, with a smooth solid surface. They are also called *boundary angles*. For liquids, the term *wetting angles* is frequently used.

As mentioned above, the coefficients σ, σ_0, and $\tilde{\sigma}$ have constant values in the case of a homogeneous medium. Consequently, the values α and α_0, which are expressed in terms of these coefficients, are also constant. Henceforth, we shall assume that these values are given.

2.1.3 Equilibrium of a Capillary Free Surface

It follows from (2.1.1) and (2.1.2) that $\nabla p = -\rho \nabla \Pi$, i.e.,

$$p = -\rho \Pi + \text{const} \qquad (\text{in } \Omega). \tag{2.1.6}$$

The Laplace condition (2.1.3) then assumes the form

$$\sigma(k_1 + k_2) = \rho \Pi + c, \tag{2.1.7}$$

where c is an arbitrary constant.

Clearly, the system of conditions (2.1.2–4) is equivalent to the system of equations (2.1.6), (2.1.7), and (2.1.4). Note that (2.1.6) does not impose any restrictions on the position of a liquid, determining only the pressure distribution inside it.

Thus, *for a liquid to be in its equilibrium state, it is necessary and sufficient that condition* (2.1.7) *be satisfied on the free surface and* (2.1.4) *be satisfied on the contact line.* These conditions will be used for determining the shapes of equilibrium capillary surfaces. Equation (2.1.7) will serve as the differential equation of the surface, while the corresponding boundary condition will be given by (2.1.4). The specific form of these relations will depend on the form in which the required surface is represented (see Sect. 2.2).

When solving specific problems, the above conditions are usually supplemented by

---

[2] Let us recall their definition. Let A be a point on a certain surface Γ. We shall orient Γ in a certain neighborhood of A; i.e., we shall consider one side of Γ to be internal and the other external. Next, we choose a system of Cartesian coordinates $\tilde{x}$, $\tilde{y}$, $\tilde{z}$, having its origin at A such that the $\tilde{z}$-axis lies along the outward normal to Γ. Then each section of Γ formed by a plane passing through the $\tilde{z}$-axis (normal section) will have a certain curvature $k \gtreqless 0$ at point A (for this section, the curvature is equal to $\tilde{z}''|_A$). The curvature generally depends on the choice of the section. It can be shown that if $k \not\equiv \text{const}$, it assumes the minimum and maximum values k_1 and k_2, respectively, for two mutually perpendicular sections which are called the principal sections. Generally speaking, the values k_1 and k_2 depend on the choice of point A on Γ. If Γ is the free surface of a liquid, the $\tilde{z}$-axis is directed from the liquid to the gas.

some additional geometrical conditions; for example, the volume of the domain Ω may be assumed as given.

2.1.4 Derivation of Equilibrium Conditions from the Variational Principle of Stationary Potential Energy

Let us consider the expressions for the potential energy $\mathscr{U}$ of a system and its first variation $\delta\mathscr{U}$ which we shall require later. At the same time, we shall derive equilibrium conditions (2.1.7) and (2.1.4) from the principle of stationary potential energy.

The potential energy for the mechanical system "liquid + vessel wall" under consideration has the following form:[3]

$$\mathscr{U} = \sigma|\Gamma| + \tilde{\sigma}|\Sigma| + \sigma_0|\Sigma_0| + \rho \int_\Omega \Pi \, d\Omega, \tag{2.1.8}$$

where $|\cdot|$ denotes the area of the corresponding surface.

According to the above principle, this system will be in equilibrium if and only if

$$\delta\mathscr{U} = 0 \tag{2.1.9}$$

for all allowed variations of the surface, Γ. In the present case, the only allowed variations of Γ are those which leave the volume of the liquid unchanged (the liquid is incompressible by definition):

$$\delta \int_\Omega d\Omega = 0. \tag{2.1.10}$$

However, these variations may displace the contact line γ along the vessel wall.

If each point on the surface Γ with a radius vector $\boldsymbol{x}$ is displaced by a small vector $\delta\boldsymbol{x}$, we obtain from the Gaussian formula (see [230])

$$\delta|\Gamma| = -\int_\Gamma (k_1 + k_2)\boldsymbol{n}\cdot\delta\boldsymbol{x}\, d\Gamma + \int_\gamma \boldsymbol{e}\cdot\delta\boldsymbol{x}\, d\gamma, \tag{2.1.11}$$

where $\boldsymbol{n}$ and $\boldsymbol{e}$ are unit vectors normal to Γ (outward to Ω) and to γ in the plane tangential to Γ (outward to Γ), respectively. Further, it is obvious from Fig. 2.2 that

$$\delta|\Sigma| = -\delta|\Sigma_0| = \int_\gamma \boldsymbol{e}_1\cdot\delta\boldsymbol{x}\, d\gamma,$$

where $\boldsymbol{e}_1$ is a unit vector normal to γ in a plane tangential to Σ (outward to Σ). Finally, we have

$$\delta \int_\Omega \Pi\, d\Omega = \int_\Gamma \Pi\boldsymbol{n}\cdot\delta\boldsymbol{x}\, d\Gamma.$$

It would be more convenient to change the form of the last integral in (2.1.11). For this purpose, we draw the inward unit vector normal $\boldsymbol{n}_1$ to Σ (Fig. 2.2) and note that there is no flow through the wall. This gives

$$\delta\boldsymbol{x}\cdot\boldsymbol{n}_1 = 0 \qquad (\text{on } \gamma). \tag{2.1.12}$$

[3] As regards the stability of the equilibrium state of rotating systems, the potential energy functional may have a form differing from (2.1.8); see [114, 149–152] and Sect. 3.1.

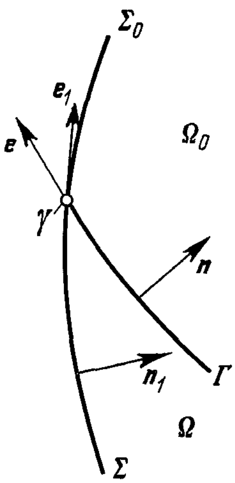

Fig. 2.2

Since the vectors e, e_1, n, and n_1 are coplanar on γ, we get

$$e \cdot \delta x = (n \cdot n_1) e_1 \cdot \delta x \qquad (\text{on } \gamma).$$

Combining the variations of parts of $\mathscr{U}$, we obtain

$$\delta \mathscr{U} = \int_\Gamma [-\sigma(k_1 + k_2) + \rho \Pi] n \cdot \delta x \, d\Gamma + \int_\gamma [\sigma(n \cdot n_1) + (\tilde{\sigma} - \sigma_0)] e_1 \cdot \delta x \, d\gamma. \tag{2.1.13}$$

Condition (2.1.10) can be written in the following form:

$$\int_\Gamma n \cdot \delta x \, d\Gamma = 0. \tag{2.1.14}$$

According to the Lagrangian multipliers method, which is applicable to (2.1.14), there exists a constant c such that for all δx satisfying condition (2.1.12) only, we obtain $\delta \mathscr{U} + c \int_\Gamma n \cdot \delta x \, d\Gamma = 0$; i.e.,

$$\int_\Gamma [-\sigma(k_1 + k_2) + \rho \Pi + c] n \cdot \delta x \, d\Gamma + \int_\gamma [\sigma(n \cdot n_1) + (\tilde{\sigma} - \sigma_0)] e_1 \cdot \delta x \, d\gamma = 0.$$

Obviously, this leads to condition (2.1.7) and the equality

$$\sigma(n \cdot n_1) + (\tilde{\sigma} - \sigma_0) = 0 \qquad (\text{on } \gamma),$$

which is identical to (2.1.4), since $n \cdot n_1$ is the cosine of the contact angle, α, formed by the liquid. Assuming that the value of $\cos \alpha = (\sigma_0 - \tilde{\sigma})/\sigma$ is given, this equality can be written in the form

$$n \cdot n_1 = \cos \alpha \qquad (\text{on } \gamma). \tag{2.1.15}$$

In conclusion, it can be mentioned that several authors have recently derived the equilibrium conditions by using the variational principle; see, in particular, [20, 95, 114, 131, 149, 190].

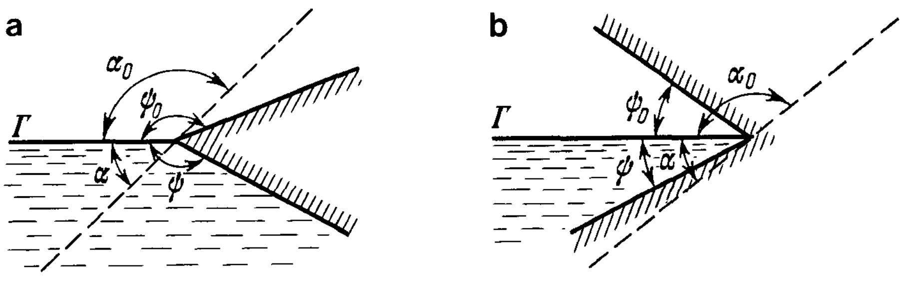

Fig. 2.3

2.1.5 Vessel with a Nonsmooth Surface

Earlier, it was assumed that the surface of a vessel is smooth; otherwise, the equilibrium problem would have singularities. Suppose that the contact line, γ, completely or partially passes along an edge of the vessel surface. In this case, (2.1.7) retains its form while the boundary condition changes. Mentally replacing the edge with the curvature of an infinitely small radius, we require that condition (2.1.4) be satisfied at some point on the curvature. It can be easily verified that this is equivalent to the following condition: at every point on the edge, the dihedral angles ψ and ψ_0 formed by the liquid and the gas must be simultaneously not smaller (Fig. 2.3a) than or not larger (Fig. 2.3b) than the corresponding contact angles α and α_0 formed with a rigid smooth wall in accordance with condition (2.1.4).

Let us now suppose that the contact line between the free surface of the liquid and the vessel wall intersects the edge of the vessel at a certain point A in such a way that a part of the edge is completely wetted. For the smooth equilibrium surface of a liquid, this is possible only if the following condition is satisfied:

$$\cos 2\alpha + \cos \mu \leqslant 0; \quad \text{i.e.,}\ |\pi - \mu| + |\pi - 2\alpha| \leqslant \pi, \tag{2.1.16}$$

where μ is the internal dihedral angle formed by the vessel surface at A.

In order to prove this statement, we express the plane angle φ formed by the liquid surface at A in terms of μ and α. We denote the inward unit vectors normal to the vessel faces and the unit vector normal to the liquid surface at point A by $\boldsymbol{n}_1$, $\boldsymbol{n}_2$, and $\boldsymbol{n}$, respectively (the vector $\boldsymbol{n}$ is directed from the liquid to the gas). Then

$$\boldsymbol{n}\cdot\boldsymbol{n}_1 = \boldsymbol{n}\cdot\boldsymbol{n}_2 = \cos\alpha, \quad \boldsymbol{n}_1\cdot\boldsymbol{n}_2 = -\cos\mu,$$

and φ is the angle between the vectors $\boldsymbol{n}_1 \times \boldsymbol{n}$ and $\boldsymbol{n} \times \boldsymbol{n}_2$. Hence, from the formula

$$(\boldsymbol{a} \times \boldsymbol{b})\cdot(\boldsymbol{c} \times \boldsymbol{d}) = (\boldsymbol{a}\cdot\boldsymbol{c})(\boldsymbol{b}\cdot\boldsymbol{d}) - (\boldsymbol{b}\cdot\boldsymbol{c})(\boldsymbol{a}\cdot\boldsymbol{d})$$

we obtain

$$\cos\varphi = (\cos^2\alpha + \cos\mu)/\sin^2\alpha. \tag{2.1.17}$$

Considering that the result must not exceed unity, we arrive at condition (2.1.16).

If the faces of the vessel are made of different materials so that the contact angles α_1 and α_2 are different, the right-hand side of (2.1.17) becomes $(\cos\alpha_1 \cos\alpha_2 + \cos\mu)/(\sin\alpha_1 \sin\alpha_2)$. Consequently, condition (2.1.16) will assume the form $\cos(\alpha_1 + \alpha_2) + \cos\mu \leqslant 0$. It is, however, not clear what would happen if inequality (2.1.16) becomes an equality.

Condition (2.1.16) can also be written in the form

$$\alpha_- \leqslant \alpha \leqslant \alpha_+,$$

where

$$\alpha_- = \tfrac{1}{2}|\pi - \mu|, \quad \alpha_+ = \pi - \tfrac{1}{2}|\pi - \mu|.$$

If this condition is violated all along the edge, the equilibrium surface at point A for $\mu > \pi$ will have an infinite curvature. If $\mu < \pi$, the equilibrium surface will not reach the edge anywhere, i.e., point A does not exist. If $\mu < \pi$, then for $\alpha < \alpha_-$, the entire edge will be completely wetted; i.e., the edge seems to "suck in" the liquid, while for $\alpha > \alpha_+$, the edge is not wetted at all, i.e., the edge expels the liquid. For example, in the case of a vessel in the form of a right-angled prism, all the edges will be wetted for $0 \leqslant \alpha < \pi/4$, while for $3\pi/4 < \alpha < \pi$, none of the edges will be wetted.

An interesting situation may arise upon slow variation of the system parameters (for example, a change in the liquid volume) if condition (2.1.16) is violated only along part of the edge. For the sake of definiteness, let us assume that $\mu < \pi - 2\alpha$ on this part of the edge. In this case, if the addition of the liquid brings it to the "danger" region, the contact point jumps over this region in an infinitely short time. This leads to the formation of an infinitely narrow tongue of liquid which then draws finite masses of the liquid. The subsequent decrease in the volume may lead to a peculiar type of hysteresis: the free surface may not coincide with the surface of the "added" liquid corresponding to the same volume (a part of the liquid remains near the "danger" region and may "tear away" from the main part).

All the arguments presented above in connection with condition (2.1.16) are independent of the external force field.

2.1.6 Other Generalizations

A) So far, we have assumed that the surface tensions satisfy condition (2.1.5). Let us now suppose that this condition is not satisfied and $\sigma_0 - \tilde{\sigma} > \sigma$. In this case, the surface of the vessel "sucks" in a liquid film of microscopic thickness. During macroscopic calculations, the volume of this film can be neglected; its presence, however, means that the gas is in touch with the liquid only. Hence, the condition of mechanical equilibrium on the line of contact between the film and the main part of the liquid simply leads to $\cos\alpha = 1$; i.e., the contact angle for the liquid is equal to zero. The case of complete wetting considered above is realized, for example, for cryogenic fluids in contact with glass. Apparently, the case $\tilde{\sigma} > \sigma_0 + \sigma$ cannot be realized from a physical point of view.

B) Suppose that the domain Ω is unconnected; i.e., it consists of two or more mutually isolated parts, while Ω_0 is connected as before. In this case, conditions (2.1.7) and (2.1.4) must be satisfied on each of these parts (components of the domain Ω), the constant c depending on the number of components.

Obviously, every possible k-component form of equilibrium generates a $(k-1)$-parametric set of such forms, since any small mass redistribution is possible. The case in which Ω_0 is unconnected can be analyzed in a similar manner.

C) Suppose that a vessel is filled with $k \geqslant 2$ immiscible fluids (one of them may be a gas). We denote the domains occupied by these fluids by $\Omega_1, \ldots, \Omega_k$, the corresponding densities by ρ_i, the surface tensions at the boundaries between domains Ω_i and Ω_j by σ_{ij}, and the surface tensions between domains Ω_i and the wall by σ_i. (If the domain occupied by some fluid is unconnected, each connectivity component must be numbered separately, i.e., we assume that there are different fluids with the same physical properties.) The following condition must then be satisfied on the contact surface Γ_{ij} between domains Ω_i and Ω_j in the equilibrium state:

$$-\sigma_{ij}(k_1 + k_2) + (\rho_i - \rho_j)\Pi + c_{ij} = 0,$$

where curvatures k_1 and k_2 are assumed to be positive if the corresponding normal sections are convex toward Ω_i. On each of lines γ_{ij} along which domains Ω_i and Ω_j come in contact with the wall, corresponding dihedral angles α_{ij} and α_{ji} must assume constant values determined by a condition similar to (2.1.4):

$$\sigma_{ij}\cos\alpha_{ij} = \sigma_j - \sigma_i, \quad \sigma_{ij}\cos\alpha_{ji} = \sigma_i - \sigma_j.$$

There may also be lines along which *three* liquids are in mutual contact. Suppose, for example, that these liquids occupy domains Ω_1, Ω_2, and Ω_3 shown in Fig. 2.4. In this case, dihedral angles α_1, α_2, and α_3 corresponding to these domains are such that the vector sum $\boldsymbol{\sigma}_{12} + \boldsymbol{\sigma}_{23} + \boldsymbol{\sigma}_{13}$ is equal to zero (Fig. 2.4). Hence

$$\alpha_1 = \arccos[(\sigma_{23}^2 - \sigma_{12}^2 - \sigma_{13}^2)/(2\sigma_{12}\sigma_{13})].$$

(It is assumed that each of the coefficients σ_{ij} does not exceed the sum of the remaining two.) For other angles, the formulas are obtained by cyclic permutation of the indices.

Problems involving the contact lines between three fluids have been investigated comparatively recently [33, 71, 185, 216].

D) If the material of the vessel is inhomogeneous (for example, if different parts of the vessel are made of different materials), the surface tension and the contact angle are generally not constant and change along the vessel surface according to a given law.

In this connection, it should be noted that while determining the contact angle, the values of α obtained experimentally are generally spread over a wide range. As a matter of fact, the contact angle depends on whether the liquid flows onto the surface or away

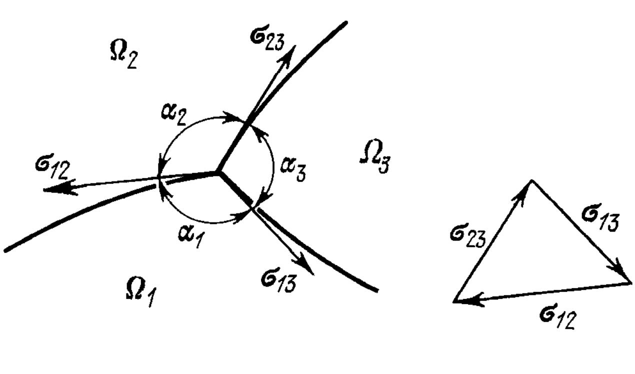

Fig. 2.4

Table 2.1. "Flow-in" and "flow-back" contact angles for some systems

System	Contact angle	
	Flow-in [deg]	Flow-back [deg]
Distilled water on azobenzol	90	62
0.05% Soap solution on paraffin	48	27

from it. The "flow-in" angle is a always larger than the "flow-back" angle (see Table 2.1). The difference between these two angles is called *the wetting hysteresis*. The reason behind this hysteresis is not yet clear. Some authors attribute it to a constant frictional resistance to the flow of the contact perimeter over a rigid surface, i.e., to a sort of dry friction. However, it is hard to fancy a constant frictional resistance. Another explanation is that the adhesive forces between a solid and a liquid have different values for dry and wet surfaces, even over short intervals of time [124].

Experimental data indicate that the cleaner the surface of a solid, the lower the wetting hysteresis. A large value of the "flow-in" angle is possible due to the presence of a film which hinders strong adhesion of the liquid to the solid surface. After coming in contact with the liquid, this film is partially removed; hence, the contact between the liquid and the solid surface becomes closer, the adhesive forces are intensified and the contact angle is smaller during the "flow back".

The roughness of a solid surface has a considerable effect on the contact angle. The formula connecting the roughness with the contact angle was proposed in the following form by *Wenzel* [223], although without a proper derivation:

$$\cos\alpha = k\cos\alpha_1, \tag{2.1.18}$$

where α is the macroscopic contact angle obtained by usual observations and measurements, leaving the microscopic pattern of the surface imperceptible; α_1 is the microscopic contact angle appearing during detailed analysis, revealing the microscopic pattern of the surface [$\cos\alpha_1 = (\sigma_0 - \tilde{\sigma})/\sigma$]; and k is the roughness constant equal to the ratio of the real to apparent surface area. *Deryagin* [55] derived formula (2.1.18) and indicated the conditions and limits of its applicability.

All this is supported by modern concepts of wetting hysteresis on a clean surface. They maintain that the wetting line is held back on microscopic inhomogeneities of the vessel surface (see, for example, [15, 116]). Without going into details, we refer the reader to some works [59, 81, 123, 138, 142′, 148, 218, 219, 227, 228] dealing with the problem of the contact angle for a movable contact line.

It would be interesting to develop general mathematical principles similar to the principle of stationary potential energy leading to an interval of contact angles, and to apply these principles to investigate specific problems. The simplest problem in which the above-mentioned effects play a decisive role is the analysis of a liquid drop hanging on a vertical wall.

E) It was assumed for the sake of simplicity that the mass-force potential $\Pi(\boldsymbol{x})$ does not depend on the domain Ω occupied by a liquid. However, the points discussed in this section remain valid even when the potential of the forces depends on the shape of the fluid mass. The potential of self-gravitational forces caused by the gravitational interaction of liquid particles is an example of such a potential:

$$\Pi_\Omega(x) = -G_\rho \int_\Omega \frac{1}{\sqrt{(x-y)^2}} d\Omega_y.$$

Here, G is the gravitational constant, and integration is carried out over the coordinates of point y, running through the entire domain Ω.

F) Certain liquid media (for example, ferromagnetic suspensions) have a pronounced tendency toward magnetization. An investigation of the behavior of such interesting liquids under zero gravity, taking magnetic fields into account, is beyond the scope of this book. *Borisov* [22] has given a general formulation of the problem on equilibrium shapes of interfaces of magnetized liquids, taking magnetic fields, capillary and mass forces into account. He has also derived the equilibrium conditions from the variational principle of stationary potential energy. Generally, the problem of finding the equilibrium shape of a liquid being magnetized is inseparable from the problem of finding the corresponding magnetic field. In some cases, however, these problems can be separated. Such problems are also considered by *Borisov* [22] for linear magnetization and saturation induction. The analogous problem for liquid dielectrics in an electric field has been analyzed in [77].

2.2 The Equilibrium Surface Problem

We return to conditions (2.1.7) and (2.1.15) and rewrite them in the form of a differential equation and its boundary condition.

2.2.1 Arbitrary Parametric Representation of a Surface

In order to concretely formulate the problem of determining the equilibrium surface Γ, we must precisely specify the type of surface we wish to determine. For this purpose, we can use, say, some known surface Γ' which can be mapped in a mutually continuous one-to-one manner onto Γ with the help of a certain function ·(,x)$x = x$. We shall confine ourselves to the relatively simple case in which we choose Γ' in the form of a certain *known* domain in a plane with Cartesian coordinates ξ, η, bounded by a smooth or piecewise smooth curve γ'. The above equation then assumes the form

$$x = x(\xi, \eta) \tag{2.2.1}$$

The function $x(\xi, \eta)$ maps the curve γ' onto the contact line γ.[4]

We introduce the coefficients of the first and second quadratic forms on Γ (see, for example, [246], pp. 108, 125):

---

[4] A more general type of surface can be obtained by assuming that the one-to-one nature of the mapping on γ' is violated. For example, if Γ' is the unit circle $\xi^2 + \eta^2 \leqslant 1$, we obtain a spherical surface by imposing the condition $x(\xi, \eta) = x_0$ for $\xi^2 + \eta^2 = 1$. Taking the ring $\rho_1^2 \leqslant \xi^2 + \eta^2 \leqslant \rho_2^2$ for Γ' and applying the condition $x(\rho_1 \cos\theta, \rho_1 \sin\theta) = x(\rho_2 \cos\theta, \rho_2 \sin\theta)$ for $0 \leqslant \theta \leqslant 2\pi$, we obtain a toroidal surface.

$$E = \boldsymbol{x}_\xi^2, \quad F = \boldsymbol{x}_\xi \cdot \boldsymbol{x}_\eta, \quad G = \boldsymbol{x}_\eta^2;$$

$$L = \boldsymbol{n} \cdot \boldsymbol{x}_{\xi\xi}, \quad M = \boldsymbol{n} \cdot \boldsymbol{x}_{\xi\eta}, \quad N = \boldsymbol{n} \cdot \boldsymbol{x}_{\eta\eta}.$$

Here the unit normal vector $\boldsymbol{n}$ is defined by the relation

$$\boldsymbol{n} = \pm \frac{\boldsymbol{x}_\xi \times \boldsymbol{x}_\eta}{\sqrt{EG - F^2}}, \tag{2.2.2}$$

the sign being chosen in such a way that the vector $\boldsymbol{n}$ is directed from Ω to Ω_0 (see Sect. 2.1.4).

The following formula then describes the sum of the principal curvatures (see [246], p. 138):

$$k_1 + k_2 = \frac{EN - 2FM + GL}{EG - F^2}.$$

Substituting the expressions obtained above into (2.1.7) and considering that $\Pi = \Pi(\boldsymbol{x})$ is a given function of $\boldsymbol{x}$, we obtain a second-order nonlinear scalar differential equation in the vector–function (2.2.1):

$$\pm \frac{\boldsymbol{x}_\xi^2 \boldsymbol{x}_{\eta\eta} - 2(\boldsymbol{x}_\xi \cdot \boldsymbol{x}_\eta)\boldsymbol{x}_{\xi\eta} + \boldsymbol{x}_\eta^2 \boldsymbol{x}_{\xi\xi}}{[\boldsymbol{x}_\xi^2 \boldsymbol{x}_\eta^2 - (\boldsymbol{x}_\xi \cdot \boldsymbol{x}_\eta)^2]^{3/2}} \cdot (\boldsymbol{x}_\xi \times \boldsymbol{x}_\eta) = \frac{\rho}{\sigma} \Pi(\boldsymbol{x}) + c, \tag{2.2.3}$$

where the constant c differs from the analogous constant in (2.1.7) by a factor $1/\sigma$.

Let us now consider the boundary conditions for the function $\boldsymbol{x}(\xi, \eta)$. For this purpose, it is convenient to assume that the equation for the surface Σ of the vessel is given in the form

$$\Phi(\boldsymbol{x}) = 0$$

where $\Phi(\boldsymbol{x})$ is a scalar function, $\Phi(\boldsymbol{x}) > 0$ inside the vessel, and $|\nabla\Phi| \neq 0$ on Σ. (When constructing the free surface, it is sufficient to consider instead of the entire surface Σ of the vessel only the part where the contact line γ is expected.)

Since the required equilibrium surface of the liquid must lie inside the vessel, we get

$$\Phi(\boldsymbol{x}(\xi, \eta)) > 0 \quad \text{for } (\xi, \eta) \in \Gamma'. \tag{2.2.4}$$

One of the boundary conditions for $\boldsymbol{x}(\xi, \eta)$ will be

$$\Phi(\boldsymbol{x}(\xi, \eta))|_{\gamma'} = 0. \tag{2.2.5}$$

The second boundary condition is obtained from (2.1.15) by rewriting it in the following form:

$$\pm \frac{\boldsymbol{x}_\xi \times \boldsymbol{x}_\eta}{\sqrt{\boldsymbol{x}_\xi^2 \boldsymbol{x}_\eta^2 - (\boldsymbol{x}_\xi \cdot \boldsymbol{x}_\eta)^2}} \cdot \frac{\nabla\Phi(\boldsymbol{x})}{|\nabla\Phi(\boldsymbol{x})|}\bigg|_{\gamma'} = \cos\alpha. \tag{2.2.6}$$

Thus, the boundary-value problem consisting of differential equation (2.2.3), inequality (2.2.4) and boundary conditions (2.2.5) and (2.2.6) reflects all information available about the equilibrium surface, except the condition that the domain occupied by a liquid have a given volume.

This problem can also be written in a tensor-invariant form. For this purpose, we denote the coordinates on Γ by u^1 and u^2 (instead of ξ and η), and introduce in place of E, F and G the covariant metric tensor with components

$$a_{\alpha\beta} = \frac{\partial \boldsymbol{x}}{\partial u^\alpha} \cdot \frac{\partial \boldsymbol{x}}{\partial u^\beta} \qquad (\alpha, \beta = 1, 2)$$

and the contravariant tensor $a^{\alpha\beta}$ corresponding to it [the matrix $(a^{\alpha\beta})$ is inverse to the matrix $(a_{\alpha\beta})$]. After this, we can write formula (2.2.2) in the form

$$\boldsymbol{n} = \pm \frac{1}{\sqrt{a}} \frac{\partial \boldsymbol{x}}{\partial u^1} \times \frac{\partial \boldsymbol{x}}{\partial u^2} \qquad (a = a_{11}a_{22} - a_{12}^2).$$

It can be verified that the following formulas hold:

$$\Delta \boldsymbol{x} = \boldsymbol{n}(\boldsymbol{n} \cdot \Delta \boldsymbol{x}), \qquad \boldsymbol{n} \cdot \Delta \boldsymbol{x} = k_1 + k_2 \tag{2.2.7}$$

(see [241]). Here $\Delta = \Delta_\Gamma$ is the Laplace-Beltrami differential operator whose invariant expression has the form

$$\Delta_\Gamma \varphi = \frac{1}{\sqrt{a}} \frac{\partial}{\partial u^\alpha} \left(\sqrt{a} a^{\alpha\beta} \frac{\partial \varphi}{\partial u^\beta} \right).$$

which assumes summation over recurring indices.

Using formulas (2.2.7) and the expressions for $\boldsymbol{n}$ and Δ_Γ, we can write (2.1.7) in the following two forms, one of which is vector and the other, scalar:

$$\frac{1}{\sqrt{a}} \frac{\partial}{\partial u^\alpha} \left(\sqrt{a} a^{\alpha\beta} \frac{\partial \boldsymbol{x}}{\partial u^\beta} \right) = \pm \frac{\rho \Pi(\boldsymbol{x}) + c\sigma}{\sigma \sqrt{a}} \frac{\partial \boldsymbol{x}}{\partial u^1} \times \frac{\partial \boldsymbol{x}}{\partial u^2}, \tag{2.2.8}$$

$$\pm \left(\frac{\partial \boldsymbol{x}}{\partial u^1} \times \frac{\partial \boldsymbol{x}}{\partial u^2} \right) \cdot \frac{1}{a} \frac{\partial}{\partial u^\alpha} \left(\sqrt{a} a^{\alpha\beta} \frac{\partial \boldsymbol{x}}{\partial u^\beta} \right) = \frac{\rho}{\sigma} \Pi(\boldsymbol{x}) + c. \tag{2.2.9}$$

It can be easily seen from formulas (2.2.7) that these equations are equivalent. Only one of the three scalar equations corresponding to system (2.2.8) is independent.

To within obvious changes of notation, conditions (2.2.4–6) remain unchanged.

The nonclosure of the equilibrium surface problem (for three unknown scalar functions we have one independent scalar equation, two scalar boundary conditions and one inequality) is due to the arbitrariness in the parametrization of the surface. Thus, we can impose additional restrictions on the function $\boldsymbol{x}(u^1, u^2)$; viz., two additional scalar equations and, perhaps, some additional boundary conditions.

Let us consider the basic case from our point of view when the required surface Γ is simply connected and smooth together with its boundary γ. Here, we can take any simply connected domain with a smooth boundary γ' as the domain Γ' of variation of coordinates u^1 and u^2; this is what we shall actually assume in the future. (For example, we can choose for Γ' a unit circle having its center at the origin.) Furthermore, we can require that the function $\boldsymbol{x} = \boldsymbol{x}(u^1, u^2)$ establish a conformal correspondence between the domain Γ' and the surface Γ. The necessary and sufficient condition for this is the validity of the proportionality condition between the metric tensors $a_{\alpha\beta}$ on Γ and $a'_{\alpha\beta}$ on Γ' ([237], p. 123)

$$a_{\alpha\beta} = \lambda a'_{\alpha\beta},$$

where $\lambda = \lambda(u^1, u^2)$ is a certain bounded function which can be assumed to be positive. In our case, this condition leads to the equalities

$$a_{11} = a_{22} \quad \text{and} \quad a_{12} = 0 \quad (\text{in } \Gamma'). \tag{2.2.10}$$

It follows from these conditions that $\sqrt{a}a^{\alpha\beta} = \delta_{\alpha\beta}$ (Kronecker delta). Reverting to the original notation of coordinates $u^1 = \xi$ and $u^2 = \eta$, we can write (2.2.8) and conditions (2.2.10) in the form

$$\boldsymbol{x}_{\xi\xi} + \boldsymbol{x}_{\eta\eta} = \pm\left[\frac{\rho}{\sigma}\Pi(\boldsymbol{x}) + c\right]\boldsymbol{x}_\xi \times \boldsymbol{x}_\eta, \tag{2.2.11}$$

$$A \equiv \boldsymbol{x}_\eta^2 - \boldsymbol{x}_\xi^2 = 0; \quad B \equiv 2\boldsymbol{x}_\xi \cdot \boldsymbol{x}_\eta = 0 \qquad (\text{in } \Gamma'). \tag{2.2.12}$$

Note that (2.2.11) without conditions (2.2.12) is not equivalent to the original equation (2.2.8). All three scalar equations corresponding to vector equation (2.2.11) are now independent. From the form of the principal part of (2.2.11), it can be concluded that we cannot subject its solutions to additional conditions (in the form of equalities) which are independent of (2.2.11) in the entire domain Γ'. This means that conditions (2.2.12) must be reduced to certain boundary conditions. We shall describe such a transformation of these conditions as presented in the book by *Courant* [233], where equation $\boldsymbol{x}_{\xi\xi} + \boldsymbol{x}_{\eta\eta} = \boldsymbol{0}$ is considered for the minimal surfaces ($k_1 + k_2 = 0$).

Differentiating the expressions for A and B in (2.2.12), we get

$$A_\xi - B_\eta \equiv -2\boldsymbol{x}_\xi \cdot (\boldsymbol{x}_{\xi\xi} + \boldsymbol{x}_{\eta\eta}), \quad A_\eta + B_\xi \equiv 2\boldsymbol{x}_\eta \cdot (\boldsymbol{x}_{\xi\xi} + \boldsymbol{x}_{\eta\eta}).$$

Obviously, if $\boldsymbol{x}(\xi, \eta)$ is a solution of (2.2.11), the right-hand sides of the above equalities are equal to zero. Hence,

$$A_\xi - B_\eta = 0, \quad A_\eta + B_\xi = 0;$$

i.e., $A + iB$ is an analytic function of the complex variable $\xi + i\eta$. This means that $A + iB$ will be identically equal to zero if A is equal to zero on the boundary γ' and B is equal to zero at some point. Hence we can replace (2.2.12) by the conditions

$$\boldsymbol{x}_\xi^2 = \boldsymbol{x}_\eta^2 \quad (\text{on } \gamma'), \quad \boldsymbol{x}_\xi \cdot \boldsymbol{x}_\eta = 0 \quad (\text{at the point } (\xi_0, \eta_0) \in \bar{\Gamma}'). \tag{2.2.13}$$

Here,

$$\bar{\Gamma}' = \Gamma' \cup \gamma'.$$

Thus we can consider problem (2.2.11), (2.2.4–6), (2.2.13) instead of problem (2.2.3–6) for the equilibrium surface of a liquid.

In conclusion, let us briefly consider the most general formulation of the mathematical problem of the equilibrium of a capillary liquid, making no assumptions concerning the connectivity of the domain occupied by the liquid. This formulation is significant from a physical point of view as well. Let $\mathfrak{M}$ be a given closed domain which can be partially occupied by a liquid having a given volume v. For the sake of simplicity, we shall assume that $\mathfrak{M}$ and $\int_{\mathfrak{M}} |\Pi| \, d\mathfrak{M}$ are finite. We denote by $\mathfrak{F}$ the totality of all possible sets $\Omega \subseteq \mathfrak{M}$, $\operatorname{mes} \Omega = v$, which are the closures of the open subsets of $\mathfrak{M}$. Each $\Omega \in \mathfrak{F}$ has its corresponding value of potential energy $\mathscr{U}(\Omega)$ given by formula (2.1.8) where the conventional area should be replaced in the general case by the so-called Hausdorff area. Moreover, the area of the boundary of $\mathfrak{M}$ must be assumed to be finite.

Using the above notation and assumptions, we can formulate the problem of minimizing the functional $\mathscr{U}(\Omega)$ $(\Omega \in \mathfrak{F})$. It can be easily verified that this functional has a lower bound and is semicontinuous from below in the Hausdorff metric. Consequently, it attains its absolute minimum value on a certain set $\tilde{\Omega}$ which is the solution of this problem. It can be expected that if the potential Π is quite smooth, parts of the boundary of $\tilde{\Omega}$ inside $\mathfrak{M}$ will also be quite smooth and then relation (2.1.7) will be valid for them. In order to obtain stationary values of the functional $\mathscr{U}(\Omega)$ in $\mathfrak{F}$, we must go over to a "finer" metric, as in the transition from C to C^1.

From a mathematical point of view, it is quite interesting to analyze in detail some more general problems on the extrema and the stationary values of functionals in the spaces of closed sets.

2.2.2 Equilibrium Surface with an Equation of the Type $z = f(x, y)$

Let us consider the particular case in which the equation of an equilibrium surface Γ in a Cartesian system of coordinates x, y, z can be expressed in the form $z = f(x, y)$. In this case, we can put $\xi = x$ and $\eta = y$. After simple transformations, problem (2.2.3–6) assumes the form

$$\pm \operatorname{div} \frac{\nabla f}{\sqrt{1 + (\nabla f)^2}} = \frac{\rho}{\sigma} \Pi + c \quad (\text{in } \Gamma'), \tag{2.2.14}$$

$$\left.\begin{aligned} &\Phi(x, y, f(x, y)) > 0 \quad (\text{in } \Gamma'), \\ &\Phi(x, y, f(x, y)) = 0 \quad (\text{on } \gamma'), \end{aligned}\right\} \tag{2.2.15}$$

$$\pm \frac{-f_x \Phi_x - f_y \Phi_y + \Phi_z}{\sqrt{1 + (\nabla f)^2} \, |\nabla \Phi|} = \cos \alpha \quad (\text{on } \gamma'). \tag{2.2.16}$$

Here, the upper or lower sign is chosen depending on whether the liquid; i.e., the domain Ω, lies below or above the surface Γ with respect to the z-axis.

Integrating both sides of (2.2.14) over the projection Γ' of the surface Γ onto the plane $z = 0$ and using the Ostrogradskii formula, we obtain the equality

$$\mp \int_{\gamma'} \frac{\partial f / \partial n_1}{\sqrt{1 + (\nabla f)^2}} \, d\gamma' = \left(\frac{\rho}{\sigma} \overline{\Pi|_\Gamma} + c \right) |\Gamma'|, \tag{2.2.17}$$

where n_1 is the direction of the inward normal to γ', and the bar indicates averaging over Γ'.

If the part of the vessel surface containing the contact line γ is cylindrical with its generatrix parallel to the z-axis, we obtain

$$(\nabla\Phi/|\nabla\Phi|)_\gamma = \boldsymbol{n}_1.$$

In this case, boundary condition (2.2.16) assumes the form

$$\mp\frac{\partial f/\partial n_1}{\sqrt{1+(\nabla f)^2}} = \cos\alpha \quad (\text{on } \gamma'). \tag{2.2.18}$$

Consequently, (2.2.17) can be written in the following form:

$$|\gamma'|\cos\alpha = \left(\frac{\rho}{\sigma}\overline{\Pi|_\Gamma} + c\right)|\Gamma'| \tag{2.2.19}$$

($|\gamma'|$ is the length of γ'), and the value of c can be obtained from this equation.

2.2.3 Axisymmetric Equilibrium Problem

The axisymmetric problem of equilibrium is comparatively simple and at the same time important from the point of view of applicability. Frequently (but by no means necessarily), such a problem arises when the vessel surface and the external force field have a common symmetry axis, since in this case the equilibrium surface may also turn out to be axisymmetric with the same axis.[5]

We introduce a cylindrical system of coordinates r, θ, z, and make the z-axis coincide with the axis of symmetry (Fig. 2.5). The axisymmetric equilibrium surface Γ will then be defined by the line L of its intersection with the half-plane θ = const. Henceforth, we shall call this line the *equilibrium line*.[6] Let ξ be any parameter measured along L. In this case, it is natural to take ξ and θ as coordinates on Γ. Calculations of the curvature in accordance with the formulas of Sect. 2.2.1 lead to the result

$$k_1 + k_2 = \pm\frac{1}{rr'}\left(\frac{rz'}{\sqrt{r'^2+z'^2}}\right)', \quad \left(' = \frac{d}{d\xi}\right), \tag{2.2.20}$$

where the upper (lower) sign must be taken if the domain Ω remains to the right (left) as we move along L in the direction of increasing ξ.

---

[5] It would be very important to find various sufficient conditions under which the equilibrium form of a liquid for a vessel and a force field admitting some transformation group (rotations, in case the vessel and the field are axisymmetric, parallel translations in the "problem in a channel" (Sect. 2.2.4), parallel translations and symmetry transformations under the additional requirement of symmetry, etc.) must be invariant to this group. Such an "extension of symmetry" may be obtained from the conditions of statics or from the additional requirement of stability (Ch. 3) and makes the analysis of problems with a given transformation group much more convincing, since it precludes the possibility of a liquid assuming an asymmetric shape in the symmetry conditions under consideration. Of course, the extension of symmetry is possible, in particular, if the equilibrium shape (in any case, the stable equilibrium shape) is unique for the given system parameters. For example, such a situation arises in an upright cylindrical immovable vessel containing a liquid in a uniform gravitational field covering the bottom completely; see *Samsonov* [155] in this connection. In conclusion, it should be noted that there are examples in which stable invariant forms exist together with stable noninvariant forms, as well as examples in which the stable forms are necessarily noninvariant.

[6] The term equilibrium arc may perhaps to more accurate, although the pedantic difference between the terms "arc" and "line" is insignificant in this case.

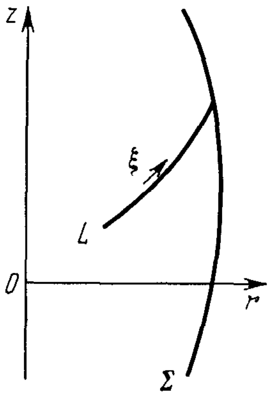

Fig. 2.5

For further discussion, it is convenient to take for the parameter ξ the length of the arc s of the line L, measured from a certain point. The equations of the line should be sought in the form $r = r(s)$, $z = z(s)$. Let $\beta = \beta(s)$ be the angle of inclination of an element of the line L, obtained with increasing s, to the r-axis. Then

$$\begin{aligned} &r' = \cos\beta, \quad z' = \sin\beta, \quad \text{whence} \\ &r'' = -\beta' z', \quad z'' = \beta' r', \quad (' = d/ds), \end{aligned} \tag{2.2.21}$$

while the sum of the principal curvatures, obtained with the help of formula (2.2.20), is equal to

$$k_1 + k_2 = \pm[\beta' + (\sin\beta)/r] = \pm(\beta' + z'/r). \tag{2.2.22}$$

(This result also follows directly from Meusnier's theorem; see, for example [247], p. 233). Using formulas (2.2.21), (2.2.22) and (2.1.7), we obtain the following system of equations for determining the equilibrium line:

$$\left.\begin{aligned} r'' &= -z'\left\{\pm\left[\frac{\rho}{\sigma}\Pi(r,z) + c\right] - \frac{z'}{r}\right\}, \\ z'' &= r'\left\{\pm\left[\frac{\rho}{\sigma}\Pi(r,z) + c\right] - \frac{z'}{r}\right\}, \end{aligned}\right. \quad \left(' = \frac{d}{ds}\right). \tag{2.2.23}$$

(Here the same sign rule is used as in the above paragraph.)

On the basis of the above system equations, it can be formally concluded that for any solution, $r'^2 + z'^2 = \text{const}$. Hence, if the equality

$$r'^2 + z'^2 = 1 \tag{2.2.24}$$

is satisfied for some value of s, it will be satisfied for all values of s. Thus, if this equality is valid and if we consider the possibility of arbitrarily changing the reference point for s, we obtain a two-parameter family of integral lines for system (2.2.23) in the r, z plane for fixed parameters on the right-hand side, as expected.

2.2.4 Plane Equilibrium Problem

Let us now assume that the potential Π is independent of the coordinate y and the vessel containing the liquid is an infinite cylinder of an arbitrary cross section with its generatrix parallel to the y-axis (such vessels will henceforth be called infinite *channels*). Then the equilibrium surface Γ also may (not necessarily!) be cylindrical with its generatrix parallel to the y-axis. Cylindrical equilibrium surfaces are also apparently possible in a channel of finite length bounded by plane walls $y = y_1$ and $y = y_2$, corresponding to a contact angle $\alpha = 90°$.

The cylindrical equilibrium surface is determined by the *equilibrium line L* of intersection of Γ with the plane $y = \text{const}$. Consequently, we can forget about the existence of the coordinate y and consider the *plane equilibrium problem*[7] of determinating the equilibrium line L in the x, z plane.

If ξ is any parameter along L, we obtain

$$k_1 + k_2 = \pm\frac{x'z'' - z'x''}{(x'^2 + z'^2)^{3/2}}, \quad \left(' = \frac{d}{d\xi}\right)$$

with the same sign rule as in Sect. 2.2.3. Arguments similar to those used in the derivation of system (2.2.23) lead to the following system of equations:

$$\begin{aligned} x'' &= \mp z'\left[\frac{\rho}{\sigma}\Pi(x,z) + c\right], \\ z'' &= \pm x'\left[\frac{\rho}{\sigma}\Pi(x,z) + c\right], \end{aligned} \quad \left(' = \frac{d}{ds}\right). \tag{2.2.25}$$

While solving this system, we must take into consideration the relation

$$x'^2 + z'^2 = 1.$$

2.2.5 Equation for a Bundle of Equilibrium Surfaces

Suppose that for a given force field and physical parameters of a system, we have a one-parametric family of mutually nonintersecting equilibrium surfaces Γ_λ occupying a certain known domain $\mathfrak{M}$. These could be, for example, surfaces obtained by gradually adding liquid to a vessel if the surfaces so obtained do not intersect.

Since the quantity c introduced in Sect. 2.1.3 assumes a constant value on each equilibrium surface, we can write the equation for the family in the form

$$\Gamma_\lambda\colon c(\boldsymbol{x}) = \lambda \tag{2.2.26}$$

and consider the problem of finding the field $c(\boldsymbol{x})$ in $\mathfrak{M}$, whose value will also enable us to find the equilibrium surfaces. For this purpose, we use the formula for the sum of principal curvatures of the surface defined by (2.2.26) (see [241]):

$$k_1 + k_2 = \pm\operatorname{div}(\nabla c/|\nabla c|).$$

[7] Not to be confused with the plane equilibrium surface which, as usual, means a part of a plane.

(The sign is determined by the side of the surface containing the liquid.) Hence, in view of (2.1.7), we obtain a differential equation for $c(\boldsymbol{x})$:

$$\pm\sigma\,\mathrm{div}(\nabla c/|\nabla c|) = \rho\Pi(\boldsymbol{x}) + c \quad (\text{in } \mathfrak{M}).$$

The boundary condition for the field $c(\boldsymbol{x})$ is determined from the boundary condition for equilibrium surfaces. For example, if we are adding a liquid to the vessel, it can be easily verified that this condition will have the form

$$\mp(\partial c/\partial n_1)/|\nabla c| = \cos\alpha \quad (\text{on the boundary of } \mathfrak{M}).$$

We shall not investigate the boundary value problem obtained here, particularly since the conditions under which the family of equilibrium surfaces has the property of mutual nonintersection are not quite clear.

2.2.6 On Mass Force Potential and Similitude Numbers

In the equilibrium surface equations described above, the density of the mass force potential $\Pi(\boldsymbol{x})$ is assumed to be a known function. Henceforth, we shall consider as basic the case in which a liquid is acted upon by a homogeneous gravitational field of intensity g,[8] directed along the z-axis, as well as by the centrifugal force field due to the homogeneous rotation of a mechanical system about the same axis with an angular velocity ω. In this case, the mass density of the potential will be

$$\Pi = gz - \omega^2 r^2/2,$$

where $r = \sqrt{x^2 + y^2}$ is the distance from the rotation axis. If $g > 0$, we speak of a positive loading, while for $g < 0$, the loading is said to be negative. The case $g = 0$ corresponds to zero-gravity conditions.

Dividing both sides of (2.2.14) by ± 1 and using the notation $\pm c = q$, we get[9]

$$\mathrm{div}\frac{\nabla z}{\sqrt{1 + (\nabla z)^2}} = bz - pr^2 + q. \tag{2.2.27}$$

The following notation has been used in this case:

$$b = \pm\rho g/\sigma, \quad p = \pm\rho\omega^2/(2\sigma). \tag{2.2.28}$$

This notation will be retained throughout the book, the signs being chosen in the manner indicated in Sect. 2.2.2. The quantities b and p have the dimensions $(\text{length})^{-2}$ and $(\text{length})^{-3}$, respectively.[10]

---

[8] It should be recalled that the inertial forces of the translational motion of advance of a vessel are also reduced to a homogeneous field. It is usually assumed that $g = ng_0$, where $g_0 = 981$ cm/s^2 is the standard value of the acceleration due to gravity and n is a dimensionless loading factor which can be of either sign. Hence we shall be speaking of loading instead of gravity in some cases.

[9] The condition that the equilibrium surface in (2.2.14) can be represented in the form $z = f(x, y)$ is not significant in this section.

[10] Instead of the parameter b, the *capillary constant* a is sometimes used in the literature. This constant is defined by the equality $a^2 = 2\sigma/(\rho|g|)$ and is connected with b by the relation $a = \sqrt{2/|b|}$.

Using the characteristic length l for the system under consideration, we obtain two dimensionless parameters

$$\mathbf{Bo} = bl^2 = \pm\rho g l^2/\sigma \quad (\textit{Bond number}) \quad \text{and} \quad \mathbf{P} = pl^3 = \pm\rho\omega^2 l^3/(2\sigma).$$

The first of these parameters establishes a relation between gravitational and capillary forces, while the second parameter connects the centrifugal and capillary forces. This leads to the following possibility of *modelling*: the geometrically similar transformation of an equilibrium system again leads to an equilibrium system if the values of the parameters **Bo** and **P** are the same for both systems. (Thus, it follows that the boundary angles α must also be the same for both systems if a wetting line exists.) Moreover, it can be verified that the stability of equilibrium surfaces is also conserved as a result of such a transformation. In particular, the above statement (which can be obviously extended to force fields of a general kind) is used for physical models of a weakening force field by reducing the system's size (see, for example, [62, 80]).

2.3 The Construction of Simply Connected Axisymmetric Equilibrium Shapes

Generally, it is quite difficult to construct the equilibrium shapes of a liquid while taking surface tension into account. It is sufficient to remark that the classical Plateau problem of finding the minimal surface extending over a given contour is just a special particular case of this problem. The solution, however, is considerably simplified in the axially symmetric and plane cases where the dimensionality of the problem is reduced. In this section, we consider the axially symmetric problem of determining simply connected equilibrium surfaces.

2.3.1 Family of Equilibrium Lines

Taking formula (2.2.20) for $\xi = r$ into account and using the notation introduced in Sect. 2.2.6, we can rewrite the equilibrium equation (2.1.7) in the following form:

$$\frac{1}{r}\left(\frac{rz'}{\sqrt{1+z'^2}}\right)' = bz - pr^2 + q, \quad \left(' = \frac{d}{dr}\right). \tag{2.3.1}$$

Similarly, (2.2.23) can be reduced to the system

$$\begin{aligned} r'' &= -z'(bz - pr^2 + q - z'/r), \\ z'' &= r'(bz - pr^2 + q - z'/r), \end{aligned} \qquad (' = d/ds). \tag{2.3.2}$$

Let us consider the case of simply connected surfaces Γ. We shall measure the length of the arc s along L from the point lying on the z-axis. The signs of the parameters b (for a given value of g) and p depend on whether the liquid is above or below the surface Γ in the vicinity of the point $s = 0$ (Fig. 2.6). *Unless otherwise stated, we shall always assume that the liquid is below the equilibrium surface Γ (when it is simply connected) with respect*

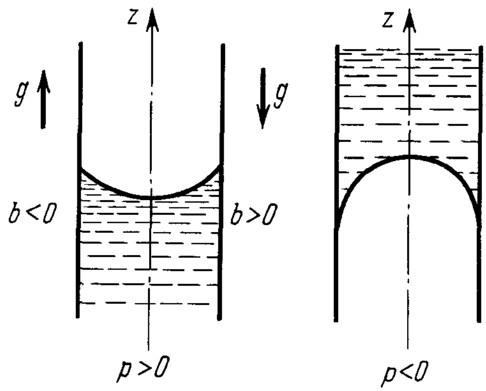

Fig. 2.6

to the direction of the z-axis. In this case, the plus sign must be used in both formulas in (2.2.28) and the signs of b and g will be the same. It can be easily deduced from (2.3.2) that for given values of b, p, and q, each equilibrium line is uniquely defined by the initial conditions

$$r(0) = z'(0) = 0, \quad z(0) = z_0, \quad r'(0) = 1.$$

Thus, for fixed values of b and p, all possible simply connected equilibrium surfaces of rotation form a two-parametric family with parameters z_0 and q. However, system (2.3.2) is invariant to the substitution $z(s) \to z(s) + c/b$, $q \to q - c$, where c is an arbitrary constant. Hence, if z_0 and q are changed in such a way that the quantity $(bz_0 + q)$ remains constant, the corresponding equilibrium curve is simply displaced as a whole along the z-axis. This means that all geometrically different simply connected equilibrium surfaces of rotation form a one-parametric family. Without any loss of generality, the initial conditions of system (2.3.2) for these surfaces can be written in the following form:

$$r(0) = z(0) = z'(0) = 0, \quad r'(0) = 1. \tag{2.3.3}$$

In this case the parameter q has a simple geometrical meaning: since $k_1 + k_2 = bz - pr^2 + q$, we get $q = (k_1 + k_2)_{r=0} = 2k(0)$, where $k(0)$ is the curvature of the equilibrium line at the point $s = 0$.

In concluding this section, we mention a formula which will be found useful in the future:

$$\left(2rz' - qr^2 - br^2 z + \frac{p}{2}r^4\right)\Bigg|_{s=s_1}^{s=s_2} = -b\int_{s_1}^{s_2} r^2 z'\, ds. \tag{2.3.4}$$

This formula is obtained by integrating the product of r and the second of equations (2.3.2).

2.3.2 Determination of an Equilibrium Line from Known Values of α and v

Suppose that we are given the meridian of a certain simply connected surface of rotation, intersecting the rotation axis at the point O (Fig. 2.7). To every point a on this meridian, there corresponds a definite value of the integral

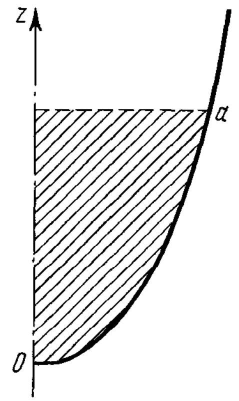

Fig. 2.7

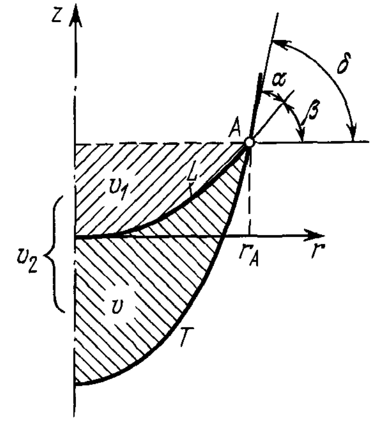

Fig. 2.8

$$\pi \int_{Oa} r^2\, dz. \tag{2.3.5}$$

To within the algebraic sign, this integral is equal to the volume enclosed between the surface under consideration and the plane $z = \text{const}$ passing through the point a. Such an integral is denoted by v_1 for the equilibrium surface of a liquid and by v_2 for the vessel surface. The angle between the r-axis and the tangent to the meridian T of the vessel surface is denoted by δ. Naturally, the values of v_1, v_2, and δ depend on point a.

Suppose that we are given a vessel, contact angle α, and volume v of the liquid in it. The problem of determining the free surface of the liquid then consists of finding an equilibrium line L for which the following conditions are satisfied at point A of its contact with the vessel surface (Fig. 2.8):

$$\beta = \delta - \alpha, \quad v_1 = v_2 - v. \tag{2.3.6}$$

We shall describe two methods of solving this problem.

1) *By Using the First Integral.* Let us first consider the method proposed by *Temkin* et al. [208]. This method is applicable when the gravitational forces are not equal to zero ($b \neq 0$), and is based on the application of formula (2.3.4). If point $s = s_1$ lies on the rotation axis and $s = s_2$ is the point of contact A, we obtain the following expression from (2.3.4), allowing for conditions (2.3.6) and the equality $z' = \sin\beta$:

$$q = \frac{2}{r_A}\sin(\delta_A - \alpha) - bz_A + \frac{b}{\pi}\frac{v_{2A} - v}{r_A^2} + \frac{p}{2}r_A^2. \tag{2.3.7}$$

If the position of point A were known for the required equilibrium line, we would find the value of q and construct the entire equilibrium line by integrating system (2.3.2) with the initial conditions

$$r = r_A, \quad z = z_A, \quad r' = \cos(\delta_A - \alpha), \quad z' = \sin(\delta_A - \alpha), \tag{2.3.8}$$

toward decreasing s.

In order to find point A, we choose a sufficiently dense network of points A_k ($k = 1, 2, \dots, n$) on the meridian of the vessel wall and successively construct the integral lines L_k of system (2.3.2) with conditions (2.3.7–8) for $A = A_k$. Each line has two possibilities: either it reaches the z-axis while remaining within the vessel and without intersecting itself (in this case it will be one of the required equilibrium lines), or it reaches the vessel wall, in which case it is not a meridian of the simply connected equilibrium surface in the vessel. If the point of contact A lies between A_k and A_{k+1}, this will be revealed by the qualitative difference between the lines L_k and L_{k+1}: at the closest point to the z-axis with $r' = 0$, we shall have $z' = 1$ for one of these lines and $z' = -1$ for the other (Fig. 2.9).

2) *Graphic Method.* The problem of finding an equilibrium line can be solved graphically [187, 189]. For this purpose, when numerically integrating system (2.3.2) with initial conditions (2.3.3) together with the equations and the initial conditions

$$\beta' = bz - pr^2 + q - z'/r, \quad v_1' = \pi r^2 z', \quad \beta(0) = 0, \quad v_1(0) = 0,$$

we must construct, for given b and p and for different fixed values of q, quite dense families of curves $\beta(r)|_{q=\text{const}}$, $v_1(r)|_{q=\text{const}}$ and the corresponding family of equilibrium lines $z(r)|_{q=\text{const}}$.

The equilibrium lines can be easily found for each specific case with the help of these families of curves. Knowing α, v, and the shape of the vessel, we can plot two auxiliary graphs: $\delta(r)$–α and $v_2(r)$–v. Finding the points of intersection of the curves $\delta(r)$–α and $\beta(r)|_{q=\text{const}}$, we construct the curve $q = q(r)$, on whose points the first of (2.3.6) is satisfied. The points of intersection of the curves $v_2(r)$–v and $v_1(r)|_{q=\text{const}}$ are used to construct the second $q(r)$ curve on which the second of conditions (2.3.6) is satisfied. The points of intersection of both curves $q(r)$ define approximately the possible pairs of values of q_L and r_A for the equilibrium line. Knowing q_L and r_A, we can find the point of contact r_A, z_A on the family of curves $z(r)|_{q=\text{const}}$. The corresponding equilibrium line is then constructed by interpolation and it can be verified whether it lies entirely within the vessel. If necessary, the equilibrium line can be constructed more accurately by integrating system (2.3.2) with initial conditions (2.3.3) for the obtained value of q. Further refinement can be achieved analytically, for example, by applying Newton's (linearization) method; the derivatives with respect to q can be roughly calculated using constructed curves, or, more accurately, by numerically integrating the variational system of equations corresponding to system (2.3.2).

Certain difficulties arise in view of the fact that, generally speaking, the obtained value of r_A ambiguously defines a point on the integral line as well as a point on line T. If such a

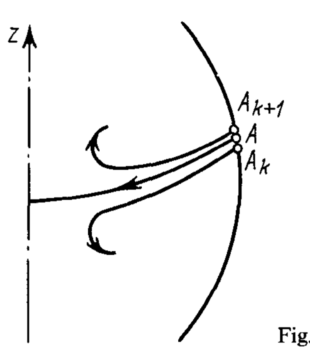

Fig. 2.9

situation arises, we can either verify the values of α and v for each combination of the obtained points, or break up all the lines into monotonic segments $z(r)$ and independently construct each segment. Moreover, some combinations can be discarded by considering that line L must not intersect itself and must lie completely within the vessel.

This method is especially convenient for solving real problems when it is necessary to find a series of equilibrium shapes for different values of v when the parameters b, p, and α, as well as the shape of the vessel, are given.

In conclusion, it should be noted that the same method is also applicable for potentials of the type $\Pi = gz + f(r)$, where $f(r)$ is an arbitrary function. A similar method can be used for determining the axisymmetric surface Γ when the line of contact passes along the edge of the vessel surface (see Sect. 3.9.4).

2.4 The Axisymmetric Problem for a Vessel at Rest

If there is no rotation, the method described in Sect. 2.3 can be given a more complete form, as is shown in this section.

2.4.1 General Remarks

Let $b \neq 0$. We introduce the dimensionless variables

$$\rho = \sqrt{|b|}\,r, \quad \zeta = \sqrt{|b|}\,z, \quad \tau = \sqrt{|b|}\,s, \quad \kappa = q/\sqrt{|b|}, \tag{2.4.1}$$

where ρ is the radius in the new cylindrical system of coordinates (it should not be confused with the density of the liquid!). Then system (2.3.2) assumes the following form for $p = 0$:

$$\rho'' = -\zeta'(\varepsilon\zeta + \kappa - \zeta'/\rho), \quad \zeta'' = \rho'(\varepsilon\zeta + \kappa - \zeta'/\rho), \quad (' = d/d\tau), \tag{2.4.2}$$

where $\varepsilon = 1$ for $b > 0$ and $\varepsilon = -1$ for $b < 0$. In order to find the simply connected equilibrium surfaces, this system must be integrated under the initial conditions

$$\rho(0) = \zeta(0) = \zeta'(0) = 0, \quad \rho'(0) = 1. \tag{2.4.3}$$

Since system (2.4.2) (but certainly not the required solution!) has a singularity at $\rho = 0$, it is advantageous to use for small values of τ expansions that can easily be obtained by the method of indeterminate coefficients:

$$\begin{aligned} \rho &= \tau - \tfrac{1}{24}\kappa^2\tau^3 + (-\tfrac{1}{160}\varepsilon\kappa^2 + \tfrac{1}{1920}\kappa^4)\tau^5 + \cdots, \\ \zeta &= \tfrac{1}{4}\kappa\tau^2 + (\tfrac{1}{64}\varepsilon\kappa - \tfrac{1}{192}\kappa^3)\tau^4 + \cdots, \end{aligned} \tag{2.4.4}$$

Numerical integration can then be performed.

If both sides of the second equation in (2.4.2) are multiplied by ρ, we obtain a formula similar to (2.3.4) after integration and simple transformations:

$$2\rho\sin\beta = \varepsilon\rho^2\zeta + \kappa\rho^2 - (\varepsilon/\pi)V_1, \tag{2.4.5}$$

where the dimensionless volume V_1 is introduced as in Sect. 2.3.2.

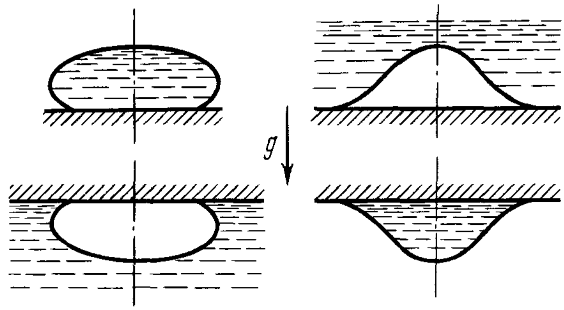

Fig. 2.10

System (2.4.2) and initial conditions (2.4.3) are invariant under the substitution $\{\zeta \to -\zeta, \kappa \to -\kappa\}$. Hence, as κ changes sign, the integral line undergoes a mirror reflection with respect to the ρ-axis. This means that in order to analyze the shape of this line, it is sufficient to confine ourselves to the case $\kappa \geqslant 0$ and to remember that $\beta(\rho)|_{-\kappa} = -\beta(\rho)|_{\kappa}$ and $V_1(\rho)|_{-\kappa} = -V_1(\rho)|_{\kappa}$.

This symmetry is not connected with the axial symmetry of the problem. If there is no rotation, the following simple but remarkable fact emerges from (2.2.27): each equilibrium state of a liquid in *any* vessel has another corresponding state which is obtained as a result of the mirror reflection of the entire system with respect to the equipotential plane with a simultaneous replacement of the liquid by gas and vice versa, and of the contact angles by supplementary angles. Typical duality patterns are shown in Fig. 2.10.[11]

Before concluding this discussion, let us make a remark. It will be shown in Chap. 3 that on each integral line of the system (2.4.2) under conditions (2.4.3), a point $\tau = \tau_1^*$ exists such that for $\tau < \tau_1^*$ the segment $(0, \tau)$ defines an equilibrium surface which will be stable in a certain vessel for certain values of the contact angle α. If, however, $\tau > \tau_1^*$, the corresponding surface is known beforehand to be unstable in any vessel and for any values of the contact angle α. Hence we shall devote particular attention to the segments $(0, \tau_1^*)$ which will be called *maximal stability regions*. These regions are singled out in Chap. 3; here, we mention these results in order to draw attention to the most interesting shapes.

2.4.2 Positive Loading

Figure 2.11 shows the typical form of integral lines obtained by numerical integration of problem (2.4.2–3) for $\varepsilon = 1$. This diagram could also be substantiated by a qualitative analysis of (2.4.2). It will be shown in Chap. 3 that the maximal stability regions for the lines shown in Fig. 2.11 extend only to the first point at which $\beta = \pi$ (this region is represented by the semi-axis $\rho \geqslant 0$ for $\kappa = 0$). Figure 2.12 depicts a family of maximal stability regions. It will be shown in Sect. 2.10.1 that as $\kappa \to 0$, the ordinates of the tips of these segments tend to the value 2. For small κ it is natural to use the approximate methods described in Sects. 2.7 and 2.8. For large values of κ, the shape of the maximal stability regions approaches a semicircle of radius $2/\kappa$. At the terminal points of these regions we have (to within the terms of higher order)

[11] Skipping ahead, we can also note that since an identical (to within the algebraic sign) variation of dual systems leads to identical increments in their potential energies, these states are either both stable or both unstable.

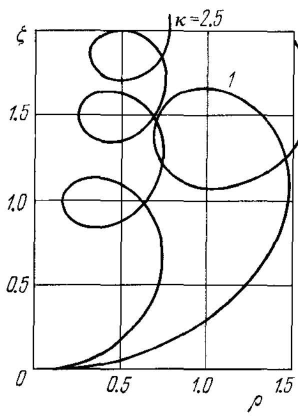

Fig. 2.11

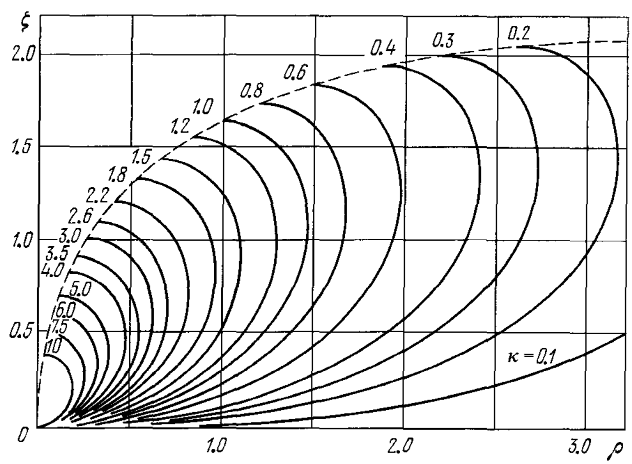

Fig. 2.12

$$\rho = \left(\frac{2}{3}\right)^{1/2} \frac{4}{\kappa^2}, \quad \zeta = \frac{4}{\kappa} - \frac{8}{3\kappa^3}\left[2 + \ln\left(\frac{3}{2}\kappa^2\right)\right], \quad V_1 = \frac{32\pi}{3\kappa^3}\left(1 - \frac{4}{\kappa^2}\right),$$

while at the points with a vertical tangent, we get

$$\rho = \frac{2}{\kappa} - \frac{4}{3\kappa^3}, \quad \zeta = \frac{2}{\kappa} - \frac{4}{3\kappa^3}(1 + \ln 4), \quad V_1 = \frac{16\pi}{\kappa^3}\left(\frac{1}{3} - \frac{1}{\kappa^2}\right).$$

Figures 2.13–2.15 show curves $\beta(\kappa, \rho)$ and $V_1(\kappa, \rho)$ for maximal stability regions at $\kappa \geqslant 0$. It should be recalled that for $\kappa < 0$ these functions are odd in κ. These data are sufficient to determine the equilibrium line (belonging to the maximal stability region) for known values of $b > 0$, v, and α by going over to dimensionless coordinates and using the graphical method described in Sect. 2.3.2. Of course, the existence of a solution of the dimensionless analogue of system (2.3.6) is only necessary, but generally not sufficient, for the existence of a *stable* equilibrium state for given values of the parameters.

The obtained values of κ_L, ρ_A, β_A, and $(V_1)_A$ can be used for determining ζ_A with the help of (2.4.5). The equilibrium shape can be obtained either by numerical integration or by directly applying Fig. 2.12 after which one must go over to the original (dimensional) coordinates r and z.

2.4.3 Negative Loading

Typical form of the integral lines of problem (2.4.2–3) for $\varepsilon = -1$, obtained by numerical integration and confirmed by qualitative analysis, is shown in Fig. 2.16 for the plane $(\rho, \zeta - \kappa)$.

The following properties can be proved by using the expression obtained by integrating the first equation in system (2.4.2) from a certain $\tau_1 \geqslant 0$ to $\tau_2 > \tau_1$, as well as the expression for the curvature of an integral curve.

If $\kappa = 0$, we get $\zeta_1(\tau) \equiv \zeta(\tau) - \kappa = 0$. For quite small values of $|\kappa|$, the function $\zeta_1(\tau) = -\kappa J_0(\tau) + o(\kappa)$. For each $\kappa \neq 0$, the integral line $\rho(\tau)$, $\zeta_1(\tau)$ is defined for $0 \leqslant \tau <$

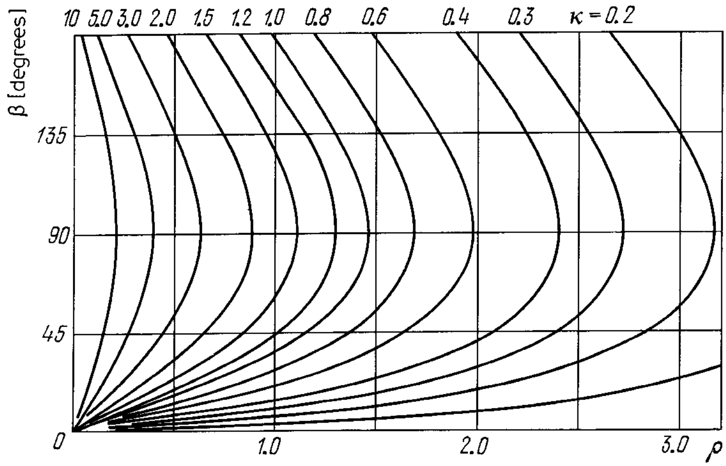

Fig. 2.13

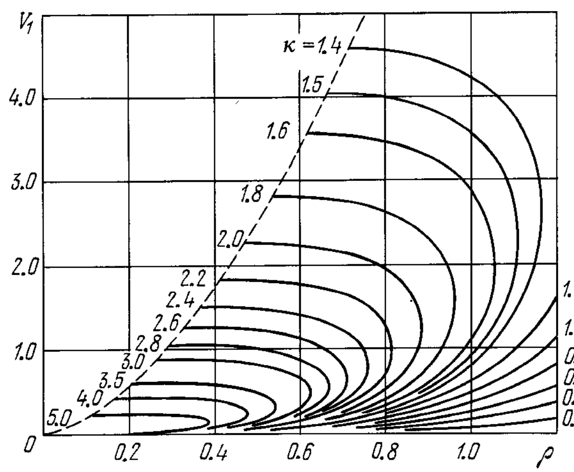

Fig. 2.14

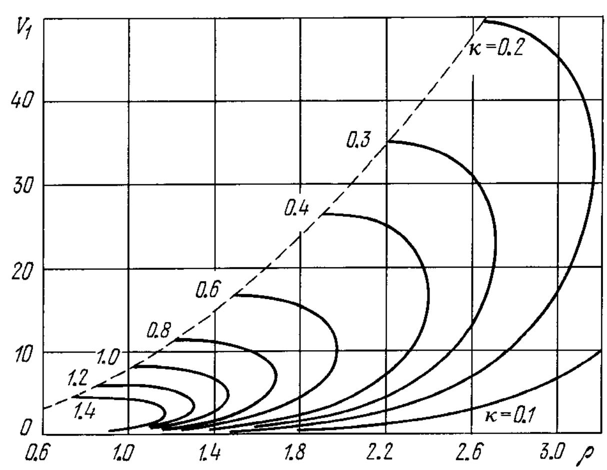

Fig. 2.15

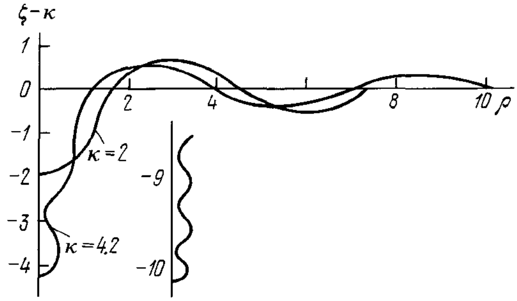

Fig. 2.16

∞; it does not meet the ζ_1-axis except at the initial point and intersects the ρ-axis an infinite number of times. Moreover, $\rho(\infty) = \infty$, $\rho'(\infty) = 1$, $\zeta_1'(\infty) = 0$, and at successive stationary points of the function $\zeta_1(\tau)$ the values of ζ_1 have alternating signs and monotonically decrease in their absolute value. The value of ρ' at the point of intersection with the ρ-axis is less than the value of ρ' for all subsequent τ. Hence, if $\rho' > 0$ at any of such points, the function $\zeta_1(\rho)$ will be single-valued for further values of τ.

Figure 2.17 shows the corresponding maximal stability regions obtained with the help of the methods described in Chap. 3. It is found that these segments can be of two types. At the tips of the segments lying on arc BC, the equilibrium lines have a horizontal tangent. Point B is obtained for $\kappa = 1.570$ while $\rho_C = 3.8317$ is the first positive zero of the Bessel function $J_1(\rho)$. Tips of the segments lying on arc OAB are otained with the help of a more complicated rule. In particular, the values of β corresponding to this arc are always less than $\pi/2$ and tend to this value as $\kappa \to \infty$. Besides, it has been established that the function $V_1(\zeta)|_{\rho=\text{const}}$ is an increasing function in the stability region and has a local maximum on arc OAB.

For large values of κ, the maximal stability region consists of two parts. The main part extends from the starting point to the point of inflection and differs only insignificantly in shape from a semicircle of radius $2/\kappa$. The second part extends from the point of

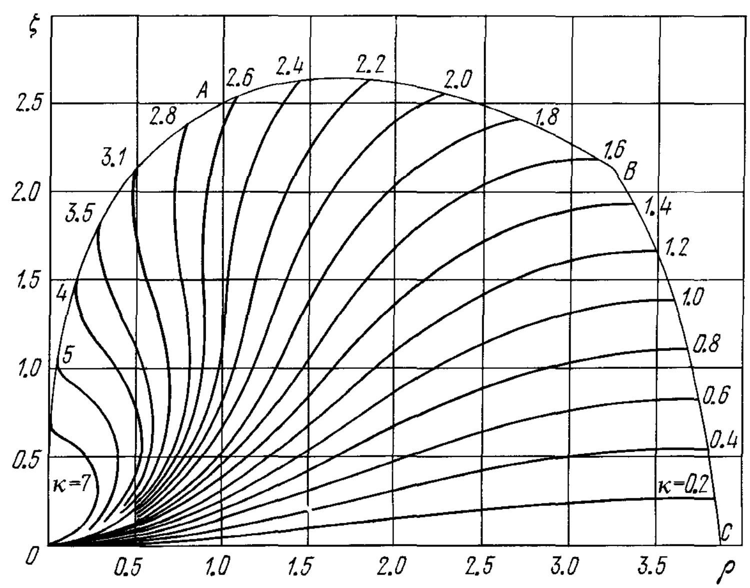

Fig. 2.17

inflection to the terminal point, forming a small neck along which a sharp change in the profile curvature occurs. As in the case for $\varepsilon = 1$, we are interested in asymptotic formulas which define the parameters of the characteristics points on the maximal stability region for $\kappa \gg 1$. At the point with a vertical tangent on the first part, we have (to within the terms of higher order)

$$\rho = \frac{2}{\kappa} + \frac{4}{3\kappa^3}, \quad \zeta = \frac{2}{\kappa} + \frac{4}{3\kappa^3}(1 + \ln 4), \quad V_1 = \frac{16\pi}{\kappa^3}\left(\frac{1}{3} + \frac{1}{\kappa^2}\right),$$

while at the point of inflection

$$\rho = \left(\frac{2}{3}\right)^{1/2}\frac{4}{\kappa^2}, \quad \zeta = \frac{4}{\kappa} + \frac{4}{3\kappa^3}\ln\left(\frac{9}{4}\kappa^4\right), \quad \beta = \pi - \left(\frac{2}{3}\right)^{1/2}\frac{4}{\kappa}\left(1 - \frac{2}{9\kappa^2}\right),$$

$$V_1 = \frac{32\pi}{3\kappa^3}\left(1 + \frac{4}{\kappa^2}\right)$$

and at the point with a vertical tangent at the neck

$$\rho = \frac{16}{3\kappa^3}, \quad \zeta = \frac{4}{\kappa} + \frac{8}{3\kappa^3}\left[1 + \ln\left(\frac{9}{4}\kappa^4\right)\right], \quad V_1 = \frac{32\pi}{3\kappa^3}\left(1 + \frac{4}{\kappa^2}\right).$$

To within higher-order terms, these last parameters are the same as those obtained for the terminal point where $\beta = \pi/2 - 128/9\kappa^6$. For $\varepsilon = \pm 1$, the shape of the free surface for large values of κ (small values of $|\mathbf{Bo}|$) can be determined by methods described in Sect. 2.13.

Figures 2.18 and 2.19 show the curves for the dependences $\beta(\kappa, \rho)$ and $V_1(\kappa, \rho)$ which can be used for the construction of the equilibrium surface in a given vessel for $\varepsilon = -1$ (see Sect. 2.3.2 and 2.4.2).

2.4.4 Zero-Gravity

If $p = 0$ and $b = 0$, the solution of system (2.3.2) under the initial conditions (2.3.3) has the form

$$r = \frac{2}{q}\sin\frac{qs}{2}, \quad z = \frac{2}{q}\left(1 - \cos\frac{qs}{2}\right). \tag{2.4.6}$$

For $r > 0$, this is a semicircle of radius $2/|q|$ having its center at point $(0, 2/q)$. It will be shown in Chap. 3 that this is a maximal stability region. Analytical expressions for the functions $\beta(q, s)$ and $v_1(q, s)$ can be easily obtained:

$$\beta = \frac{1}{2}qs, \quad v_1 = \frac{8\pi}{3q^3}\left(1 - \cos\frac{qs}{2}\right)^2\left(2 + \cos\frac{qs}{2}\right). \tag{2.4.7}$$

This enables us to apply the method described in Sect. 2.3 for finding equilibrium shapes for given values of α and v.

In particular, let $r = f(z)$ be the equation for the vessel wall being wetted by a liquid. In this case, taking the origin at the bottom of the vessel (Fig. 2.20), we can rewrite system of equations (2.3.6) by taking (2.4.7) into account:

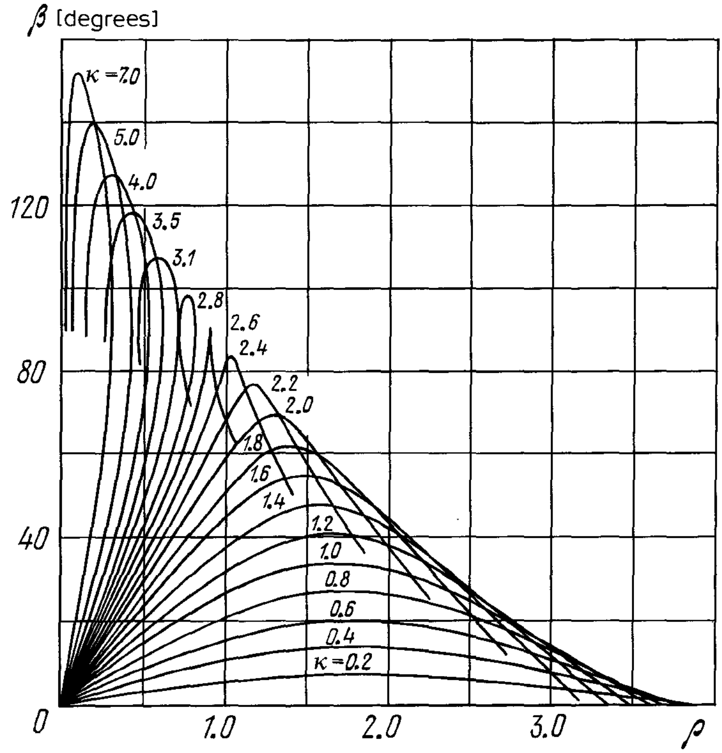

Fig. 2.18

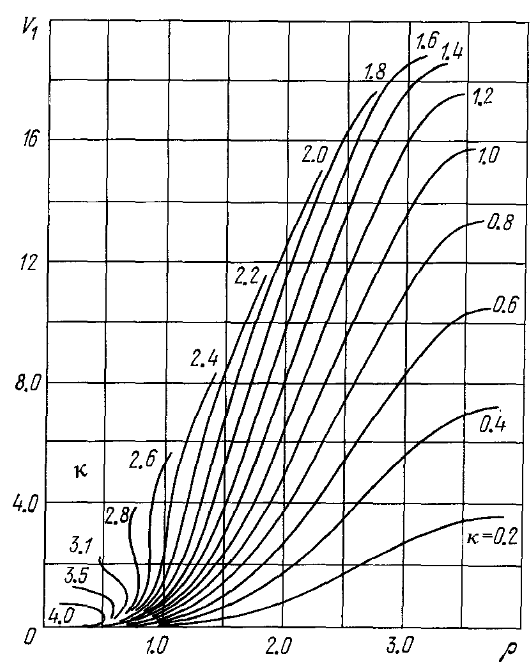

Fig. 2.19

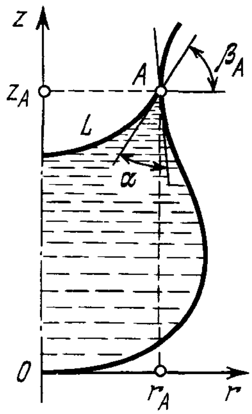

Fig. 2.20

$$f'(z_A) = \cot(\beta_A + \alpha),$$

$$\frac{\pi}{3}\frac{f^3(z_A)}{\sin^3\beta_A}(1 - \cos\beta_A)^2(2 + \cos\beta_A) = \pi\int_0^{z_A} f^2(z)\,dz - v. \tag{2.4.8}$$

The values of β_A and z_A can be obtained from this system of equations [it also gives $r_A = f(z_A)$ and $q_L = (2\sin\beta_A)/r_A$].

The following results have been obtained by directly applying (2.4.8) to vessels of simple specific shapes.

Figure 2.21 (cylinder)

$$\beta_A = \frac{\pi}{2} - \alpha, \quad z_A = \frac{v}{\pi r_1^2} + \frac{r_1}{3\cos^3\alpha}(1 - \sin\alpha)^2(2 + \sin\alpha).$$

Figure 2.22 (cone)

$$\beta_A = \delta - \alpha,$$

$$z_A = \left(\frac{3v}{\pi\cot^2\delta}\right)^{1/3}\left\{1 - \frac{\cot\delta}{\sin^3(\delta - \alpha)}[1 - \cos(\delta - \alpha)]^2[2 + \cos(\delta - \alpha)]\right\}^{1/3}.$$

Figure 2.23 (drop on a plane)

$$\beta_A = -\alpha, \quad \frac{q}{2} = -\left[\frac{\pi(1 - \cos\alpha)^2(2 + \cos\alpha)}{3v}\right]^{1/3}.$$

Figure 2.24 (sphere). We obtain the system of equations

$$\beta = \delta - \alpha,$$

$$\frac{\sin^3\delta}{\sin^3\beta}(1 - \cos\beta)^2(2 + \cos\beta) = (1 - \cos\delta)^2(2 + \cos\delta) - \frac{3v}{\pi r_1^3}$$

for determining β_A and δ_A.

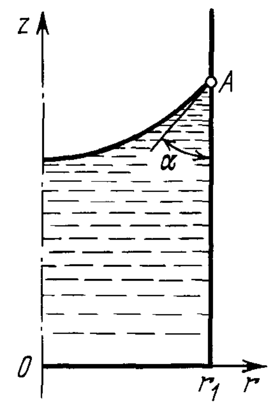

Fig. 2.21

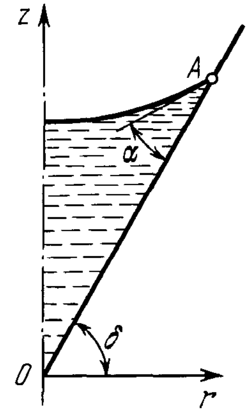

Fig. 2.22

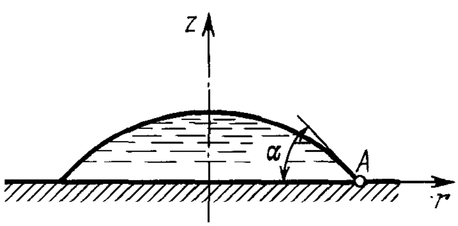

Fig. 2.23

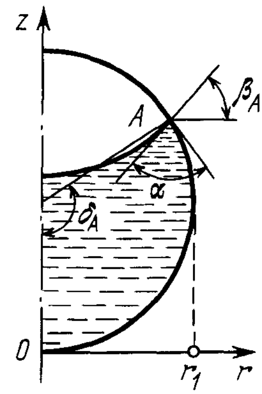

Fig. 2.24

Finally, it should be remarked that if the vessel is closed, for certain relations between the parameters of the problem the connected surface Γ may assume the form of a complete sphere, having no common points with the vessel walls. In other words, we obtain a bubble. In this case, the condition for the contact angle becomes superfluous. The radius of the bubble is determined by the values of v, while its position in the vessel is arbitrary and is determined only by the possibility of its being contained inside the vessel.[12]

2.4.5 Examples

(a) Suppose that an elongated ellipsoid of revolution with semiaxes 100 cm and 50 cm is partially filled by a liquid with parameters $\rho = 1$ gm cm^{-3}, $\sigma = 49.05$ dyne cm^{-1}, $\alpha = 30°$. The *filling coefficient* (ratio of liquid volume to vessel volume) $k_f = 0.1$. There is no rotation and the z-axis is directed from liquid to gas (Fig. 2.25). A uniform force field

[12] The above is apparently due to the absence of an external force field and rotation, rather than to axial symmetry.

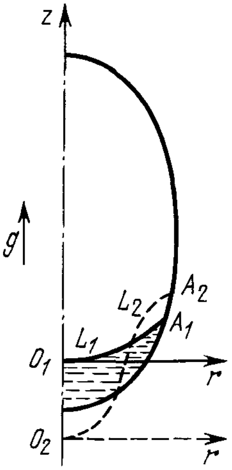

Fig. 2.25

is applied in the same direction, and $g = -8 \times 10^{-5} \times 981$ cm s^{-2}. Find the possible simply connected axially symmetric equilibrium shapes of the liquid.

Having calculated $b = \rho g/\sigma = -1.6 \times 10^{-3}$ cm^{-2}, we go over to the dimensionless parameters (2.4.1), in which the semiaxes of the vessel are $G = 2$ and $H = 4$, and hence its volume $V_{el} = 4\pi G^2 H/3 = 67$. Consequently, $V = k_f V_{el} = 6.7$. The dependences $\delta(\rho)$ and $V_2(\rho)$ are given by the formulas

$$\delta = \operatorname{arccot}\left(\pm\frac{G}{H\rho}\sqrt{G^2-\rho^2}\right),$$
$$V_2 = \tfrac{2}{3}\pi GH(G \mp \sqrt{G^2-\rho^2}). \tag{2.4.9}$$

in which the upper sign corresponds to the lower half of the ellipsoid and the lower sign to the upper half.

In accordance with the graphic method described in Sect. 2.3.2, superposition of the curve $\delta(\rho) - \alpha$ on Fig. 2.18 [the curve suffers a mirror reflection with respect to the ρ-axis for $\delta(\rho) < \alpha$] leads to the dependence $\kappa(\rho)$ shown in Fig. 2.26 (curve 1).[13] The second dependence (curve 2) is obtained with the help of curve $V_2(\rho)-V$ and Fig. 2.19. These curves intersect at two points whose coordinates are $\rho_{A_1} = 1.28$, $\kappa_{L_1} = 0.94$, and $\rho_{A_2} = 1.75$, $\kappa_{L_2} = 2.16$. The coordinates of both these points are the solutions of the dimensionless analogue of system (2.3.6) and correspond to the lower half of the ellipsoid. In view of formulas (2.4.9) and (2.4.5), we get the values $\delta = 58.8°$, $\beta = 28.8°$, $V_2 = 7.69$, $V_1 = 0.99$, and $\zeta = 0.38$ for the first solution, and $\delta = 74.5°$, $\beta = 44.5°$, $V_2 = 17.28$, $V_1 = 10.58$, and $\zeta = 2.46$ for the second. It can be easily verified that the surface corresponding to the second solution cannot be contained inside the vessel (dotted line in Fig. 2.25). This leaves only one surface which is shown in Fig. 2.25.

(b) The problem of constructing the equilibrium liquid surface in a cylindrical vessel can be solved quite easily. The abscissa ρ_A is known in this case, as it coincides with the

[13] Here, the values of κ were taken with the opposite sign at the points of intersection of the reflected part of the curve $\delta(\rho) - \alpha$.

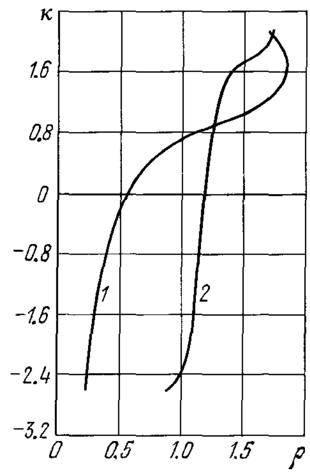

Fig. 2.26

dimensionless radius ρ_0 of the cylinder. All that remains is to determine $\kappa = \kappa_L$ from the point of intersection of the straight lines $\beta = \pi/2 - \alpha$ and $\rho = \rho_0$ in Fig. 2.18. The position of the surface in the cylinder is determined by its distance ζ_0 from the bottom measured along the axis of symmetry. This is obtained from the relation

$$\zeta_0 = (V + V_1)/(\pi\rho_0^2) - \zeta_A, \tag{2.4.10}$$

where V_1 is determined for $\kappa = \kappa_L$, $\rho = \rho_0$ graphically from the dependence $V_1(\kappa, \rho)$ while ζ_A is obtained from the relation (2.4.5). Naturally, if the volume of the liquid changes slowly, the free surface moves as a whole along the axis of symmetry, the change in volume ΔV corresponding to the displacement $\Delta V/(\pi\rho_0^2)$.

It can be seen that the *shape* of the liquid surface in a cylinder is determined by the quantities α and ρ_0 (or $\mathbf{Bo} = br_0^2 = \varepsilon\rho_0^2$). It is interesting to determine the extent to which the change in the Bond number (caused, for example, by a change in the value of g) affects the shape of the liquid surface. For the sake of definiteness, let us assume that $\mathbf{Bo} \geqslant 0$. As has been stated above, the graphical data given in Sect. 2.4.2 can be used to determine the shape of the surface for values of **Bo** lying in the range from ~ 0.1 to ~ 10. The case $\mathbf{Bo} = 0$ is described in Sect. 2.4.4. The asymptotic expression for the shape for $\mathbf{Bo} \ll 1$ is given in Sect. 2.13.4, and for $\mathbf{Bo} \gg 1$, in Sect. 2.7. Figures 2.27a and b depict the equilibrium surface shape for $\mathbf{Bo} = 1000$, 100, 10, 1, and 0, respectively, for $\alpha = 0$ and $\alpha = 30°$. These results are borrowed from an article by *Concus* [51] (similar results were obtained by *Shuleikin* [162] who used the data published by W. Thomson as early as 1891).

2.4.6 Reference Commentaries

Axially symmetric simply connected equilibrium liquid surfaces in a uniform force field have been investigated by several authors. The first fairly comprehensive results were published by *Bashforth* and *Adams* [13] in 1883. In this work, which has since become a bibliographical rarity, the authors started with the equilibrium equation in the form of (2.3.1) (for $p = 0$) and, with the help of numerical integration, compiled tables for the

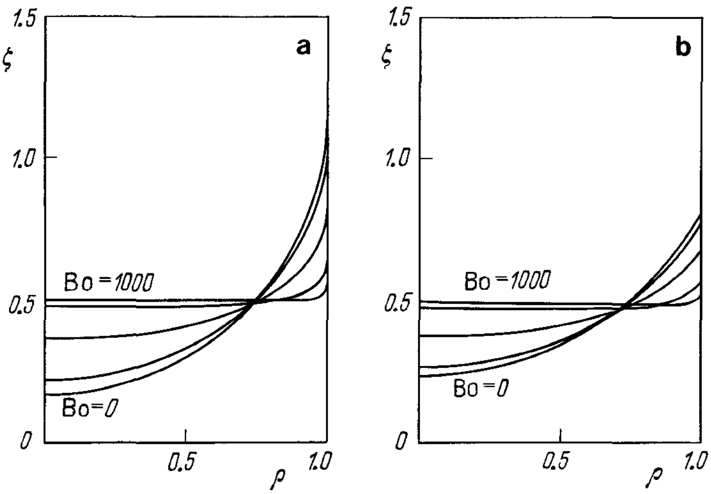

Fig. 2.27

values of r/R_0, z/R_0, and $v_1/(\pi R_0^3)$ ($R_0 = 2/|q|$) for given values of β and for Bond numbers $\mathbf{Bo} = bR_0^2 \gtrless 0$.

The equilibrium problem has once again drawn the attention of researchers in the last 20 years. Detailed analysis of various cases has been carried out with the help of modern methods and extensive use of computers. The results of calculations of axisymmetric profiles, frequently extended considerably beyond the maximal stability regions, are given by *Padday* and *Pitt* [127, 128]. A large body of numerical data on axisymmetric equilibrium shapes is contained in the monograph by *Hartland* and *Hartley* [72]. Detailed tables and plots given in [86] describe the characteristics of maximal stability regions for $\varepsilon = -1$ (i.e., for $b < 0$) and supplement the data given in Sect. 2.4.3. An approximate description of the shape of maximal stability regions for large κ and $\varepsilon = \pm 1$ is given by *Chesters* [48].

Important special cases have been considered by a number of authors whose results can also frequently be used in a more general formulation of the problem. The case of an axisymmetric equilibrium surface abutting a smooth horizontal plane or the edge of a rigid body (forming a horizontal circle) has been analyzed and attributed to numerous applications of the problem of equilibrium and a slow evolution of drops and bubbles. The analysis of this case for $\varepsilon = -1$ is given by *Tamada* and *Shibaoka* [206], *Hida* and *Nakanishi* [74], *Buevich* and *Butkov* [40], *Marmur* and *Rubin* [103], *Boucher*, *Evans*, *Kent* and *Jones* [25, 27, 30], *Michael* and *Williams* [110], as well as by the authors of this book [188, 192]. For $\varepsilon = +1$, the problem has been considered by *Shuleikin* [163], *Robertson* and *Lehman* [143], *Michael* and *Williams* [111], as well as in [27, 30, 74]. The data on the geometry of drops for $\varepsilon = \pm 1$ can be found in the work of *Vacek* et al. [213], a sort of review article. The investigations by various authors on the shape of a sessile drop are analyzed in detail by *Ivashchenko* and *Eremenko* in their book [78].

The problem of equilibrium shapes of a liquid in a right circular cylinder was studied by *Shuleikin* [162], *Concus* [51], and later by *Siekmann*, *Scheideler* and *Tietze* [167, 169].

The shape of a bubble floating on a liquid surface and separated from the external gaseous medium by just a thin liquid film was investigated by *Medrow* and *Chao* [107].

Several authors have used series expansions of the solutions. Thus, *Barnyak* [9–11] investigated in detail the series (2.4.4) and their analytical extensions. By considering the equilibrium problem ($b > 0$) in a vessel having a meridian of the form $z = f(r)$, *Keleberdenko* [83] obtained the solution as the sum of a power series whose coefficients are numerically computed, the additional conditions being satisfied by solving transcendental equations. Results of specific computations are also given in this work. The expansion of the function $z(r)$ into a power series was considered earlier by *Li* [95].

The conditions under which the formation of a bubble under zero gravity (see end of Sect. 2.4.4) ultimately leads to a decrease in the potential energy of the system, i.e., becomes advantageous from the energy point of view, was considered by *Zenkevich* [226]. A detailed bibliography of other works on equilibrium shapes under zero gravity conditions is given in the review article by *Habip* [70].

The present section is based on the work of the authors and *Svechkareva* as well as of *Moiseev, Chernous'ko* and *Chesters* [4, 16–18, 20, 46, 48, 112, 113, 115, 187, 189, 191].

2.5 Axisymmetric Shapes of a Rotating Liquid Under Zero-Gravity

In this section, we carry out investigations similar to those in Sect. 2.4 for the other limiting case when $b = 0$, $p \neq 0$.

2.5.1 Properties of the Solutions of Equilibrium Differential Equations

Let us turn to (2.3.1). If $b = 0$ and the z-axis at the point $z = 0$ is directed from the liquid to the gas, i.e., $p > 0$, the introduction of dimensionless variables in accordance with the formulas

$$\rho = \sqrt[3]{p}r, \quad \zeta = \sqrt[3]{p}z, \quad \tau = \sqrt[3]{p}s, \quad \kappa = q/\sqrt[3]{p} \tag{2.5.1}$$

leads to the equation

$$\frac{1}{\rho}\left(\frac{\rho\zeta'}{\sqrt{1+\zeta'^2}}\right)' = -\rho^2 + \kappa, \quad \left(' = \frac{d}{d\rho}\right) \tag{2.5.2}$$

with the following initial conditions for a simply connected surface:

$$\zeta(0) = 0, \quad \zeta'(0) = 0. \tag{2.5.3}$$

A similar transformation of problem (2.3.2–3) leads to

$$\rho'' = -\zeta'(-\rho^2 + \kappa - \zeta'/\rho), \quad \zeta'' = \rho'(-\rho^2 + \kappa - \zeta'/\rho), \quad (' = d/d\tau), \tag{2.5.4}$$

$$\rho(0) = \zeta(0) = \zeta'(0) = 0, \quad \rho'(0) = 1. \tag{2.5.5}$$

It follows from the invariance of the original problem to the mirror reflection in the plane $z = \text{const}$ that if in the solution of problem (2.5.4–5) $|\zeta'(\tau_c)| = 1$ at a certain point $\tau = \tau_c$, the integral line will be symmetric with respect to the plane $\zeta = \zeta(\tau_c)$; i.e., the corresponding surface of rotation will be closed, although it may have self-intersections. Because of this symmetry, it is sufficient to depict the integral line just up to the "equatorial point."

Multiplying the second equation in (2.5.4) by ρ, integrating, and taking conditions (2.5.5) into account, we obtain

$$\zeta' = -\tfrac{1}{4}\rho^3 + \tfrac{1}{2}\kappa\rho. \tag{2.5.6}$$

On the basis of this equation and the expression $k = -\rho^2 + \kappa - \zeta'/\rho$ for the curvature of an integral line, the following properties of these lines were obtained in [171] [these results were confirmed by numerical integration; Figure 2.28 shows the integral lines extended to the value $\beta = \pm\pi/2$, i.e., $\zeta' = \pm 1$ at the point (ρ_1, ζ_1)]:

for $-\infty < \kappa < 3/\sqrt[3]{2}$, the value $\beta = -\pi/2$ is attained for

$$\rho = \rho_1(\kappa) = \sqrt[3]{2 + \sqrt{d}} + \sqrt[3]{2 - \sqrt{d}}, \quad d = 4 - \tfrac{8}{27}\kappa^3; \tag{2.5.7}$$

the dependence $\rho_1(\kappa)$ is increasing, $\rho_1(-\infty) = 0$, $\rho_1(3/\sqrt[3]{2} - 0) = 2\sqrt[3]{2}$;

for $\kappa \leqslant 0$, the line is convex upward;

for $0 < \kappa < 3/\sqrt[3]{2}$, the line is convex downward (upward) for $0 \leqslant \rho \leqslant \sqrt{2\kappa/3}$ (resp. $\sqrt{2\kappa/3} \leqslant \rho \leqslant \rho_1(\kappa)$), and the maximum value of $\zeta(\rho)$ is attained for $\rho = \sqrt{2\kappa}$;

for $\kappa = 3/\sqrt[3]{2}$, the line is convex downward and has an asymptote $\rho = \sqrt[3]{2}$;

for $3/\sqrt[3]{2} < \kappa < \infty$, the line is convex downward and the value $\beta = \pi/2$ is attained for

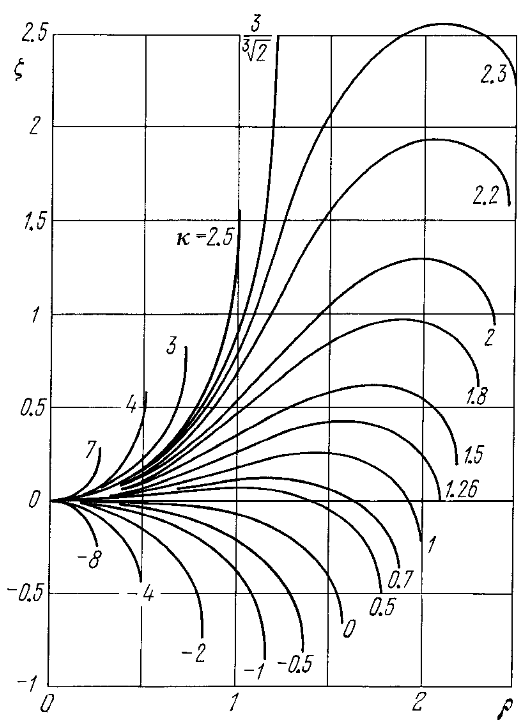

Fig. 2.28

$$\rho = \rho_1(\kappa) = \sqrt{\tfrac{2}{3}\kappa}\left(\cos\frac{\mu}{3} - \sqrt{3}\sin\frac{\mu}{3}\right),$$
$$\cos\mu = \sqrt{27/(2\kappa^3)}, \quad 0 < \mu < \pi/2; \tag{2.5.8}$$

the dependence $\rho_1(\kappa)$ is decreasing, $\rho_1(3/\sqrt[3]{2} + 0) = \sqrt[3]{2}$ and $\rho_1(\infty) = 0$.

The following expansions can be used for numerical integration of system (2.5.4) for small τ:

$$\rho = \tau - \tfrac{1}{24}\kappa^2\tau^3 + (\tfrac{1}{1920}\kappa^4 + \tfrac{1}{40}\kappa)\tau^5 + \cdots,$$

$$\zeta = \tfrac{1}{4}\kappa\tau^2 - (\tfrac{1}{192}\kappa^3 + \tfrac{1}{16})\tau^4 + \cdots.$$

2.5.2 Solution in Elliptic Integrals

Integrating, we obtain from (2.5.2) and (2.5.3)

$$\frac{\zeta'}{\sqrt{1+\zeta'^2}} = -\frac{1}{4}\rho^3 + \frac{1}{2}\kappa\rho, \quad \left(' = \frac{d}{d\rho}\right). \tag{2.5.9}$$

First, let $\kappa < 3/\sqrt[3]{2}$. In this case, $\zeta'(\rho_1) = -\infty$ (see Sect. 2.5.1); then

$$-1 = -\tfrac{1}{4}\rho_1^3 + \tfrac{1}{2}\kappa\rho_1, \quad \text{i.e.} \quad \kappa = \tfrac{1}{2}\rho_1^2 - 2/\rho_1, \tag{2.5.10}$$

leading to (2.5.7). Substituting (2.5.10) into (2.5.9), introducing the variable $t = \rho/\rho_1$ $(0 \leqslant t \leqslant 1)$, and integrating, we get

$$\zeta = -\rho_1 \int_0^{\rho/\rho_1} t(1 - \tfrac{1}{4}\rho_1^3 + \tfrac{1}{4}\rho_1^3 t^2)[1 - t^2(1 - \tfrac{1}{4}\rho_1^3 + \tfrac{1}{4}\rho_1^3 t^2)^2]^{-1/2}\,dt.$$

Using the transformation

$$t^2 = 1 - h\tan^2\frac{\varphi}{2}, \quad h = \frac{4}{\rho_1^3}\sqrt{1 + \tfrac{1}{2}\rho_1^3}$$

we can reduce this integral to the form

$$\zeta = \frac{2}{\rho_1^2\sqrt{h}} \int_{\psi_0}^{\psi} \frac{1 - \frac{1}{4}\rho_1^3 h \tan^2\frac{\varphi}{2}}{\sqrt{1 - l^2\sin^2\varphi}}\,d\varphi, \tag{2.5.11}$$

where

$$l^2 = \frac{1}{2} + \frac{8 + \rho_1^3}{8\sqrt{4 + 2\rho_1^3}} < 1,$$

$$\psi_0 = 2\arctan\frac{1}{\sqrt{h}}, \quad \psi = 2\arctan\sqrt{\frac{1}{h}\left[1 - \left(\frac{\rho}{\rho_1}\right)^2\right]}.$$

From (2.5.11) we get an expression for the dependence $\zeta(\rho)$ in terms of elliptic integrals of the first and second kind:

$$\zeta = \rho_1\sqrt{h}\{E(\psi,l) - E(\psi_0,l) + [2/(\rho_1^3 h) - \tfrac{1}{2}]\cdot[F(\psi,l) - F(\psi_0,l)]$$
$$-\sqrt{1-l^2\sin^2\psi}\tan(\psi/2) + \sqrt{1-l^2\sin^2\psi_0}\tan(\psi_0/2)\}.$$

Let us now suppose that $\kappa \geqslant 3/\sqrt[3]{2}$. In this case, we get the following equality instead of (2.5.10):

$$\kappa = \tfrac{1}{2}\rho_1^2 + 2/\rho_1,$$

whence $\rho_1 \in (0, \sqrt[3]{2})$ is uniquely determined by formula (2.5.8). As in the previous case, using the substitutions

$$u = \rho/\rho_1, \quad u^2 = 1 - q\cot^2\theta, \quad q = 4/\rho_1^3 - \tfrac{1}{2} + \sqrt{4/\rho_1^3 + \tfrac{1}{4}},$$

we get

$$\zeta = \rho_1\sqrt{q}\left\{\frac{4}{\rho_1^3 q}[F(\delta,m) - F(\theta_0,m)] - E(\delta,m) + E(\theta_0,m)\right.$$
$$\left.-\sqrt{1-m^2\sin^2\delta}\cot\delta + \sqrt{1-m^2\sin^2\theta_0}\cot\theta_0\right\},$$

where

$$m^2 = \frac{1}{q}\left(1 + 2q - \frac{8}{\rho_1^3}\right), \quad \theta_0 = \arctan\sqrt{q},$$
$$\delta = \arctan\sqrt{q[1-(\rho/\rho_1)^2]^{-1}}.$$

2.5.3 Equilibrium Surfaces in a Vessel

In order to construct a simply connected equilibrium surface in contact with the vessel walls, we can use, as before, the method described in Sect. 2.3 for a given value of the contact angle and a given volume of the liquid. For this purpose, we go over to dimensionless variables (2.5.1) and draw the family of maximal stability segments (determined in the same way as in Sect. 2.4.1) of the equilibrium lines (Fig. 2.29). It should be mentioned that for $\kappa > 3/\sqrt[3]{2} = 2.381$, these segments reach the point where the integral line meets the ζ-axis. Figures 2.30 and 2.31 show the families of curves $\beta(\kappa,\rho)$ and $V_1(\kappa,\rho)$ ($V_1 = pv_1$) for these segments. These results, obtained by numerical integration of problem (2.5.4–5), enable us to apply the graphic method described in Sect. 2.3.2.

Note the following relation obtained by integrating the first equation in (2.5.4) with the help of (2.5.5) and (2.5.6):

$$\rho' = 1 + \frac{3}{4\pi}V_1 - \frac{1}{2}\kappa\zeta. \tag{2.5.12}$$

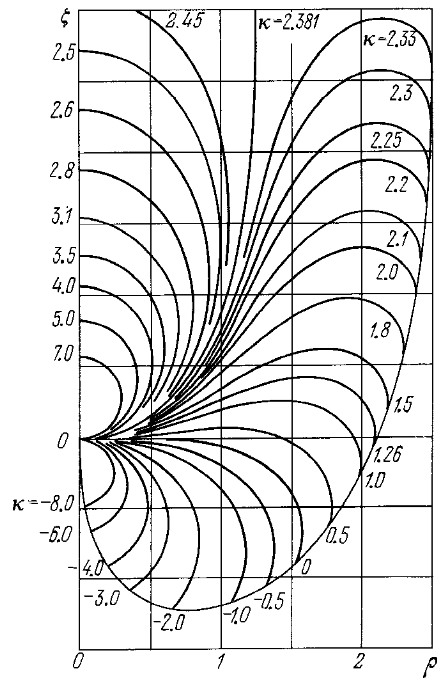

Fig. 2.29

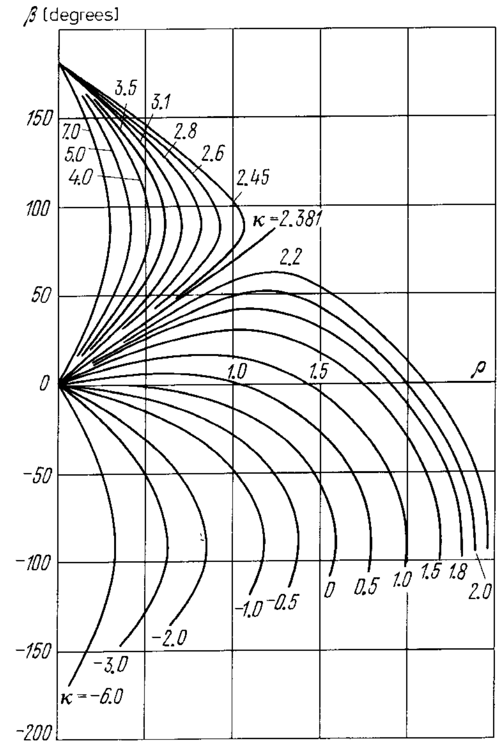

Fig. 2.30

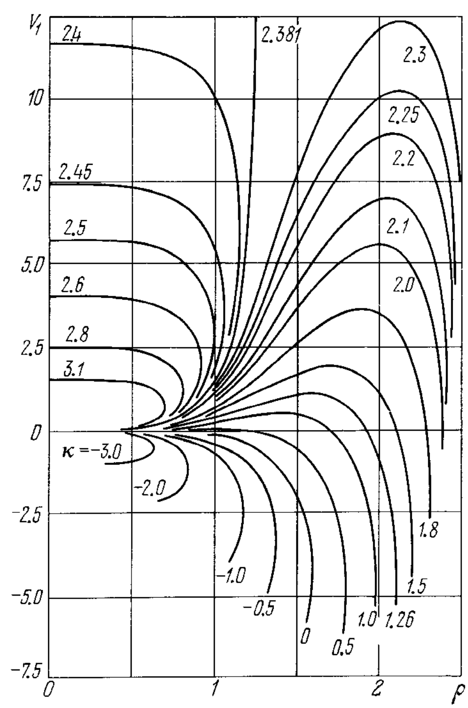

Fig. 2.31

Table 2.2. Parameters of a bubble in a rotating zero-gravity liquid

κ	V_g	ρ_1	H	κ	V_g	ρ_1	H
11.898	0.020	0.168	0.168	2.432	8.312	1.084	1.638
8.057	0.064	0.249	0.250	2.402	11.368	1.146	1.962
6.000	0.160	0.337	0.340	2.3875	15.452	1.195	2.382
4.741	0.340	0.430	0.439	2.3848	17.512	1.211	2.591
3.923	0.644	0.529	0.549	2.3829	19.928	1.226	2.837
3.372	1.120	0.630	0.672	2.3819	22.836	1.237	3.129
3.001	1.828	0.732	0.812	2.38139	26.488	1.246	3.495
2.754	2.820	0.830	0.971	2.381185	31.376	1.252	3.984
2.591	4.180	0.924	1.157	2.381113	38.824	1.257	4.732
2.491	6.188	1.010	1.376	2.381102	54.736	1.259	6.328
				$\frac{3}{\sqrt[3]{2}} = 2.3811016$	∞	$\sqrt[3]{2} = 1.2599$	∞

The equilibrium surface may not even come in contact with the vessel walls and form a gas bubble whose position with respect to the axis of rotation is determined only by the posibility of its containment inside the vessel. It can be seen from Fig. 2.28 that such surfaces can be obtained only for $\kappa \geqslant 3/\sqrt[3]{2}$. Each such value of κ has corresponding (dimensionless) values of volume V_g, equatorial radius ρ_1, and height $2H$ of the bubble (see Table 2.2 which has been compiled by using the results obtained by *Rosenthal* [144]). If the volume v_g of a bubble is known, we can find the corresponding dimensionless volume $V_g = pv_g$, after which we can determine ρ_1 and H (and the entire equilibrium line, if necessary) and then revert to dimensional variables with the help of formulas (2.5.1).

Besides (2.5.8), the bubble parameters are also connected by the relation

$$3V_g/(8\pi) - \kappa H/2 = -1,$$

which follows from (2.5.12).

If $V_g \to \infty$, we get $\rho_1 \to \sqrt[3]{2}$, and thus, $V_g \sim 2\sqrt[3]{4}\pi H$, whence $v_g \sim 2\sqrt[3]{4}\pi p^{-2/3}h$, $r_1 \sim \sqrt[3]{2}p^{-1/3}$. Hence, if $\omega \to \infty$ and the other parameters remain unchanged, the dimensional height $h \propto \omega^{4/3}$ and $r_1 \propto \omega^{-2/3}$. If $V_g \to 0$, the bubble surface becomes spherical.

Slobozhanin [171] (see also [20], pp. 30–31) has described a method for approximating the bubble surface to an elongated ellipsoid of revolution on the basis of minimization of the potential energy of the system (Sect. 2.1.4). The approximation is found to be quite satisfactory for not too large values of V_g (for example, the error in the radius values does not exceed 4% for $V_g \leqslant 12$) and improves with decreasing V_g. As $V_g \to 0$, the elongation of the ellipsoid; i.e., $(a_\zeta - a_\rho)/a_\zeta$ (where the symbols are used in the obvious sense), tends to $(3/16\pi)V_g$.

Analogous asymptotic properties of an exact equilibrium surface have not been investigated so far.

2.5.4 Equilibrium Shapes of a Rotating Drop

It can be seen from Fig. 2.28 that closed equilibrium surfaces without self-intersection are also possible for all $\kappa \leqslant \kappa^*$, where $\kappa^* = 1.2633$ is the value of κ for which the equatorial point is at the same height as the "pole" O. However, such surfaces now contain liquid *inside* them; i.e., they confine an equilibrium rotating drop.

Table 2.3. Parameters of a rotating drop under zero gravity

κ	V	T	ρ_1	$2H$	κ	V	T	ρ_1	$2H$
−8.000	0.064	0.003	0.249	0.496	−0.771[b]	5.738	0.478	1.269	1.634
−6.000	0.150	0.007	0.330	0.655	−0.500	6.720	0.643	1.379	1.582
−4.000	0.467	0.023	0.486	0.944	−0.208[b]	7.734	0.883	1.500	1.477
−3.000	0.968	0.050	0.626	1.179	0[b]	8.378	1.106	1.587	1.369
−2.500	1.454	0.078	0.724	1.322	0.300	9.107	1.539	1.713	1.162
−1.942[b]	2.334	0.135	0.864	1.486	0.550[a]	9.460	2.048	1.817	0.939
−1.672[b]	2.928	0.179	0.944	1.556	0.703[a]	9.526	2.461	1.880	0.780
−1.402[b]	3.647	0.239	1.033	1.611	0.763[b]	9.515	2.652	1.904	0.712
−1.115[b]	4.541	0.328	1.136	1.643	0.900	9.402	3.179	1.960	0.544
−0.907	5.253	0.412	1.215	1.645	1.000[a]	9.235	3.661	2.000	0.409
−0.884[b]	5.333	0.422	1.224	1.644	1.079[b]	9.046	4.125	2.031	0.296
−0.794[a]	5.656	0.466	1.260	1.637	1.2633[b]	8.378	5.671	2.104	0

[a] Results obtained by Ross.
[b] Results obtained by Chandrasekhar.

The analysis of a drop is carried out in the same way as that of the bubble in Sect. 2.5.3. Table 2.3 contains the values of the functions $V(\kappa)$, $T(\kappa)$, $\rho_1(\kappa)$, and $2H(\kappa)$, where ρ_1 is the equatorial radius, $2H$ is the distance between poles and $T = G^2/(\rho\sigma v^{7/3})$ is a dimensionless parameter characterizing the angular momentum G of the drop with respect to the rotational axis ($G = I\omega$, I is the moment of inertia of the liquid, and ρ is its density). By compiling this table we made use of the results obtained by *Ross* [145] (denoted by superscript a) and *Chandrasekhar* [43] (superscript b). In accordance with (2.5.12), the following relation is valid for the drop:

$$3V/(8\pi) - \kappa H/2 = 1.$$

It can be seen that as V increases to $V = 8.378$ ($\kappa = 0$), the surface near the poles becomes flatter although it still remains convex. A recess appears at the poles upon a further increase in the value of V, and *two* equilibrium surfaces correspond to each value of V from 8.378 right up to $V_{max} = 9.526$ ($\kappa = 0.703$). It will be seen in Chap. 3 that the figures corresponding to the region of decreasing $V(\kappa)$ are unstable. Both poles merge at $\kappa = 1.2633$ and V assumes the same values as for $\kappa = 0$.

The discussion at the end of Sect. 2.5.3 leads to an oblate ellipsoid whose oblateness is asymptotically equal to $(3/16\pi)V$ for $V \to 0$.

2.5.5 Reference Commentaries

The well-known experiments of Plateau, lively discussed in connection with cosmological questions, raised the problem of the equilibrium figures of a rotating drop (isolated portion of a capillary fluid). Theoretical investigations in this field were initiated early in the 20th century by Rayleigh and Appell, and were continued by Boussinesq, Globa-Mikhailenko and Charrueau (see bibliography in *Appell*'s book [1] and in *Habip*'s paper [70]). In particular, *Charrueau* (in [1]) expressed the solution in terms of elliptic integrals (Sect. 2.5.2), investigated the properties of equilibrium shapes as a function of the parameter $h = \rho\omega^2 r_1^3/(8\sigma)$, where r_1 is the equatorial radius, and obtained the value of h_{max}

corresponding to $\kappa = 1.2633$. (We can easily derive the relation $\kappa = (h-1)\sqrt[3]{2/h}$ between the parameters h and κ from (2.5.7).) Later, these investigations were continued by *Sperber* [198], *Chandrasekhar* [43] and *Ross* [145] (see also review [220]). Characteristics of a wide range of shapes of a rotating drop are tabulated in [197].

Rosenthal [144] carried out similar studies on a gas bubble in a rotating liquid by taking the dimensionless volume V_g as the characteristic parameter. He also considered the asymptotic behavior of the shape of the bubble as $V_g \to \infty$. Numerical results of this problem are also given by *DiMaggio* [57], *Ross* [145] and *Princen* et al. [141]. The latter have determined the value of σ from the shape of a drop in a rotating tube containing a denser liquid. The equilibrium shape of a rotating liquid containing a gas bubble was investigated by *Bauer* and *Siekmann* [14]. *Barnyak* and *Lukovskii* [11, 12] used the power series expansion of the solutions for finding the equilibrium shapes (see Sect. 2.4.6).

This Sect. 2.5 is based on the results reported in [20, 43, 144, 145, 171, 187, 191, 197].

2.6 Axisymmetric Rotation Problem in a Gravitational Force Field

2.6.1 General Remarks

Let us return to the general case described by the system of Eqs. (2.3.2) and initial conditions (2.3.3). To begin with, it should be noted that the following expansions can be used for numerical integration for small values of s:

$$r = s - \tfrac{1}{24}q^2s^3 + \left(-\tfrac{1}{160}bq^2 + \tfrac{1}{40}pq + \tfrac{1}{1920}q^4\right)s^5 + \cdots,$$

$$z = \tfrac{1}{4}qs^2 + \left(\tfrac{1}{64}bq - \tfrac{1}{16}p - \tfrac{1}{192}q^3\right)s^4 + \cdots.$$

The number of parameters (b, p, q) in the Cauchy problem (2.3.2–3) can be reduced by going over to dimensionless parameters. For example, by using variables (2.4.1), we obtain the system

$$\begin{aligned}\rho'' &= -\zeta'(\varepsilon\zeta - \nu\rho^2 + \kappa - \zeta'/\rho),\\ \zeta'' &= \rho'(\varepsilon\zeta - \nu\rho^2 + \kappa - \zeta'/\rho),\end{aligned} \tag{2.6.1}$$

where $\varepsilon = \pm 1 (b \gtrless 0)$, $\nu = p|b|^{-3/2} (>0)$; in this case, only two parameters are left. The system in variables (2.5.1) has a similar form (here we must put $\mu\zeta - \rho^2$ for $\varepsilon\zeta - \nu\rho^2$, where $\mu = bp^{-2/3} = \varepsilon\nu^{-2/3}$).

The presence of two parameters complicates the visual representation of the family of integral lines in the entire volume but does not hinder the application of the graphic method described in Sect. 2.3.2 for any specific value of ν. (Some special solutions of system (2.6.1) are given in [20, 225]. However, it is possible to construct the family of equilibrium lines in several problems containing only one intrinsic parameter. One of the most universal methods for such constructions is the method of continuation of solutions with respect to the parameter. It is well known in the theory of approximate calculation and involves a transition to differential equations which determine the evolution of the required quantities with changing parameter and can be solve numerically.

It should be recalled that for the finite equation $F(x; \lambda) = 0$ with parameter λ and a known solution $x = x_0$ for a certain value of $\lambda = \lambda_0$, the method consists in a transition to the Cauchy problem

$$dx/d\lambda = -F'_\lambda(x; \lambda)/F'_x(x; \lambda), \quad x|_{\lambda=\lambda_0} = x_0,$$

which can be numerically solved using any scaling scheme. We can thus continue the solution of $x(\lambda)$ for a finite (not small) interval λ as long as it remains finite and $F'_x(x(\lambda); \lambda) \neq 0$. If this condition is violated for a certain value of λ, a branching of the solution takes place in the neighborhood of this point (Sect. 4.1).

While using this method for constructing equilibrium lines, we have to observe the change in a function and not in a number. This somewhat complicates the calculations although the method remains the same in principle. For simplicity of notation, we shall speak of the dependence $z(r)$ and assume that it is required to construct a system of equilibrium surfaces if $b = \text{const}$ and p changes. The volume v of the liquid and the contact angle α are assumed to be given (*slow accelerating rotation problem*). Let us write (2.3.1) in the general form:

$$z'' = f(r, z, z'; p, q).$$

The initial and final conditions, as well as the condition of conservation of volume are written as follows:

$$z(0) = z_0, \quad z'(0) = 0, \quad \varphi(r_A, z(r_A)) = 0,$$

$$\psi(r_A, z(r_A), \quad z'(r_A)) = 0, \quad \int_0^{r_A} F(r, z)\, dr = 0.$$

Here functions f, φ, ψ, and F are given, the values of p are specified; function $z(r)$ $(0 \leqslant r \leqslant r_A)$ and the values of q, z_0 and r_A are unknown. Suppose that this problem can be solved for a certain value of p with the help of, say, the methods described in Sect. 2.3. Then, denoting the derivative with respect to p by a bar, we obtain

$$\bar{z}'' = f'_z\bar{z} + f'_{z'}\bar{z}' + f'_p + f'_q\bar{q}, \quad \bar{z}(0) = \bar{z}_0, \quad \bar{z}'(0) = 0, \tag{2.6.2}$$

$$\left.\begin{aligned} &\varphi'_r\bar{r}_A + \varphi'_z(\bar{z}(r_A) + z'(r_A)\bar{r}_A) = 0,\\ &\psi'_r\bar{r}_A + \psi'_z(\bar{z}(r_A) + z'(r_A)\bar{r}_A) + \psi'_{z'}(\bar{z}'(r_A) + z''(r_A)\bar{r}_A) = 0,\\ &\int_0^{r_A} F'_z\bar{z}\, dr + F(r_A, z(r_A))\bar{r}_A = 0. \end{aligned}\right\} \tag{2.6.3}$$

In view of relations (2.6.2), we get

$$\bar{z}(r) = u(r) + \bar{q}v(r) + \bar{z}_0 w(r), \tag{2.6.4}$$

where u, v and w are solutions of problem (2.6.2) in which $(f'_p + f'_q\bar{q})$ and $\bar{z}_0$ are replaced by f'_p and 0, f'_q and 0, and 0 and 1, respectively. Having found u, v and w and substituting (2.6.4) into (2.6.3), we obtain a first-degree system of equations from which we can find $\bar{q}$, $\bar{z}_0$ and $\bar{r}_A$. This enables us to take a small step along p and we can use any recalculation method for finding the values of q, z_0 and r_A upon a change in the value of p. Taking such steps, we can construct the equilibrium line until branching takes place.

We now show that the procedure for constructing families of equilibrium lines can be considerably simplified for vessels of simplest shapes by using special methods for choosing the parameter.

2.6.2 Cylinder

The equilibrium shape of a free surface leaning against the walls of a cylinder is determined by three dimensionless parameters: the Bond number $\mathbf{Bo} = br_0^2 = \varepsilon\rho_0^2$ (r_0 is the dimensional radius of the cylinder), the number $\mathbf{P} = pr_0^3 = v|\mathbf{Bo}|^{3/2}$, and the contact angle α. A change in the liquid volume causes only an apparent displacement of the equilibrium surface as a whole along the z-axis.

Suppose that a family of equilibrium shapes is to be constructed for given **Bo** and **P** by taking α as the parameter. For this purpose we can integrate system (2.6.1) (under standard initial conditions (2.4.3), not to be mentioned henceforth) for different values of κ over the smallest interval $(0, \tau_0)$ for which $\rho(\tau_0) = \rho_0 = |\mathbf{Bo}|^{1/2}$. The lines thus obtained are marked by the values of $\alpha = \arccos \zeta'(\tau_0)$.

Let us now consider the case in which α and v are given and **Bo** serves as the parameter. Here, we can integrate system (2.6.1) for different κ to the smallest value of τ_0 for which $\zeta'(\tau_0) = \cos\alpha$. The lines are marked by the values of $\mathbf{Bo} = \varepsilon[\rho(\tau_0)]^2$. Certain results of numerical construction of equilibrium surfaces of a liquid rotating in a cylinder for $\mathbf{Bo} > 0$ are given in the paper by *Wasserman* and *Slattery* [221].

2.6.3 Cone and Sphere

(1) For a cone with slope angle δ of the generatrix, we can take for the characteristic length $l = \sqrt[3]{v}$, whence $\mathbf{Bo} = bl^2 = \varepsilon V^{2/3}$, $\mathbf{P} = pl^3 = vV$. We assume that α and v are given and V serves as the parameter. In this case, we can integrate system (2.6.1) for different κ up to the smallest τ_0 for which $\delta - \beta(\tau_0) = \alpha$. The lines obtained in this way are marked by the values of

$$V = \tfrac{1}{3}\pi[\rho(\tau_0)]^3 \tan\delta - \pi \int_0^{\tau_0} \rho^2\zeta'\, d\tau.$$

(2) For a sphere of radius r_0, we can take $\mathbf{Bo} = br_0^2 = \varepsilon\rho_0^2$ and $\mathbf{P} = pr_0^3 = v|\mathbf{Bo}|^{3/2}$. Suppose that v, α, and the filling coefficient $k_f = v/(\frac{4}{3}\pi r_0^3)$ are given and **Bo** serves as the parameter. We can then integrate system (2.6.1) for different κ up to the lowest value of τ_0 for which a circle with its center on the ζ-axis, leaning at a given angle α to the equilibrium line, ensures the given coefficient k_f. It can be easily verified that this condition is equivalent to the equality

$$V(\tau_0) \equiv \pi\rho_0^3(\tfrac{2}{3} - \cos\delta_0 + \tfrac{1}{3}\cos^3\delta_0) - \pi \int_0^{\tau_0} \rho^2\zeta'\, d\tau = \tfrac{4}{3}\pi k_f \rho_0^3,$$

where $\rho_0 = \rho(\tau_0)/\sin\delta_0$, $\delta_0 = \alpha + \beta(\tau_0)$. The line thus obtained is marked by the value of $\mathbf{Bo} = \varepsilon\rho_0^2$.

In practical calculations for $p = 0$, it is advantageous to use the following properties of the function $k_f = k_f(\kappa, \tau_0)$ for a sphere:

(a) $\lim_{\tau_0 \to 0} k_f(\kappa, \tau_0) = k_\alpha \equiv (2 - 3\cos\alpha + \cos^3\alpha)/4$,

where k_α is the filling coefficient for a spherical vessel for the horizontal equilibrium surface Γ;

(b) for $\kappa > 0$, the function $k_f(\kappa, \tau_0)$ increases with τ_0, while for $\kappa < 0$ it decreases;

(c) for $\kappa = 0$, we get $k_f(0, \tau_0) \equiv k_\alpha$.

Hence, if α and k_f are given, we should choose the values $\kappa > 0$ for $k_f > k_\alpha$ in the Cauchy problem (2.4.2–3), and the values $\kappa < 0$ in the opposite case.

(3) The method described above for a sphere can be used for any axially symmetric vessel. The only complication (which, by the way, is not a matter of principle) is that when the axial cross section with the equation, say, of the type $r = \varphi(t)$, $z = \psi(t)$ is inclined to the equilibrium line, we shall have to solve the following equation at each step in τ, generally numerically:

$$\tan[\alpha + \beta(\tau)] = \psi'(t)/\varphi'(t). \tag{2.6.5}$$

Generally speaking, the volume also has to be found numerically:

$$V_2 = \left(\frac{\rho(\tau)}{\varphi(t)}\right)^3 \pi \int_{t_{\min}}^{t} r^2 z' \, dt. \tag{2.6.6}$$

If small steps are taken in τ, (2.6.5) can be solved using Newton's method, for example, in the following form: having written the equation in the form $u(\tau) = w(t)$, we get

$$t_{k+1} = \theta_{k+1} + [u(\tau_{k+1}) - w(\theta_{k+1})]/w'(\theta_{k+1}), \quad \text{where}$$

$$\theta_{k+1} = t_k + \frac{\Delta\tau_k}{\Delta\tau_{k-1}} \Delta t_{k-1}.$$

2.6.4 Application of the First Integral of the Equilibrium Equation

If the problem is confined to finding the equilibrium surface in a given vessel for fixed values of the physical quantities, numerical integration using the first integral of the equilibrium equation (Sect. 2.3.2) proves effective. For this purpose, we go over to dimensionless variables in (2.3.2) and (2.3.6), taking the characteristic length of the vessel as the unit of the scale. In this case, these equations retain their form but b and p are now replaced by **Bo** and **P** respectively.

Figure 2.32 shows the equilibrium surfaces of a liquid filling an elongated ellipsoid of revolution with the semiaxes ratio 1 : 2. These surfaces were constructed in [208] by using the method described above. Curve 1 corresponds to the filling coefficient $k_f = 0.3$, $\alpha = 60°$, **Bo** = 2, **P** = 10, while curve 2 corresponds to the values $k_f = 0.7$, $\alpha = 120°$, **Bo** = 1, and **P** = 5 (the minor semiaxis of the ellipsoid is taken as the characteristic length). Curves 3 and 4 correspond to the case in which **P** = 0, while the other quantities have the values indicated above. A comparison of curves 1 and 2 with curves 3 and 4,

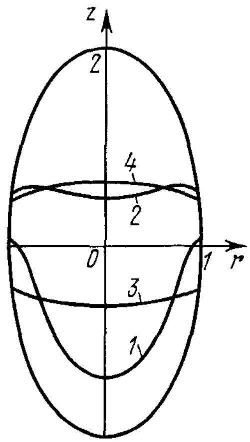

Fig. 2.32

respectively, helps in drawing a qualitative conclusion about the change in the shape of the equilibrium surface upon a slow increase in the value of ω. In this case, a depression is formed at the axis of rotation and gradually increases until the free surface touches the bottom. A further increase in the value of ω makes the surface doubly connected.

In conclusion, it should be mentioned that it is interesting to work out a simple method for constructing the families of equilibrium surfaces for the most natural case in which the vessel and the contact angle α are given, while of the three quantities b, p and v, two are fixed and the third serves as the parameter.

2.7 Axisymmetric Problem for Large Bond Numbers

For large values of the Bond number, the form of the equilibrium surface can be determined using the methods of the boundary-layer theory. Such a situation arises when the forces of surface tension are small in comparison with the gravitational forces, and occurs not only for large values of g, but also for small values, if the dimensions of the vessel are quite large. This section is based on the results obtained by *Srubshchik* and *Yudovich* [200].

2.7.1 Formulation of the Problem

For the sake of simplicity, let us first assume that the dependence $z(r)$ is single-valued for a free surface so that we can use (2.3.1). Having chosen the characteristic length l of the vessel, we introduce the dimensionless variables r/l and z/l, denoting then again by the letters r and z. Taking $\mathbf{Bo} = bl^2 \gg 1$, we can rewrite (2.3.1) in the form

$$\varepsilon^2 \frac{1}{r}\left(\frac{ru'}{\sqrt{1+u'^2}}\right)' - u + \frac{1}{2}\omega_0^2 r^2 = 0, \quad \left(' = \frac{d}{dr}\right), \tag{2.7.1}$$

where the following notation has been used:

$$\varepsilon = (\mathbf{Bo})^{-1/2}, \quad u = z - c \quad (c = ql/\mathbf{Bo}), \quad \omega_0 = \sqrt{l/g}\,\omega \quad (g > 0).$$

Henceforth, we shall assume that the quantity ω_0 is either finite (rotation) or equal to zero (state of rest), while $\varepsilon \ll 1$. Essentially, this is equivalent to the assumption that the value of σ/ρ is relatively small. The other version, where the condition **Bo** $\gg 1$ is achieved by increasing g (hence, the last term on the left-hand side of (2.7.1) contains the factor ε^2), can be analyzed in a similar manner.

If $\varepsilon = 0$, (2.7.1) has the obvious solution $u = u_0(r) = (1/2)\omega_0^2 r^2$, which is called degenerate. In this case, $z_0(r) = c_0 + (1/2)\omega_0^2 r^2$, where the constant c_0 is chosen in such a way that the liquid has a given volume.

For the sake of definiteness, let us assume that in the neighborhood of the point $(\eta, z(\eta))$ (η is not specified beforehand!) at which the equilibrium line adjoints the axial cross section of the wall, the cross section has the equation $z = f(r)$. In this case, $f(\eta) = z(\eta)$, i.e., $f(\eta) - u(\eta) = c$, while the boundary conditions for the equilibrium line assume the form

$$u'(0) = 0, \quad \{(1 + u'f')[(1 + u'^2)(1 + f'^2)]^{-1/2}\}|_{r=\eta} = \cos\alpha. \tag{2.7.2}$$

The requirement of constant volume leads to the additional condition

$$\int_0^{\eta_0} (z - z_0) r\,dr + \int_{\eta_0}^{\eta} (z - f) r\,dr = 0, \tag{2.7.3}$$

where $z_0(r)$ and η_0 correspond to the value $\varepsilon = 0$ (i.e., $\sigma = 0$) and can therefore be easily found from the known volume of the liquid [in this case, $c_0 = f(\eta_0) - (1/2)\omega_0^2 \eta_0^2$].

Since (2.7.1) contains a small parameter as the coefficient of the highest derivative, it can be naturally expected that the solution of problem (2.7.1–3) will differ considerably from the degenerate solution only in the vicinity of the contact line, and the necessary correction can be found by the boundary–layer method.

2.7.2 Construction of the Asymptotic Expansion

According to the methods of the boundary-layer theory (see, for example, [199, 243, 249]), the solution containing the function $u = u_\varepsilon(r)$ and the quantities η_ε and c_ε should be sought in the form

$$u_\varepsilon(r) \sim \sum_{i=0}^{\infty} \varepsilon^i w_i(r) + \varepsilon \sum_{i=0}^{\infty} \varepsilon^i v_i\left(\frac{\eta_\varepsilon - r}{\varepsilon}\right), \tag{2.7.4}$$

$$\eta_\varepsilon \sim \sum_{i=0}^{\infty} \varepsilon^i \eta_i, \quad c_\varepsilon \sim \sum_{i=0}^{\infty} \varepsilon^i c_i. \tag{2.7.5}$$

Here the series $\sum_i \varepsilon^i w_i$ is obtained from the condition that (2.7.1) is formally satisfied (first iterative process). In particular, we get

$$w_0 = \tfrac{1}{2}\omega_0^2 r^2, \quad w_1 = 0, \quad w_2 = (2\omega_0^2 + \omega_0^6 r^2)(1 + \omega_0^4 r^2)^{-3/2}.$$

(We could have easily written down a rather involved recurrence relation in which the function $w_i(r)$ for each i is expressed in terms of the preceding functions.) Hence we get $z_0 = c_0 + (1/2)\omega_0^2 r^2$, as expected (see Sect. 2.7.1).

The constructed sum $\sum_i \varepsilon^i w_i$ satisfies the first of the boundary conditions (2.7.2). The second boundary condition is ensured by choosing the series $\varepsilon \sum_i \varepsilon^i v_i$, obtained as a result of the so-called second iterative process. For this purpose, we use the substitution $\eta_\varepsilon - r = \varepsilon t$ and expand all terms of (2.7.1) and of the second boundary condition in (2.7.2), in which we have substituted expression (2.7.4), into power series in ε. In particular, we obtain the following differential equation for $v_0(t)$:

$$v_0'' - v_0(1 + \omega_0^4\eta_0^2 - 2\omega_0^2\eta_0 v_0' + v_0'^2)^{3/2} = 0 \tag{2.7.6}$$

and the following boundary conditions:

$$\begin{aligned} v_0'(0) &= \omega_0^2\eta_0 + \{f'(\eta_0) - \sin\alpha\cos\alpha[1 + f'^2(\eta_0)]\} \\ &\quad \times [f'^2(\eta_0)\sin^2\alpha - \cos^2\alpha]^{-1}, \\ v_0(\infty) &= 0 \end{aligned} \tag{2.7.7}$$

(the second condition is necessary for functions of the boundary-layer type).

For each of the subsequent functions $v_i(t)$ we obtain a linear differential equation of the type

$$[(1 + \omega_0^4\eta_0^2 - 2\omega_0^2\eta_0 v_0' + v_0'^2)^{-3/2} v_i']' - v_i = f_i(t)$$

and boundary conditions of the type

$$v_i'(0) = a_i, \quad v_i(\infty) = 0.$$

Here, function $f_i(t)$ and constant a_i are expressed in terms of functions $v_0(t), \ldots, v_{i-1}(t)$ and their derivatives, by the constants $\eta_0, \ldots, \eta_i$, and the values of functions $w_0(r), \ldots, w_{i+1}(r)$ and their derivatives for $r = \eta_0$. On the other hand, the expansion of condition (2.7.3) and the equality $f(\eta_\varepsilon) - u_\varepsilon(\eta_\varepsilon) = c_\varepsilon$ into power series in ε gives a system of two linear algebraic equations with determinant $[f'(\eta_0) - \eta_0\omega_0^2]\eta_0^2/2$ for obtaining c_i and η_i. The right-hand parts of this system are expressed by the functions $w_0(r), \ldots, w_i(r), v_0(t), \ldots, v_{i-1}(t)$ and their derivatives, as well as by the constants $c_0, \ldots, c_{i-1}, \eta_0, \ldots, \eta_{i-1}$. Knowing $w_0(r)$ and calculating η_0 and c_0, we can in principle calculate any number of terms in expansions (2.7.4) and (2.7.5) in the following order: $w_1(r)$ ($\equiv 0$), $v_0(t), c_1, \eta_1, w_2(r), v_1(t), c_2, \eta_2, \ldots$. In particular, simple calculations give

$$c_1 = 0, \quad \eta_1 = v_0(0)[f'(\eta_0) - \eta_0\omega_0^2]^{-1}.$$

The condition $f'(\eta_0) - \eta_0\omega_0^2 \neq 0$ is quite important in the construction of the boundary layer. It means that the equilibrium surface constructed without taking surface tension into account must not touch the vessel walls. Physically, it is obvious that in the special case in which the surface touches the walls, the surface tension near the contact line will play a more important role. Indeed, it can be shown that the boundary layer in this case is constructed using fractional power series in ε. This special case will not be discussed here.

2.7.3 Boundary Layer Equation

It can be easily verified that (2.7.6) for the principal term of the boundary layer under the second boundary condition (2.7.7) is integrated in elementary functions. For this purpose, we must multiply both sides of the equation by $v_0'(1 + \omega_0^4\eta_0^2 - 2\omega_0^2\eta_0 v_0' + v_0'^2)^{-3/2}$

and integrate by taking the boundary condition into account. After simple transformations, this gives

$$(\sqrt{1 + \omega_0^4 \eta_0^2} - \tfrac{1}{4} v_0^2) v_0^2 = v_0'^2 (1 + \omega_0^4 \eta_0^2 - 2\omega_0^2 \eta_0 v_0' + v_0'^2)^{-1}. \tag{2.7.8}$$

Here, we can express v_0' in terms of v_0 and integrate once again after the separation of variables. The integral is found to be elementary; i.e., we obtain an explicit expression for the function inverse to $v_0(t)$:

$$t = k - \nu^{-3/2}\left[\frac{1}{2}\ln\frac{2\sqrt{\nu} - \sqrt{4\nu - v_0^2}}{2\sqrt{\nu} + \sqrt{4\nu - v_0^2}} + \nu^{-1/2}(\sqrt{4\nu - v_0^2} - \omega_0^2 \eta_0 v_0)\right],$$

where $\nu = \sqrt{1 + \omega_0^4 \eta_0^2}$, and the constant k is equal to

$$k = \nu^{-3/2}\left\{\frac{1}{2}\ln\frac{2\sqrt{\nu} - \sqrt{4\nu - v_0^2(0)}}{2\sqrt{\nu} + \sqrt{4\nu - v_0^2(0)}} + \nu^{-1/2}[\sqrt{4\nu - v_0^2(0)} - \omega_0^2 \eta_0 v_0(0)]\right\}.$$

The quantity $v_0(0)$ appearing in this equality is expressed in terms of the value of $v_0'(0)$ (determined from the first condition in (2.7.7)) through the relation

$$\tfrac{1}{2} v_0^2 - \nu = -(\nu^2 - \omega_0^2 \eta_0 v_0')(\nu^2 - 2\omega_0^2 \eta_0 v_0' + v_0'^2)^{-1/2},$$

which follows from (2.7.8).

The qualitative nature of the behavior of the solutions of (2.7.6) can be easily understood by rewriting the equation in the form of the system

$$dv_0/dt = v_0', \quad dv_0'/dt = v_0(1 + \omega_0^4 \eta_0^2 - 2\omega_0^2 \eta_0 v_0' + v_0'^2)^{3/2} \tag{2.7.9}$$

and considering the corresponding family of trajectories in the plane v_0, v_0' (Fig. 2.33). When constructing this family, it should be noted that:

(1) the expression within the parentheses is always positive;
(2) for small values of $|v_0'|$, we obtain from (2.7.9) a system defining the saddle;
(3) for large values of $|v_0'|$, we obtain the following system from (2.7.9):

$$dv_0/dt = v_0', \quad dv_0'/dt = v_0 |v_0'|^3, \quad \text{i.e.} \quad dv_0'/dv_0 = v_0 v_0'^2 \operatorname{sgn} v_0',$$

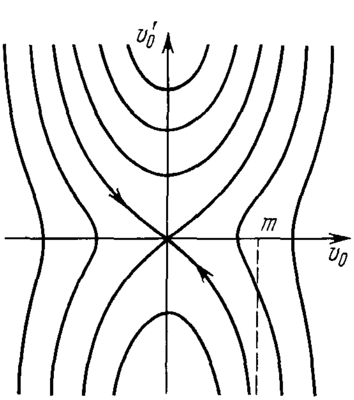

Fig. 2.33

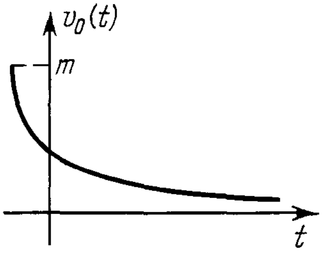

Fig. 2.34

from which, in particular, it can be seen that v_0 as well as t have finite limits as $|v_0'| \to \infty$. Separatrices marked by arrows in Fig. 2.33 correspond to solutions satisfying the second condition in (2.7.7). The onset of the motion along one of the separatrices is determined by the fist condition in (2.7.7). It can be seen from (2.7.6) that the solution under consideration is of the order $\exp[-(1 + \omega_0^4\eta_0^2)^{3/4}t]$ as $t \to \infty$. Thus, for $v_0'(0) < 0$, the solution $v_0(t)$ extended on both sides has the form shown in Fig. 2.34. As $v_0'(0)$ changes, the curve for $v_0(t)$ is obtained from this curve by simple translation. For $v_0'(0) > 0$, the pattern is more or less the same, although the curve is pressed towards the t-axis for $\omega_0 \neq 0$.

So far, we have assumed that the function $z(r)$ is single-valued. However, this may not be always true. For example, the liquid surface in a conical vessel wraps itself towards the rotation axis near the contact line for sufficiently large values of the contact angle α. When applying (2.3.1) in this case, it should be assumed that $\mathbf{Bo} = bl^2 < 0$, $|\mathbf{Bo}| \gg 1$ on the corresponding segment of the equilibrium line. Then, the first minus sign in Boundary layer equation (2.7.6) must be replaced by a plus sign. This leads to the family of trajectories shown in Fig. 2.35. In particular, the trajectory with the asymptote $v_0 = m$ corresponds to the solution whose graph is a natural extension of the curve shown in Fig. 2.34. Together, these two form a curve (Fig. 2.36) whose infinite arcs form the boundary-layer profile in the case of wrapping of the free liquid surface.

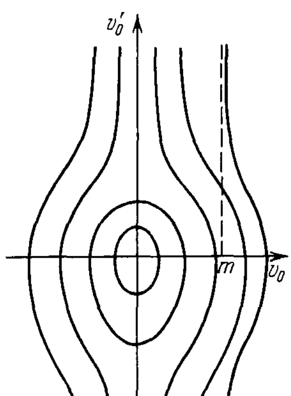

Fig. 2.35

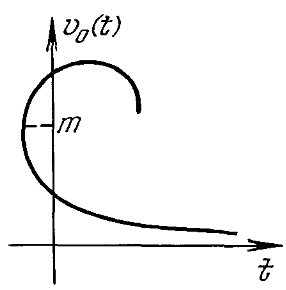

Fig. 2.36

2.7.4 Remarks

Thus, to within quantities of the order $(\mathbf{Bo})^{-1}$, we obtain for $\mathbf{Bo} \gg 1$

$$z(r) = c_0 + \frac{1}{2}\omega_0^2 r^2 + \frac{1}{\sqrt{\mathbf{Bo}}} v_0((\eta_0 - r)\sqrt{\mathbf{Bo}} + \eta_1) + O(\mathbf{Bo}^{-1}).$$

As mentioned above, we proceed in this case from the solution of the degenerate ($\mathbf{Bo} = \infty$) problem $z_0(r) = c_0 + (1/2)\omega_0^2 r^2$.

It is interesting that for certain open vessels, the degenerate solution exists, but not for all values of volume V, and for some other vessels, such a solution is not possible at all. Thus, for a conical vessel with generatrix $z = kr$, the maximum volume $V_{\max}$ will be obtained (Fig. 2.37) for

$$c_0 + \tfrac{1}{2}\omega_0^2\eta_0^2 = k\eta_0, \quad \omega_0^2\eta_0 = k; \quad \text{i.e., for}$$

$$c_0 = k^2/(2\omega_0^2), \quad \eta_0 = k/\omega_0^2,$$

whence $V_{\max} = \pi k^4/12\omega_0^6$. If $V > V_{\max}$, equilibrium of the rotating liquid is not possible for sufficiently large $\mathbf{Bo}$ and the excess liquid overflows from the vessel.

By way of another example, let us consider a vessel with axial cross section $z = kr^2$. Here, it is clear that for $k < (1/2)\omega_0^2$, the degenerate solution does not exist for any value of V. In other words, the entire liquid flows out of the vessel. For $k > (1/2)\omega_0^2$, a solution is possible for any V.

The examples described above can be generalized. Namely, we assume that the axial cross section of the vessel wall has the equation

$$z = f(r)\ (0 \leqslant r < \infty),$$

where $f(0) = 0$. It can then be easily verified that the degenerate solutions have the following properties:

(1) if $f(r) \leqslant (1/2)\omega_0^2 r^2$ $(0 \leqslant r < \infty)$, a solution with a simply connected free surface is not possible for any V;

(2) if $f''(r) < \omega_0^2$ for all values of $r > 0$ satisfying the relation $f'(r) = \omega_0^2 r$, doubly connected equilibrium shapes of the liquid are not possible (we are speaking only of shapes which do not extend to infinity);

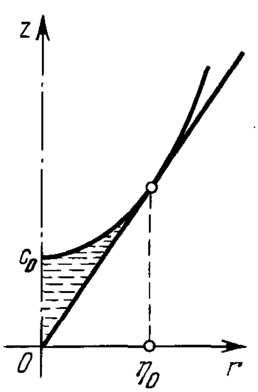

Fig. 2.37

(3) if $f(r) > (1/2)\omega_0^2 r^2$ for certain r, but $f(r) \leqslant (1/2)\omega_0^2 r^2$ for all sufficiently large values of r, a V_{max} ($< \infty$) exists for shapes with a simply connected free surface;

(4) if $(1/2)\omega_0^2 r^2 - f(r) \to \infty$ as $r \to \infty$, and $f'(r) \neq \omega_0^2 r$ for all sufficiently large r, a V_{max} exists for doubly connected shapes if such shapes exist;

(5) if conditions (2) and (3) are satisfied, V can assume all values from 0 to V_{max};

(6) if condition (2) is satisfied and $f(r) - (1/2)\omega_0^2 r^2 \to \infty$ as $r \to \infty$, V can assume all values from 0 to ∞.

In conclusion, it should be mentioned once again that the above discussion covers the special case of a liquid at rest, for which $\omega_0 = 0$. In this case the plane $z = c_0$ serves as the degenerate equilibrium surface and all the calculations are accordingly simplified.

The following fact, established by *Concus* [51], is worth noting: for $\mathbf{Bo} = br_0^2 > 100$, the relative error in the shape of the equilibrium surface of a liquid at rest in a cylinder of radius r_0, obtained by second approximation of the boundary layer methods, the shape being constructed numerically, does not exceed 1%.

2.7.5 Reference Commentaries

Apparently, the boundary-layer methods were first applied to the problems of equilibrium of a capillary liquid at rest by *Moiseev* and *Chernous'ko* [46, 112–115], and later, with more complete mathematical substantiation, by *Srubshchik* and *Yudovich* [199]. The latter also investigated the case of a rotating liquid [200]. Some problems of this kind were analyzed by *Concus* [51] and by *Turkington* and *Osborne* [211]. A similar problem on the axially symmetric equilibrium for quite large ω (the equilibrium surface in this case will be doubly connected!) has been investigated in [174].

2.8. An Axisymmetric Flat (Gently Sloping) Equilibrium Surface

If $|\nabla z| \ll 1$, the equilibrium problem can be linearized and becomes quite simple. This is possible if an equilibrium surface $z = \text{const}$ exists for certain values of system parameters close to the given values.[14] In particular, it is essential that the conditions

$$|\delta - \alpha| \ll 1, \quad |\mathbf{P}| \ll 1, \tag{2.8.1}$$

where standard notation has been used, be simultaneously satisfied. In this section we consider the corresponding axially symmetric problem. The discussion is based on the results obtained by *Chernous'ko* [45, 46] and authors [118].

2.8.1 General Remarks

If $|\nabla z| \ll 1$, (2.3.1) assumes the following form after linearization:

$$z'' + \frac{1}{r}z' - bz = q - pr^2. \tag{2.8.2}$$

Its solution, which is bounded at $r = 0$, will be

[14] In this case, we shall refrain from special situations under which the plane surface is a branching one (see Chap. 4).

$$z = \begin{cases} c\mathrm{I}_0(r\sqrt{b}) - \dfrac{q}{b} + \dfrac{4p}{b^2} + \dfrac{pr^2}{b} & (b > 0), \\ c\mathrm{J}_0(r\sqrt{|b|}) - \dfrac{q}{b} + \dfrac{4p}{b^2} + \dfrac{pr^2}{b} & (b < 0), \\ c + \dfrac{q}{4}r^2 - \dfrac{p}{16}r^4 & (b = 0), \end{cases} \tag{2.8.3}$$

where I_0 and J_0 are Bessel functions and c is an arbitrary constant.

The arbitrary constants are determined from known values of the contact angle α and the volume v of the liquid. If the axial cross section of the vessel is given by the equation $z = f(r)$, we obtain the conditions

$$z(\eta) = f(\eta), \tag{2.8.4}$$

$$\left.\frac{1 + z'f'}{\sqrt{1 + f'^2}}\right|_{r=\eta} = \cos\alpha, \tag{2.8.5}$$

$$\int_0^\eta (z - f)r\,dr\left(= \int_0^{\eta_0} (z_0 - f)r\,dr\right) = \frac{v}{2\pi}, \tag{2.8.6}$$

where η is the r-coordinate of the contact line, whose value is not known beforehand, while $z_0 \equiv \text{const}$ and η_0 correspond to the case in which there is neither surface tension nor rotation and can therefore be found directly.

Applying conditions (2.8.4–6), we can partially linearize the original problem, since the conditions themselves are nonlinear due to the variable nature of η. For a complete linearization, we use the notation $z = z_0 + \zeta(r)$ and $\eta = \eta_0 + h$. This leads to the following conditions:

$$\begin{gathered} \zeta(\eta_0) = h\tan\delta_0, \\ \zeta'(\eta_0) = [f''(\eta_0)h\cos^2\delta_0 - (\alpha - \delta_0)], \quad \int_0^{\eta_0} \zeta(r)r\,dr = 0, \end{gathered} \tag{2.8.7}$$

where $\tan\delta_0 = f'(\eta_0)$.

The first and third equalities here are obvious, while the second is obtained by linearization of condition (2.8.5) in the neighborhood of the point $r = \eta_0$. Taking the relation $\{1 + [f'(\eta_0)]^2\}^{-1/2} = \cos\delta_0$ into account, we obtain from (2.8.5)

$$\left.\left(\frac{1}{\sqrt{1 + f'^2}}\right)'\right|_{r=\eta_0} h + \left(\frac{\zeta' f'}{\sqrt{1 + f'^2}}\right)_{r=\eta_0} = -(\alpha - \delta_0)\sin\delta_0,$$

leading to the second of equalities (2.8.7).

Eliminating h from the first two equalities in (2.8.7), we get

$$f''(\eta_0)\zeta(\eta_0)\cos^3\delta_0 - \zeta'(\eta_0)\sin\delta_0 = (\alpha - \delta_0)\sin\delta_0. \tag{2.8.8}$$

The function $\zeta(r)$ has the same expressions (2.8.3), but with a different value of q. Hence the third condition in (2.8.7) can be written as

$$\left.\begin{aligned} \frac{c}{\sqrt{b}}\mathrm{I}_1(\sqrt{b}\eta_0) - \frac{q}{b}\frac{\eta_0}{2} + \frac{2p}{b^2}\eta_0 + \frac{p}{b}\frac{\eta_0^3}{4} &= 0 \quad (b > 0), \\ \frac{c}{\sqrt{|b|}}\mathrm{J}_1(\sqrt{|b|}\,\eta_0) - \frac{q}{b}\frac{\eta_0}{2} + \frac{2p}{b^2}\eta_0 + \frac{p}{b}\frac{\eta_0^3}{4} &= 0 \quad (b < 0), \\ c + q\frac{\eta_0^2}{8} - \frac{p}{48}\eta_0^4 &= 0 \quad (b = 0). \end{aligned}\right\} \tag{2.8.9}$$

This condition, together with (2.8.8) into which we have also substituted (2.8.3), forms a system of two first-degree equations for finding q and c, as well as for solving the completely linearized problem. As regards a partially linearized problem (it is natural to expect that such a problem gives a more precise description of the situation), we can use conditions (2.8.4–6), which are linear in q and c, to eliminate these quantities. This leads to a fairly cumbersome finite equation in η.

2.8.2 Cone and Cylinder

(1) For a cone with an apex angle $\pi - 2\delta_0$, we have $f(r) = (\tan\delta_0)r$, and condition (2.8.8) assumes the form $\zeta'(\eta_0) = \delta_0 - \alpha$. Suppose that $b > 0$. Then conditions (2.8.8–9) can be written as follows:

$$c\sqrt{b}\mathrm{I}_1(\sqrt{b}\eta_0) = -2\frac{p}{b}\eta_0 + \delta_0 - \alpha,$$

$$\frac{c}{\sqrt{b}}\mathrm{I}_1(\sqrt{b}\eta_0) - \frac{q}{b}\frac{\eta_0}{2} = -\frac{2p}{b^2}\eta_0 - \frac{p}{4b}\eta_0^3.$$

For the function $\zeta(r)$ of the type (2.8.3) this leads to the following values:

$$c = \frac{1}{\sqrt{b}\mathrm{I}_1(\sqrt{b}\eta_0)}\left(\delta_0 - \alpha - 2\frac{p}{b}\eta_0\right), \quad q = 2\frac{\delta_0 - \alpha}{\eta_0} + \frac{p}{2}\eta_0^2.$$

If the volume v of the liquid is given, we get

$$\eta_0 = \left(\frac{3}{\pi}v\cot\delta_0\right)^{1/3}, \quad z_0 = \left(\frac{3}{\pi}v\tan^2\delta_0\right)^{1/3}.$$

For $b < 0$, we can use the same formulas, substituting $\mathrm{J}_0(\sqrt{|b|}\,r)$ and $-\sqrt{|b|}\,\mathrm{J}_1(\sqrt{|b|}\,\eta_0)$, respectively, for $\mathrm{I}_0(\sqrt{b}r)$ and $\sqrt{b}\mathrm{I}_1(\sqrt{b}\eta_0)$.

Omitting simple calculations, we shall give the final result for the corresponding partially linearized problem: for $b > 0$, the value of η satisfies the transcendental equation

$$\frac{\sqrt{b}\mathrm{I}_1(\sqrt{b}\eta)}{\mathrm{I}_0(\sqrt{b}\eta)}\left[\frac{1}{3}\eta\tan\delta_0 + \frac{2}{b\eta\sin\delta_0}(\cos\alpha - \cos\delta_0) - \frac{v}{\pi\eta^2} - \frac{4p}{b^2} - \frac{p}{2b}\eta^2\right] + \frac{2p}{b}\eta$$
$$= \frac{\cos\alpha - \cos\delta_0}{\sin\delta_0},$$

while the constants q and c for the function $z(r)$ in (2.8.3) are expressed in terms of η by the relations

$$q = \frac{2}{\eta \sin\delta_0}(\cos\alpha - \cos\delta_0) - \frac{2}{3}b\eta\tan\delta_0 - \frac{v}{\pi\eta^2}b + \frac{p}{2}\eta^2,$$

$$c = \frac{1}{\sqrt{b}\mathrm{I}_1(\sqrt{b}\eta)}\left(\frac{\cos\alpha - \cos\delta_0}{\sin\delta_0} - \frac{2p}{b}\eta\right).$$

The case $b < 0$ is treated in the manner described in the previous paragraph. It should be noted that for $b < 0$ and $\mathrm{J}_1(\sqrt{|b|}\,\eta) = 0$, the solution for the general case does not exist. Of course, this is associated with the position of the maximal stability region for small values of q (see Sect. 2.4.3).

(2) The first condition in (2.8.1) assumes the form $|\alpha - \pi/2| \ll 1$ for a cylinder. Relations (2.8.4–6) are not applicable in this case; nevertheless, this does not give rise to any complications. For the sake of simplicity, we choose the origin of coordinates in such a way that $z_0 = 0$ (Fig. 2.38). Then the constant q can be calculated with the help of formula (2.2.19), taking into account the change of notation described in Sect. 2.2.6. After simple transformations allowing for the conservation of volume, we obtain

$$q = \frac{2}{\eta_0}\cos\alpha + \frac{1}{2}p\eta_0^2 - \frac{b}{\pi\eta_0^2}\int_0^{\eta_0} z(r)r\,dr = \frac{2}{\eta_0}\cos\alpha + \frac{1}{2}p\eta_0^2, \tag{2.8.10}$$

where η_0 is the radius of the cylinder. The constant c is calculated from the contact angle; since $z'(\eta_0) = \cot\alpha$, we obtain for $b > 0$, in view of the first formula in (2.8.3),

$$c = \left(\cot\alpha - \frac{2p}{b}\eta_0\right)\Big/[\sqrt{b}\mathrm{I}_1(\sqrt{b}\eta_0)]. \tag{2.8.11}$$

A similar result was obtained for $p = 0$ by *Chernous'ko* [46]. "Completely linearized" formulas are obtained by replacing $\cos\alpha$ and $\cot\alpha$ in (2.8.10) and (2.8.11) by $(\pi/2) - \alpha$.

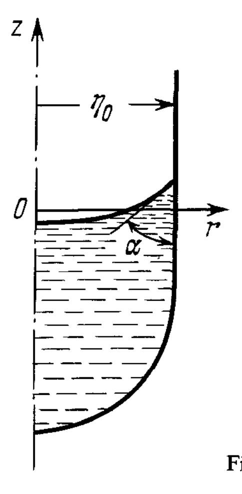

Fig. 2.38

2.8.3 Drop on a Plane

Following the works of *Bondarenko* [21] and *Chernous'ko* [46], let us consider the linearized problem on the equilibrium of a liquid on a horizontal plane. This problem is physically more natural than the ones described in Sect. 2.8.2, since the condition $\alpha \ll 1$ is satisfied much more frequently than, say, the condition $|\alpha - \pi/2| \ll 1$. We shall assume that $\omega = 0$.

Complete linearization (Sect. 2.8.1) is not possible in the present case, since $\eta_0 = \infty$. Hence we shall use only the linearized equation (2.8.2). Proceeding from solution (2.8.3) and a given contact angle α, and choosing the origin on the contact plane, we get for $b > 0$

$$z(r) = \frac{\tan\alpha}{\sqrt{b}\,\mathrm{I}_1(R_0)}[\mathrm{I}_0(R_0) - \mathrm{I}_0(\sqrt{b}r)],$$

where $R_0 = \sqrt{b}r_0$ and r_0 is the radius of the base of the drop. If we are given the volume v of the drop and $V = b^{3/2}v$, we get

$$\frac{V}{\pi\tan\alpha} = \frac{R_0}{\mathrm{I}_1(R_0)}[R_0\mathrm{I}_0(R_0) - 2\mathrm{I}_1(R_0)].$$

Similarly, denoting $R_0 = \sqrt{|b|}\,r_0$, we get for $b < 0$

$$z(r) = \frac{\tan\alpha}{\sqrt{|b|}\,\mathrm{J}_1(R_0)}[\mathrm{J}_0(\sqrt{|b|}\,r) - \mathrm{J}_0(R_0)],$$

$$\frac{V}{\pi\tan\alpha} = \frac{R_0}{\mathrm{J}_1(R_0)}[2\mathrm{J}_1(R_0) - R_0\mathrm{J}_0(R_0)].$$

The obtained dependences $V/(\pi\tan\alpha)$ on R_0 are shown in Fig. 2.39. For given values of V and α, we can find R_0 from these dependences, and hence the solution of the linearized equilibrium problem.

In particular, it follows from the formulas obtained above that $V/\tan\alpha \sim \pi R_0^3/4$ for $R_0 \to 0$. If $b > 0$, the formulas are applicable for all $R_0 > 0$, and $V/\tan\alpha \sim \pi R_0^2$ as $R_0 \to \infty$.

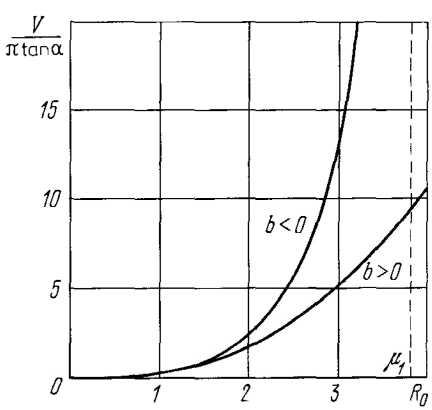

Fig. 2.39

If $b < 0$, the formulas are valid for $0 < R_0 < \mu_1$, where $\mu_1 = 3.8317$ is the smallest positive zero of the function $J_1(R)$, and $V/\tan\alpha \to \infty$ as $R_0 \to \mu_1$. If the rigid surface coincides with the plane $z = 0$ only near the contact line, the construction of the equilibrium surface may become possible even for $R_0 > \mu_1$ if $J_1(R_0) \neq 0$. However, it will be shown in Chap. 3 that the corresponding equilibrium shapes are unstable.

A special situation arises when $\alpha = 0$. In this case, no solution is possible for $b > 0$ (the liquid flows over the entire plane in the form of an infinitely thin layer), while a solution for $b < 0$ is possible only if $R_0 = \mu_1$. This solution has the form

$$z = \frac{v|b|}{\pi\mu_1^2 |J_0(\mu_1)|}[J_0(\sqrt{|b|}\,r) - J_0(\mu_1)] \quad (0 \leqslant r \leqslant \mu_1/\sqrt{|b|}).$$

2.9 Doubly Connected Axisymmetric Equilibrium Surfaces

So far, in Sects. 2.3–8, we have considered only simply connected axially symmetric equilibrium surfaces. Investigation of doubly connected surfaces becomes much more complicated due to the presence of an additional parameter. For example, if we use (2.3.1) and no longer require the boundedness of the solution at $r = 0$ (or even the existence of a solution in the region $r < r_0$), we obtain a three-parametric family of solutions by taking the arbitrariness of q into account. Formally, this increase in the number of parameters is compensated for by the introduction of a second boundary condition. However, the available algorithms for constructing the equilibrium lines are much less effective than for simply connected equilibrium surfaces.[15] It should be noted that the construction of doubly connected surfaces is considerably simplified if the position of the line of contact γ is given. This is the case when these lines serve as the lines of fracture of the vessel surface (for example, in the problem of the shape of a liquid neck when Γ rests on the edge of two coaxial circular discs). The construction of such surfaces is considered in Sect. 3.11 together with the analysis of their stability.

2.9.1 State of Rest Under Zero-Gravity

If there is no external force field or rotation, system of equations (2.3.2) assumes the form

$$r'' = -z'(q - z'/r), \quad z'' = r'(q - z'/r), \quad (' = d/ds). \tag{2.9.1}$$

For $q \neq 0$, we can use the transformation

$$\rho = |q|r, \quad \zeta = qz, \quad \tau = |q|s \tag{2.9.2}$$

and go over to a system without parameters:

$$\rho'' = -\zeta'(1 - \zeta'/\rho), \quad \zeta'' = \rho'(1 - \zeta'/\rho), \quad (' = d/d\tau).$$

From this, we can obtain, to within insignificant substitutions $\tau \to \tau +$ const and $\zeta \to \zeta +$

[15] In particular, the solution of the problem of the evolution of axially symmetric equilibrium form in a toroidal vessel upon the addition of a liquid is quite interesting.

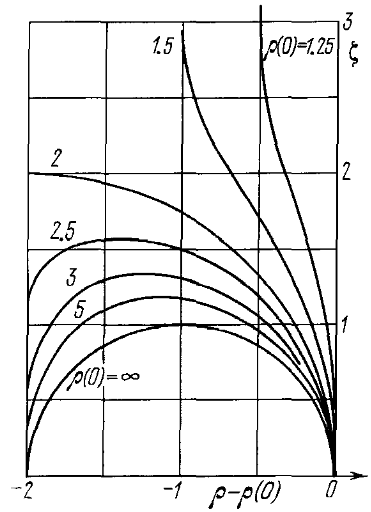

Fig. 2.40

const, the following relations:

$$\rho = \sqrt{1 + a^2 + 2a\cos\tau}, \quad \zeta = \int_0^\tau \frac{1}{\rho(\xi)}(1 + a\cos\xi)\,d\xi, \tag{2.9.3}$$

where $a \geqslant 0$ is an arbitrary constant equal to $\rho(0) - 1$. It should be noted that $\zeta(\tau)$ can be represented by elliptic integrals:

$$\zeta(\tau) = (1 + a)E(\tau/2, 2\sqrt{a}/(1 + a)) + (1 - a)F(\tau/2, 2\sqrt{a}/(1 + a)) \qquad (0 \leqslant \tau \leqslant \pi).$$

Typical forms of lines (2.9.3) for $0 \leqslant \tau \leqslant \pi$ are shown in Fig. 2.40. While extending these lines, it must be kept in mind that

$$\rho(-\tau) = \rho(\tau), \quad \zeta(-\tau) = -\zeta(\tau),$$

$$\rho(\tau + 2\pi) = \rho(\tau),$$

$$\zeta(\tau + 2\pi) = \zeta(\tau) + 2\zeta(\pi).$$

It is also clear that

(1) for $a = 0$, we get a straight line $\rho = 1$;
(2) for $0 < a < 1$, we get curves for single-valued periodic dependence $\rho(\zeta)$, $1 - a \leqslant \rho(\zeta) \leqslant 1 + a$, and for $a \to 0$, we get

$$\rho(\zeta) = 1 + a\cos\zeta + O(a^2)$$

on any finite interval of variation of ζ;
(3) for $a = 1$, we get a semicircle of radius 2; i.e., the equilibrium surface is a sphere, which is the only simply connected surface in this family;
(4) for $1 < a < \infty$, we get periodic lines reminiscent of an elongated cycloid, and $a - 1 \leqslant \rho(\zeta) \leqslant 1 + a$. The dependence $\rho(\zeta)$ is not single-valued;
(5) for $a = \infty$, line (2.9.3) degenerates into a circle of unit radius.

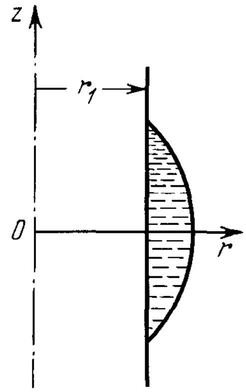

Fig. 2.41

Integral lines for system (2.9.1) are obtained from lines (2.9.3) with the help of transition (2.9.2), so that in view of the arbitrariness of q and the possibility of translation along the z-axis, we arrive at a three-parameter family of integral lines. Only after this can we make the limiting transition at $q \to 0$. This gives another family of catenaries

$$r = (c_1/2)\{\exp[(z - c_2)/c_1] + \exp[-(z - c_2)/c_1]\}.$$

It should be noted that under the assumptions made above, the domain Ω may lie on either side of the equilibrium surface.

In order to construct the equilibrium lines in a given vessel, we can use the following method which is quite cumbersome but applicable, even in the presence of mass forces and rotation [11]. Having specified the point (r_1, z_1) at which the equilibrium line abuts the axial cross section of the vessel, we can determine the initial conditions for system (2.9.1) from the angle of contact α. Numerically solving this system for a certain value of q, we find another point (r_2, z_2) where the equilibrium line meets the axial cross section (if the two do indeed meet) and the angle γ formed by these two lines at this point. Here, γ depends on q, and by trial and error (maybe, for a certain acceleration), we select a value of q for which $\gamma(q) = \alpha$. (This equation may have one, more than one, or no solutions.) Thus we construct the equilibrium line possible for a given contact angle and corresponding to a certain volume v of the liquid, calculated by means of numerical integration. Carrying out this procedure for different successive positions of point (r_1, z_1),[16] we obtain different values of v to arrive at the given value, using a modified trial and error method. One possible approach, also applicable under zero-gravity, is described in greater detail at the end of Sect. 2.9.2.

The situation is considerably simplified if the vessel has a cylindrical surface. Then we can consider either a liquid belt or a gas belt which can be either outside the cylinder, in the form of a sleeve, or inside it. In other words, four different versions are possible here and their analysis is carried out in the same way. Suppose, for example, that we are required to find the equilibrium shape of a liquid belt of volume v, located outside a cylinder of radius r_1, with a contact angle equal to α (Fig. 2.41). For this purpose, it is sufficient to draw lines of equal inclination (i.e., of equal α) and lines of equal ratio V/ρ_1^3

[16] Here, we refer to the remark made at the end of Sect. 2.6.3. The derivative $\partial\gamma/\partial q$ can be calculated by numerically integrating the system of variational equations.

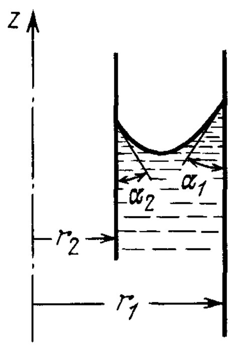

Fig. 2.42

on Fig. 2.40; here, V is the dimensionless volume:

$$V = 2\pi\left[\int_0^\tau \rho^2\zeta'\,d\tau - \rho^2(\tau)\zeta(\tau)\right].$$

Having obtained this net, we can find for given values of α and $v/r_1^3 = V/\rho_1^3$ a point which defines the value of $|q| = \rho_1/r_1$ and the shape of the equilibrium line.

Let us consider an even simpler case when the liquid is confined between two cylinders of radii r_1 and r_2 (Fig. 2.42). We go over to the dimensionless variables

$$\bar{r} = r/r_1, \quad \bar{z} = z/r_1, \quad \bar{s} = s/r_1, \quad \bar{q} = qr_1.$$

In this case, system (2.9.1) can be rewritten in the form

$$\bar{r}'' = -\bar{z}'(\bar{q} - \bar{z}'/\bar{r}), \quad \bar{z}'' = \bar{r}'(\bar{q} - \bar{z}'/\bar{r}), \quad (' = d/d\bar{s}). \tag{2.9.4}$$

The second equation has a first integral

$$\bar{r}\bar{z}' = \tfrac{1}{2}\bar{q}\bar{r}^2 + \bar{c}_1. \tag{2.9.5}$$

If the contact angles on the cylinders are equal to α_1 and α_2, respectively, we obtain the following boundary conditions:

$$\bar{z}'|_{\bar{r}=r_2/r_1} = -\cos\alpha_2,$$

$$\bar{z}'|_{\bar{r}=1} = \cos\alpha_1.$$

Substituting these conditions into (2.9.5), we can find the value of $\bar{q}$; after this, we integrate the system (2.9.4) with the initial conditions

$$\bar{r}(0) = r_2/r_1, \qquad \bar{z}(0) = 0,$$

$$\bar{r}'(0) = \sin\alpha_2, \quad \bar{z}'(0) = -\cos\alpha_2.$$

This gives an equilibrium line which must be displaced parallel to the $\bar{z}$-axis in order to ensure the given value of the volume $\bar{v}$. It should be noted that this method is also applicable to the more general case of a rotating liquid. If a uniform mass force field is also present, the method becomes somewhat complicated; for given values of α_1, α_2 and

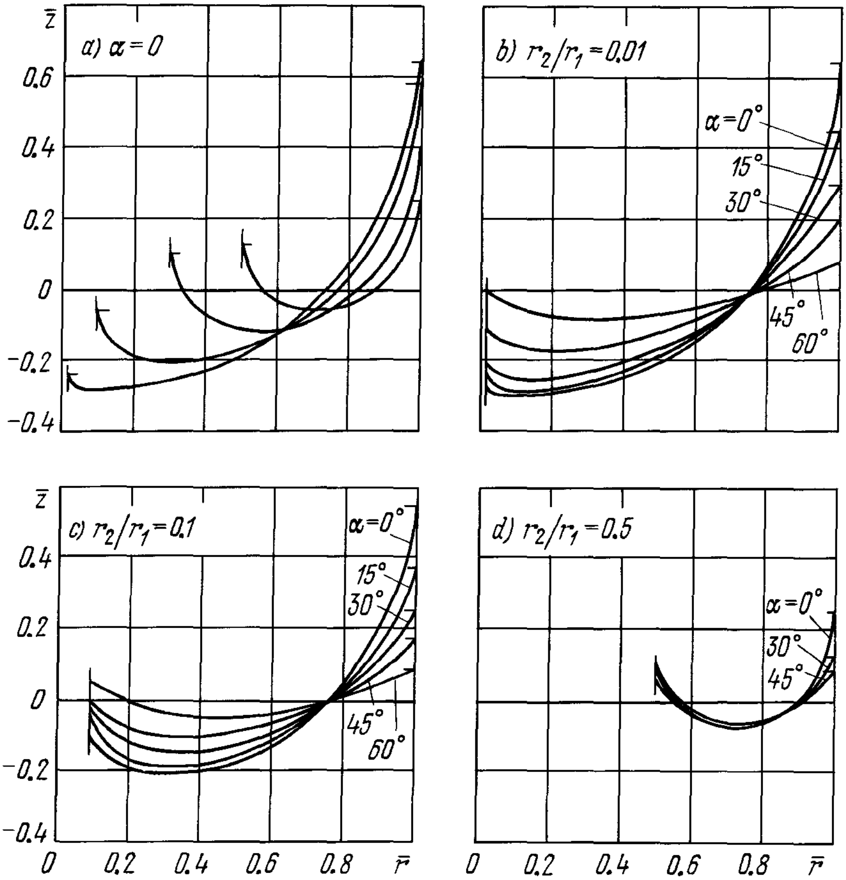

Fig. 2.43

v, we can easily find the value of q from the second equation in (2.3.2). The only remaining unknown parameter $z(0)$ can then be determined by trial and error.

It can be easily verified that for $r_1 = \text{const}$ and $r_2 \to 0$, the equilibrium surface uniformly tends to a spherical segment while for $r_1 \to \infty$ and $r_1 - r_2 = \text{const}$, the equilibrium line uniformly tends to an arc of a circle after a parallel translation. These simple statements are confirmed by the results of calculations carried out by *Seebold* et al. [159] (Fig. 2.43).

It is also appropriate to mention here the work of *Maurin* [105], in which the shape of a symmetric liquid belt surrounding a solid sphere is determined for $\alpha \simeq \pi/2$.

2.9.2 Gravitational Force Field

The family of integral curves generating doubly connected equilibrium surfaces was numerically constructed by *Padday* [127], who compiled quite comprehensive tables for them. However, the problem of constructing such surfaces in a given vessel has not been investigated thoroughly so far. We shall consider some of the results.

Let us first examine the case in which the liquid occupies an unbounded region outside a cylinder of radius r_0 (Fig. 2.44). Then, proceeding from (2.3.1) for $p = 0$, $b > 0$ and

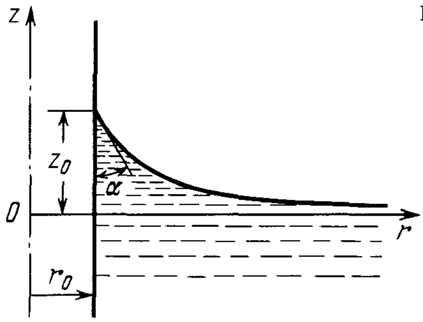

Fig. 2.44

making the change of variables (2.4.1), we arrive at an equation in dimensionless variables:

$$\zeta'' + \frac{1}{\rho}\zeta'(1 + \zeta'^2) - \zeta(1 + \zeta'^2)^{3/2} = 0, \quad \left(' = \frac{d}{d\rho}\right); \tag{2.9.6}$$

we have put $q = 0$, which only displaces the surface along the ζ-axis. The solution must satisfy the boundary conditions

$$\zeta'(\rho_0) = -\cot\alpha, \quad \zeta(\infty) = 0. \tag{2.9.7}$$

The following properties of the solutions of (2.9.6) can be easily proved:

For any $\rho_0 > 0$ and $\zeta_0 \in (0, h(\rho_0))$, there exists just one value of $\zeta_0' = \varphi(\rho_0, \zeta_0) < -\zeta_0\sqrt{4 - \zeta_0^2}/(2 - \zeta_0^2)$, for which the solution of (2.9.6) under the initial conditions $\zeta(\rho_0) = \zeta_0, \zeta'(\rho_0) = \zeta_0'$ is defined in the entire interval $\rho_0 \leqslant \rho < \infty$, decreases and $\zeta(\infty) = 0$. Here, $h(\rho_0) \in (0, \sqrt{2})$, $h(+0) = 0$ and $h(\infty) = \sqrt{2}$. For $\zeta_0 = h(\rho_0)$, the solution having these properties is obtained for $\zeta_0' = -\infty$.

For $0 < \zeta_0 < h(\rho_0)$, $\zeta_0' < \varphi$, the solution of the above Cauchy problem decreases and becomes negative.For $\zeta_0' \in (\varphi, 0)$, the decrease in the solution is followed by an increase. Both these solutions are defined only over a finite interval of variation of ρ (if we use equations in the independent variable τ, the corresponding integral curves must turn in the direction of decreasing ρ). These solutions and their derivatives estimate from below and above the solution and its derivative, indicated in the above paragraph. For $\zeta_0 \geqslant h(\rho_0)$ and any $\zeta_0' < 0$, the decrease in the solution of the Cauchy problem is followed by an increase.

φ is a continuous function of (ρ_0, ζ_0) and a decreasing function of ζ_0; moreover, $\varphi|_{\zeta_0=0} = 0$ and $\varphi|_{\zeta_0=h} = -\infty$. As $\rho_0 \to \infty$, $\varphi(\rho_0, \zeta_0)$ uniformly tends to $-\zeta_0\sqrt{4 - \zeta_0^2}/(2 - \zeta_0^2)$ (this corresponds to the plane problem in the analogous situation).

For $\zeta_0 < 0$, all these properties are appropriately reformulated.

All the statements made above are satisfied [245] for a wide range of equations of the type $\zeta'' = f(\rho, \zeta, \zeta')$, if: the function $f(\rho, \zeta, \eta)$ is continuously differentiable for $\rho_0 \leqslant \rho < \infty$, $-\infty < \zeta$, $\eta < \infty$; it increases with ζ for $\zeta\eta < 0$; $f(\rho, \zeta, 0)$ has the same sign as ζ; and $f(\rho, \zeta, \eta)$ has certain properties of increasing with η, which we shall not describe here.

From the properties enumerated above, it follows that boundary value problem (2.9.6–7) has just one solution, and it can be easily verified that as $\rho \to \infty$, this solution is asymptotic to $\text{const}\cdot\exp(-\rho)/\sqrt{\rho}$. It can be found approximately by numerically integrating (2.9.6) for $\zeta'(\rho_0) = -\cot\alpha$ and a certain $\zeta(\rho_0)$ for which the second condition

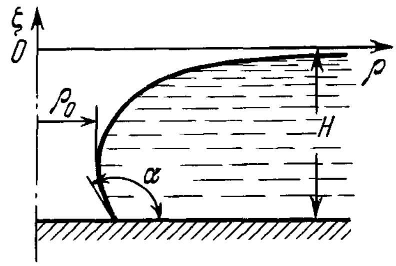

Fig. 2.45

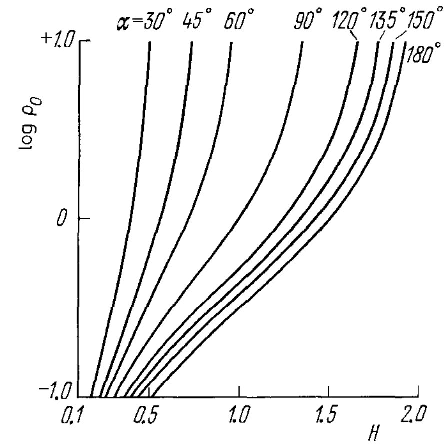

Fig. 2.46

in (2.9.7) is satisfied. (The value of $\zeta(\rho_0)$ can be found by trial and error, and is bounded between values for which $\zeta(\rho)$ and, on the other hand, $\zeta'(\rho)$ change sign.)

The results described above for the case $\alpha = 0$ ($\alpha = \pi$) were mainly obtained by *White* and *Tallmadge* [224]. Data concerning further investigations in this direction, as well as some numerical results, are contained in the article by *Padday* and *Pitt* [128]. Asymptotic expressions for the shape of the surface in the neighborhood of a cylinder of very small radius and away from it were first obtained by *Deryagin* [56] (these results were later obtained by *James* [79] as well).

A similar problem was investigated by *Taylor* and *Michael* [207], who studied the equilibrium shape of a hole in a sheet of a liquid poured on a horizontal plane (Fig. 2.45). Obviously, this shape is a part (for $\alpha < \pi/2$) or an extension (for $\alpha > \pi/2$) of the solution for the above problem involving a cylinder of dimensionless radius ρ_0 for $\alpha = \pi$. Figure 2.46 shows the relation between the height H and ρ_0 for different values of α. As $\rho_0 \to \infty$, the problem degenerates into a plane problem, and from the discussion in Sect. 2.10, it can be easily seen that H tends asymptotically to $2\sin(\alpha/2)$.

A problem of this kind, in which L is semi-infinite and has a horizontal asymptote, was later investigated by *Boucher*, *Kent* and *Jones* [28, 31]. In the case they considered, Γ is in contact with the edge of the lower end face of a cylindrical rod, the surface of a sphere, a horizontal plate or the lateral surface of a knurled rod.

Another problem concerning the equilibrium shape of a liquid in an annular tank was considered by *Seebold* et al. [159]. Three parameters are significant here: r_2/r_1 (see end of Sect. 2.9.1), α, and $\mathbf{Bo} = br_1^2$. This makes it difficult to present the results of computations in a clearly visible form. Some of them are shown in Figs. 2.47 and 2.48. The meaning of the notation used for quantities characterizing the equilibrium shape is illustrated in Fig. 2.49, where the dotted line shows the solution of the problem without taking the surface tension into account.[17] We can easily formulate statements similar to those given

[17] For problems involving more than two significant parameters, it would be important (in particular, from a practical point of view) to choose formulas which describe, with a sufficient degree of accuracy, the dependence on these parameters of the system characteristics (in this case, the basic characteristics of the equilibrium shapes).

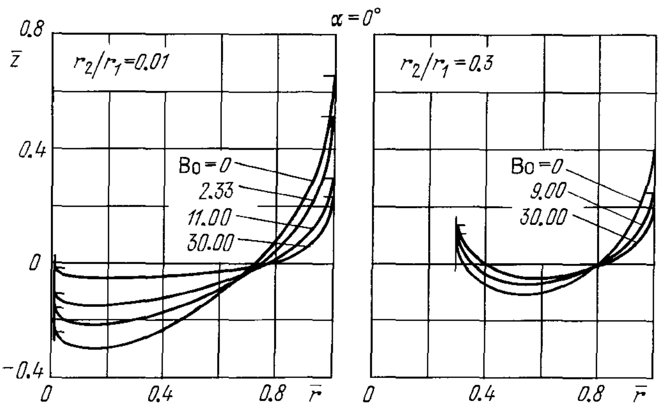

Fig. 2.47

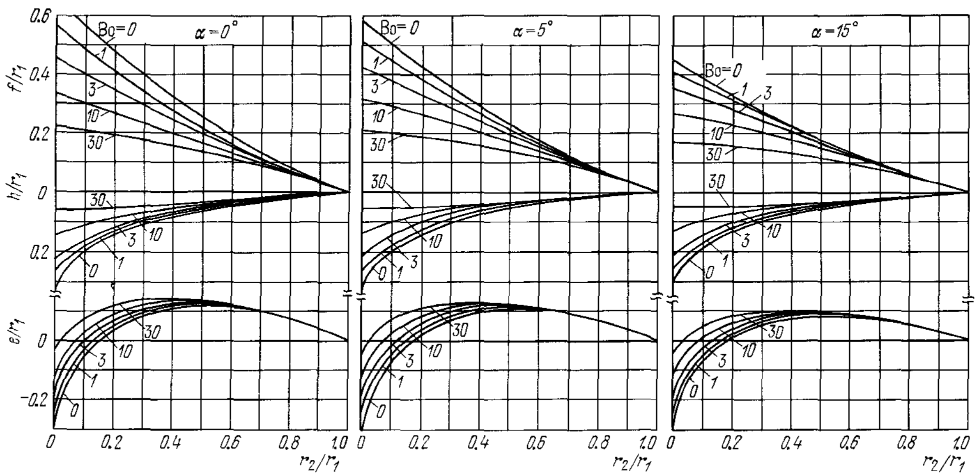

Fig. 2.48

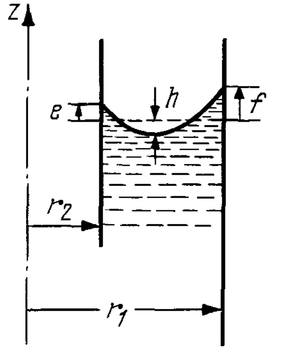

Fig. 2.49